AD NUMBER

ADB102693

NEW LIMITATION CHANGE

TO

Approved for public release, distribution unlimited

FROM

Distribution authorized to U.S. Gov't. agencies and their contractors; Critical Technology; May 1986. Other requests shall be referred to Director, U.S. Army Ballistic Research Laboratory, Attn: SLCBR-DD-T, Aberdeen Proving Ground, MD 21005-5066.

AUTHORITY

BRL ltr, 4 Apr 1988

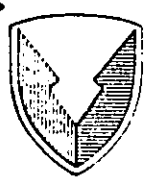

SPECIAL PUBLICATION BRL-SP-56

EXPLOSIVE LOADING OF METALS AND RELATED TOPICS

William P. Walters

May 1986

US ARMY BALLISTIC RESEARCH LABORATORY
ABERDEEN PROVING GROUND, MARYLAND

Destroy this report when it is no longer needed.
Do not return it to the originator.

Secondary distribution of this report is prohibited.

Additional copies of this report may be obtained from the Defense Technical Information Center, Cameron Station, Alexandria, Virginia 22314.

The findings in this report are not to be construed as an official Department of the Army position, unless so designated by other authorized documents.

The use of trade names or manufacturers' names in this report does not constitute indorsement of any commercial product.

DEPARTMENT OF THE ARMY
UNITED STATES ARMY LABORATORY COMMAND
BALLISTIC RESEARCH LABORATORY
ABERDEEN PROVING GROUND, MARYLAND 21005-5066

REPLY TO
ATTENTION OF

SLCBR-DD-S

4 April 1988

MEMORANDUM FOR: SEE DISTRIBUTION

SUBJECT: BRL Special Publication 56

1. Reference BRL Special Publication No. 56, "Explosive Loading of Metals and Related Topics," by W. P. Walters, May 1986, UNCLASSIFIED.

2. Request that you cancel the distribution statement shown on the front cover of your copy of the referenced report and remark it with the following distribution statement:

Approved for public release; distribution is unlimited.

FOR THE DIRECTOR:

LEONA M. SMITH
Chief

UNCLASSIFIED
SECURITY CLASSIFICATION OF THIS PAGE (When Data Entered)

REPORT DOCUMENTATION PAGE

READ INSTRUCTIONS BEFORE COMPLETING FORM

1. REPORT NUMBER: Special Publication BRL-SP-56
2. GOVT ACCESSION NO.:
3. RECIPIENT'S CATALOG NUMBER:
4. TITLE (and Subtitle): Explosive Loading of Metals and Related Topics
5. TYPE OF REPORT & PERIOD COVERED: Final
6. PERFORMING ORG. REPORT NUMBER:
7. AUTHOR(s): William P. Walters
8. CONTRACT OR GRANT NUMBER(s):
9. PERFORMING ORGANIZATION NAME AND ADDRESS:
U. S. Army Ballistic Research Laboratory
ATTN: SLCBR-TB
Aberdeen Proving Ground, MD 21005-5066
10. PROGRAM ELEMENT, PROJECT, TASK AREA & WORK UNIT NUMBERS:
11. CONTROLLING OFFICE NAME AND ADDRESS:
U. S. Army Ballistic Research Laboratory
ATTN: SLCBR-DD-T
Aberdeen Proving Ground, MD 21005-5066
12. REPORT DATE: May 1986
13. NUMBER OF PAGES: 130
14. MONITORING AGENCY NAME & ADDRESS (if different from Controlling Office):
15. SECURITY CLASS. (of this report): Unclassified
15a. DECLASSIFICATION DOWNGRADING SCHEDULE:
16. DISTRIBUTION STATEMENT (of this Report):
Distribution limited to U.S. Government Agencies and their Contractors; Test and Evaluation; May 86. Other requests for this document must be referred to Director, U.S. Army Ballistic Research Laboratory, ATTN: SLCBR-DD-T, Aberdeen Proving Ground, MD 21005-5066.
17. DISTRIBUTION STATEMENT (of the abstract entered in Block 20, if different from Report):
18. SUPPLEMENTARY NOTES:
19. KEY WORDS (Continue on reverse side if necessary and identify by block number):

Explosive Loading
Explosive Welding, Shaping and Forming
Shaped-Charges
Explosive-Metal Interactions
Visco-Plastic Jets
Gurney Calculations
Flying Plates
Shaped-Charge Jet Formation
Shaped-Charge Jet Collapse
PER

20. ABSTRACT (Continue on reverse side if necessary and identify by block number):

This document is intended to be a tutorial report covering the basic aspects of the explosive loading of metals. Chapters are given which describe the shaped-charge concept, the history of shaped-charges and several applications of shaped-charge devices. The generalized equations, such as those solved by the hydrocodes, as well as the Bernoulli Equation concept are presented. The Gurney velocity approximation for explosively driven plates is presented. Also the models used for the collapse and jet formation of a shaped-charge with a conical liner are described. Finally, the concept of explosive welding, shaping and

DD FORM 1 JAN 73 1473 EDITION OF 1 NOV 65 IS OBSOLETE

UNCLASSIFIED
SECURITY CLASSIFICATION OF THIS PAGE (When Data Entered)

forming is discussed.

TABLE OF CONTENTS

LIST OF FIGURES

LIST OF FIGURES - continued

Section IX

Section X

Section XI

EXPLOSIVE LOADING OF METALS

I. Preface

The explosive loading of metals, especially as related to shaped-charge liners and metals driven by explosives, is a vast field. Thousands of documents have been written covering many aspects of the explosive loading of materials. However, due to the intense interest in this field by the defense establishments of many nations, a great deal of the literature is either classified, not available in English, or hidden in obscure government or industry documents. Also, certain industries (e.g., drilling, mining, metal forming, etc.) engaged in explosive loading, do not readily distribute information due to their highly competitive nature. This increases the number of proprietary and minimal distribution documents. In short, a great deal of information is simply not available to, or cannot be found by, even the more diligent researcher.

I am certainly not aware of all the explosive loading information available. Furthermore, I will not even attempt to present all the information at my disposal. Instead, I will present basic introductory material and cover only the major aspects of the explosive loading of metals technology and limit my discussion to shaped-charges and the motion of metals driven by explosives. The material and literature covered will be that of important historical value and that material found to be most useful to me.

My sources stem primarily from my association with Ballistic Research Laboratory. As a direct consequence of this association, I am probably remiss in reporting the results of other government and industrial agencies, especially those which do not deal directly with the Ballistic Research Laboratory. Also, reference to foreign literature will be minimized. Several sources have been omitted as being beyond the scope of this text or merely redundant or supplemental to material already included. Nevertheless, a large shaped-charge formation and penetration bibliography is given. Again, I do not claim that this bibliography is complete.

Finally, a note of thanks to Lisa Ann Weismiller for the meticulous typing of a difficult manuscript.

II. The Shaped-Charge Concept

A cylinder of explosive with a hollow cavity in one end and a detonator at the opposite end is known as a hollow charge. The hollow cavity, which may assume almost any geometric shape such as a hemisphere, a cone or the like causes the gaseous products formed from the initiation of the explosive at the end of the cylinder opposite the hollow cavity to focus the energy of the detonation products. The focusing of the detonation products creates an intense localized force. This concentrated force when directed against a metal plate is capable of creating a deeper cavity than a cylinder of explosive without a hollow cavity, even though more explosive is available in the latter case. As discussed later, this phenomenon is known in the U.S. as the Munroe effect. Further, if the hollow cavity is lined with a thin layer of metal, glass, ceramic or the like, the liner forms a jet when the explosive charge is detonated. This focusing of the liner material causes a still deeper cavity to be formed when the explosive is detonated with the base of the liner in contact with a metal plate. The cavity formed becomes deeper yet when the explosive charge containing the liner is removed some distance away from the plate. This distance, for which an optimum exists, is called the standoff distance. Devices of this nature are called lined cavity charges or shaped-charges.

In the following sections, these concepts will be pursued in detail.

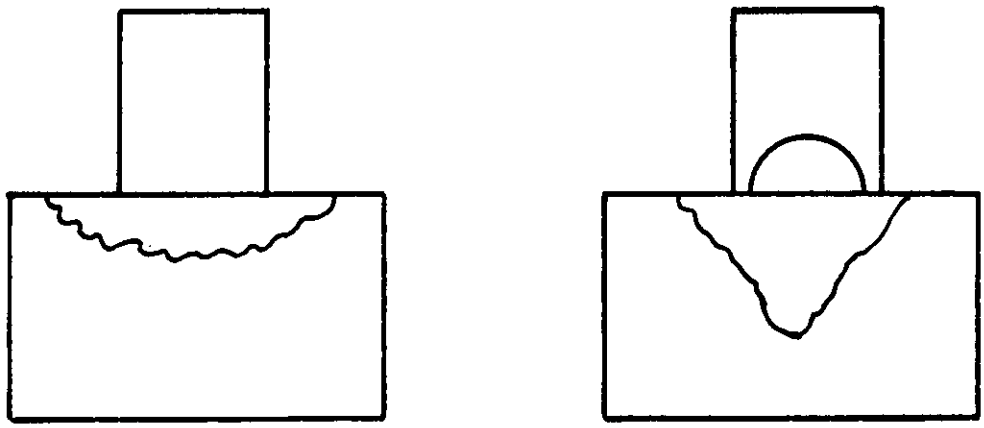

THE MUNROE EFFECT

III. History of Shaped-Charges

This section will discuss shaped-charge jets or the shaped-charge effect resulting from the interaction of an explosive with a metallic liner. Further, the discussion will be restricted to conventional shaped-charge rounds, e.g., conical, hemispherical and other arcuate metallic liners, and Self Forging Fragments (SFF) or Explosively Formed Penetrators (EFP) or P charges will only be briefly addressed. Explosive welding and cutting or tapping charges will not be considered in any detail.

The history of shaped-charge development is somewhat ambiguous in that the British, Germans and Americans all have made significant claims to the early development of lined cavity charges. I understand that currently Dr. Manfred Held of MBB, West Germany and H. H. Mohaupt of the U.S. are both preparing manuscripts on the history and/or development of Shaped-Charge research. Dr. P. C. Chou [1] and D. F. Kennedy [2] have both drafted manuscripts on their version of the history and/or development of shaped-charges. The individuals mentioned above are senior experts in the field and will certainly provide an excellent account of current and/or historical shaped-charge developments. Also, Eather and Griffiths of the U.K. [3] have provided a history of the U.K. contribution to the field of shaped-charges which includes the contributions of Evans, Ubbelohde, Taylor, Tuck, Mott, Hill, Pack and others which I will discuss later. Dr. Held may include the discussions of References 1, 2 and 3 in his manuscript.

Recently, D. F. Kennedy published a description of the shaped-charge concept [4] including jet formation, a brief history of the shaped-charge concept, jet disturbance mechanisms and modern day applications of shaped-charge devices. I highly recommend Kennedy [4] as required reading for the novice in the shaped-charge field.

We will define the term shaped-charge to apply to explosive charges with lined or unlined cavities. The cavity is formed in the end of the explosive charge opposite the point of initiation. The term shaped-charge, however, has a more general meaning, e.g., Cook [5]. The shaped-charge is also referred to as the hollow charge (in the U.K.), the cumulative charge (in the USSR), or the Hohlladung (in Germany).

The hollow cavity effect was first observed by Max von Foerster in 1883 [6,7] and apparently rediscovered by Charles Munroe in 1888 [8,9,10,11,12]. The hollow charge or cavity effect is known in the U.S. and U.K. as the Munroe effect after Munroe's well documented experiments in 1888. Munroe detonated blocks of explosive in contact with steel plates. The explosive charge had the initials U.S.N. (United States Navy) inscribed on the charge opposite the point of detonation. These initials were reproduced on the steel plate. Munroe further observed that when a cavity was formed in a block of explosive, opposite the point of initiation, the penetration, or depth of the crater produced in the target, increased. In other words, a deeper cavity could be produced in a target using a smaller mass of explosive! The increase in penetration results from the focusing of the explosive gases (detonation products) by the hollow cavity. The depth of the crater in the target can be further increased by displacing the hollow charge some optimal distance from the target, i.e., increasing the standoff-distance for a lined cavity charge.

Early German reference to the hollow cavity effect, excluding von Foerster, occurred in 1911 patents in Germany and the U.K. [13,14]. Also, in 1886, Gustov Bloem [15] of Dusseldorf patented a shell for detonating caps (U.S. Patent No. 342, 423) which resembles a shaped-charge with a hemispherical liner.

Early British development of the hollow cavity warhead was reported in 1913 according to Reference [16]. The earliest known Soviet mention of the shaped-charge effect was by Sucharewski in 1925 [17]. The first Italian paper on the shaped-charge effect was by Lodati in 1932 [18]. Kennedy [2] provides an excellent early history of the shaped-charge effect including evidence that this effect may have been known prior to von Foerster using low explosives in mining applications such as mudcapping.

Studies involving the shaped-charge effect continued from 1911 to the late 1930's, mostly by German scientists, see, e.g., Kennedy [2]. The contributions of Watson [19] on percussion fuzes and Wood [20] on SFF, EFP, Misznay-Schardin devices, ballistic discs or P-charge projectiles appeared during this period.

The lined-cavity shaped-charge research accelerated tremendously between 1935 and 1950 due primarily to World War II and the application of shaped-charges to the bazooka, panzerfaust and other devices. The discoverers of the lined cavity effect were Franz Rudolf Thomanek for Germany and the Swiss, Henry Hans Mohaupt for the U.K. and the U.S. (Unless we credit Bloem [15] with this discovery). At any rate, Thomanek and Mohaupt perfected this concept and developed the first effective lined cavity shaped-charge penetrators. Dr. Thomanek's early work is given in References [21,22,23,24] and Dr. Mohaupt's work is given in References [25,26,27,28]. Kennedy provides additional references and discussion relating to the work of Mohaupt and Thomanek [2]. Kennedy also points out that Munroe used a form of a lined cavity charge consisting of an open tin can surrounded by dynamite sticks to pierce a steel safe [12].

Mohaupt, using lined cavity charges, designed practical military devices ranging from rifle grenades, to mortars, to 100 mm diameter artillery projectiles. These devices were test fired at the Swiss Army Proving Ground at Thun, at Mohaupt's Laboratory and at the French Naval Artillery Proving Ground at Gavre. These results were also demonstrated to the U.K. who then began development programs of their own. Following the early results of World War II, the French Government authorized the release of Mohaupt's information to the U.S. and in late 1940 tests were conducted at Aberdeen Proving Ground, Maryland using several aspects of lined cavity shaped-charges [28]. The U.S. accepted the program, classified it, and thus excluded Dr. Mohaupt from the effort but produced the 2.36 in HEAT machine gun grenade and the 75 mm and 105 mm HEAT artillery projectiles in 1941. Later the machine gun grenade was modified to include a rocket motor and a shoulder launcher and became the bazooka. The bazooka was first used by the U.K. in North Africa in 1941. Other HEAT rounds were fired from tank mounted howitzers [2,28].

The military research, introduced by Mohaupt, was supported by private firms such as DuPont and the Carnegie Institute of Technology. The Carnegie group (C.I.T.) employed some outstanding researchers which contributed much of the current shaped-charge knowledge. The leaders at Carnegie were

Heine-Geldern, N. Rostoker, Emerson Pugh and his student Robert Eichelberger. Eichelberger is the former Director of the Ballistic Research Laboratory.

Shaped-charge theory continued to develop during the 1950's boosted by the Korean War [5,29,30,31,32,33,34,35,36]. During this time period tremendous progress was made toward the understanding of the phenomena associated with shaped-charge jets. Photographic techniques were employed to observe the jet process and analytical models were developed. Efforts were made to improve existing shaped-charge liners; to use detonation wave shapers; to provide spin compensation via fluted liners; to provide shaped-charge follow-through mechanisms; and to enhance the overall system performance.

Currently, shaped-charge research continues in order to devise successful countermeasures to the advanced armors currently fielded and/or contemplated, see e.g., Kennedy [4]. Studies which originated in the 1950's still continue; notably, torpedo applications of shaped-charge rounds, anti-aircraft rounds, fragmentation rounds, multi-staged or tandem liners, long standoff rounds, non-conical liners and non-copper liners. Also metallurgical and chemical aspects of the liner material was well as methods of liner fabrication remain important.

Starting in the 1950-60's significant shaped-charge developments were made possible by the advent of excellent experimental techniques such as high speed photography and flash radiography. Other improvements resulted from the transition from TNT to more energetic explosives, i.e., from TNT to Comp B to Octol and then to pressed explosives, notably LX-14. Also, alternate modes of initiation (other than point-initiation) and waveshaping techniques have provided warhead design improvements. Other advances stemmed from the development of large computer codes to simulate the collapse, formation and growth of the jet from a shaped-charge liner. These codes provide for the most part, excellent descriptions of the formation of the jet. The codes, however, are somewhat hindered by the lack of accurate equations of state of the liner material and the explosive and by inadequate constitutive relationships (i.e., the relationship betweens stress, strain, strain rate, and the velocity and velocity gradients).

The following sections will address the recent developments in more detail and will attempt to explain the shaped-charge principles and related areas. The information and references given thus far provide a brief background of shaped-charge development. Shaped-charge utilization was made possible by the discovery of blasting caps (detonators) by Alfred Nobel [28,37] in 1867. The explosive reaction initiated by these blasting caps could propagate through a column of explosive without the use of confinement. This was termed detonation or brisant explosion [28]. The hollow charge effect, described earlier, was exploited around 1910 by von Neumann [28] and was developed extensively during World War II.

The Watson patents [19] greatly enhanced the weaponization and further applications of the shaped-charge principle. The Watson percussion fuze consisted of a parabolic booster charge with a metal lined hemispherical ("or arched shield") cavity at the "output" end of the fuze body to intensify the effect of the booster charge even over an airgap. This fuze is, in effect, a detonator using the shaped-charge principle.

Further developments followed by Wood [20] who described what is known today as a self forging fragment, explosively formed penetrator, a P-charge or a Misznay-Schardin device.

The shaped-charge principle was clarified and understood as a result of the pioneering flash x-ray photographs taken by L. B. Seely and J. C. Clark of Ballistic Research Laboratory and J. L. Tuck of England, in 1943. Based on an analysis of these photographs, analytical models of the collapse of a lined conical shaped-charge were developed by Birkhoff [38], Pugh [39], Evans [40] and others as indicated in References [1 and 5]. Important contributions were carried out by the Carnegie group mentioned previously and continued by the Ballistic Research Laboratory (L. Zernow, R. Eichelberger and Associates). Other laboratories making important contributions during this time period were the Naval Ordnance Laboratory, Maryland (Solem and August), the Naval Ordnance Test Station, California (Throner, Weinland, Kennedy, Pearson and Rinehart), Picatinny Arsenal, New Jersey (Dunkle), the Standford Research Institute, California (Poulter) and others. The liner collapse and jet formation will be discussed in detail in a later section.

A bibliography and account of the weaponization of the shaped-charge and similar principles is given by J. Backofen [41-47]. Backofen's bibliography is extensive, especially regarding foreign sources. Earlier, WW II results and bibliographical information are given in References [48,49,50].

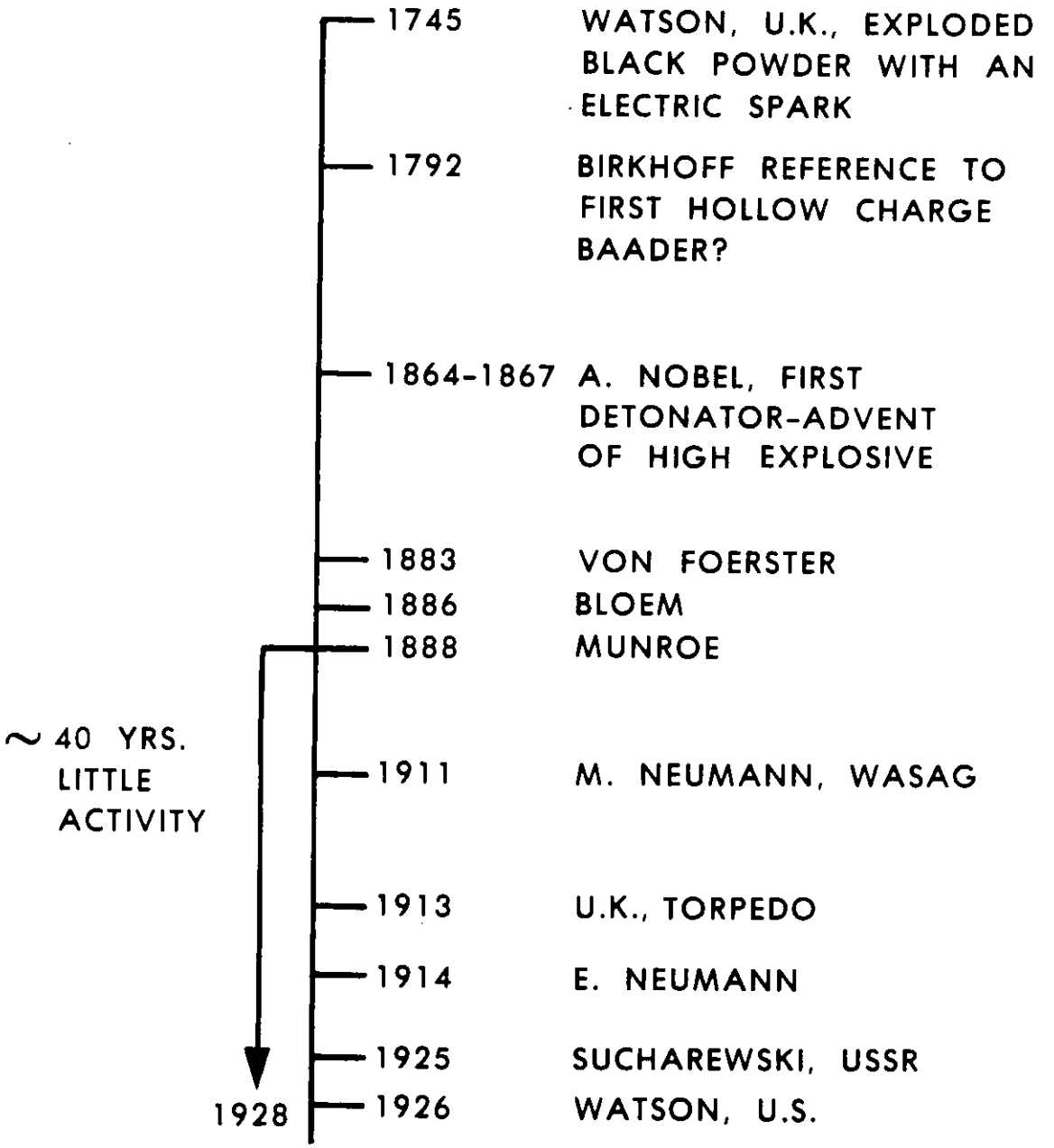

TIME LINE 1745-1928

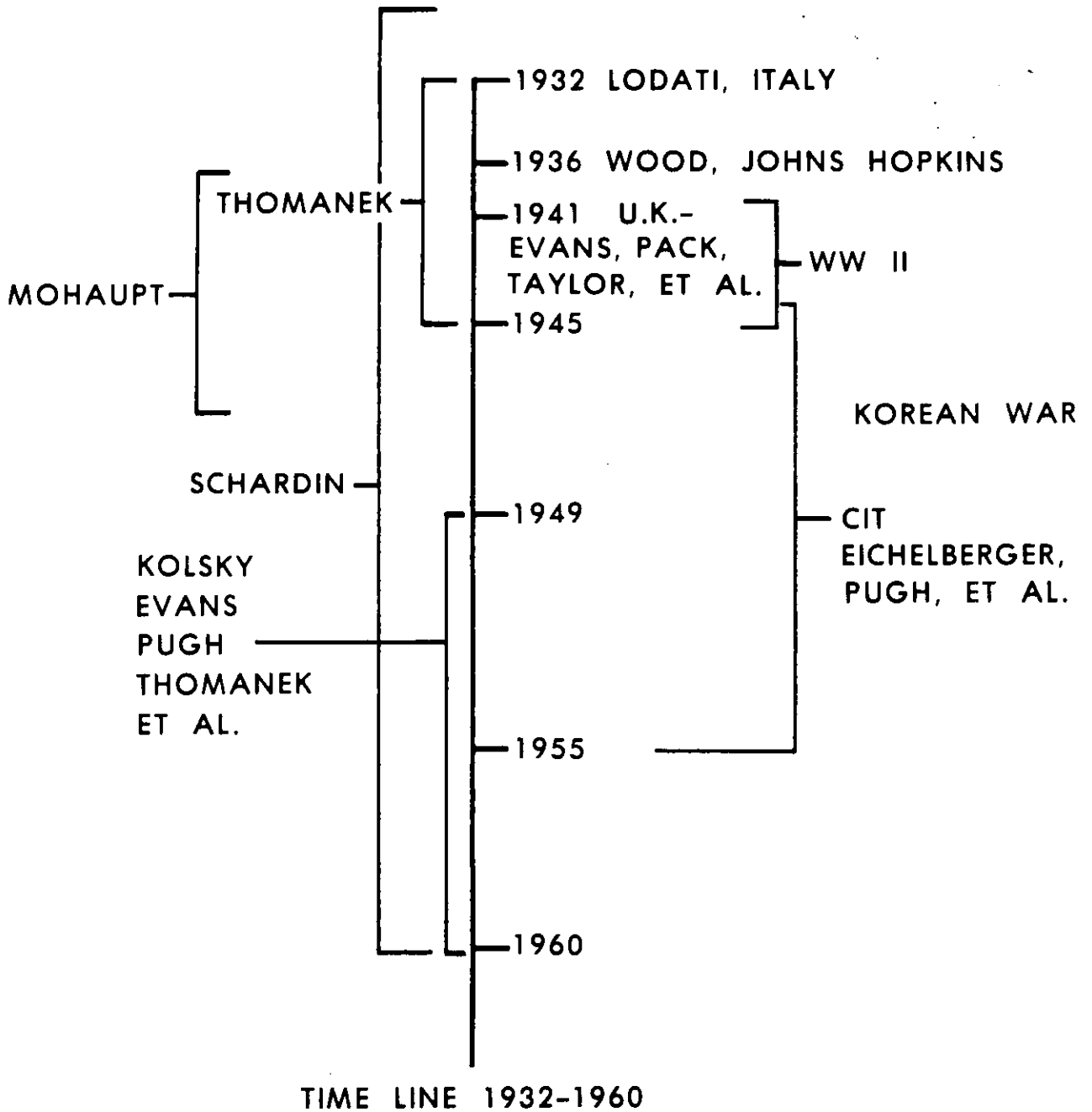
1932 LODATI, ITALY
1936 WOOD, JOHNS HOPKINS
THOMANEK
1941 U.K.-
EVANS, PACK,
TAYLOR, ET AL.
WW II
MOHAUPT
1945
KOREAN WAR
SCHARDIN
1949
CIT
EICHELBERGER,
PUGH, ET AL.
KOLSKY
EVANS
PUGH
THOMANEK
ET AL.
1955
1960
TIME LINE 1932-1960

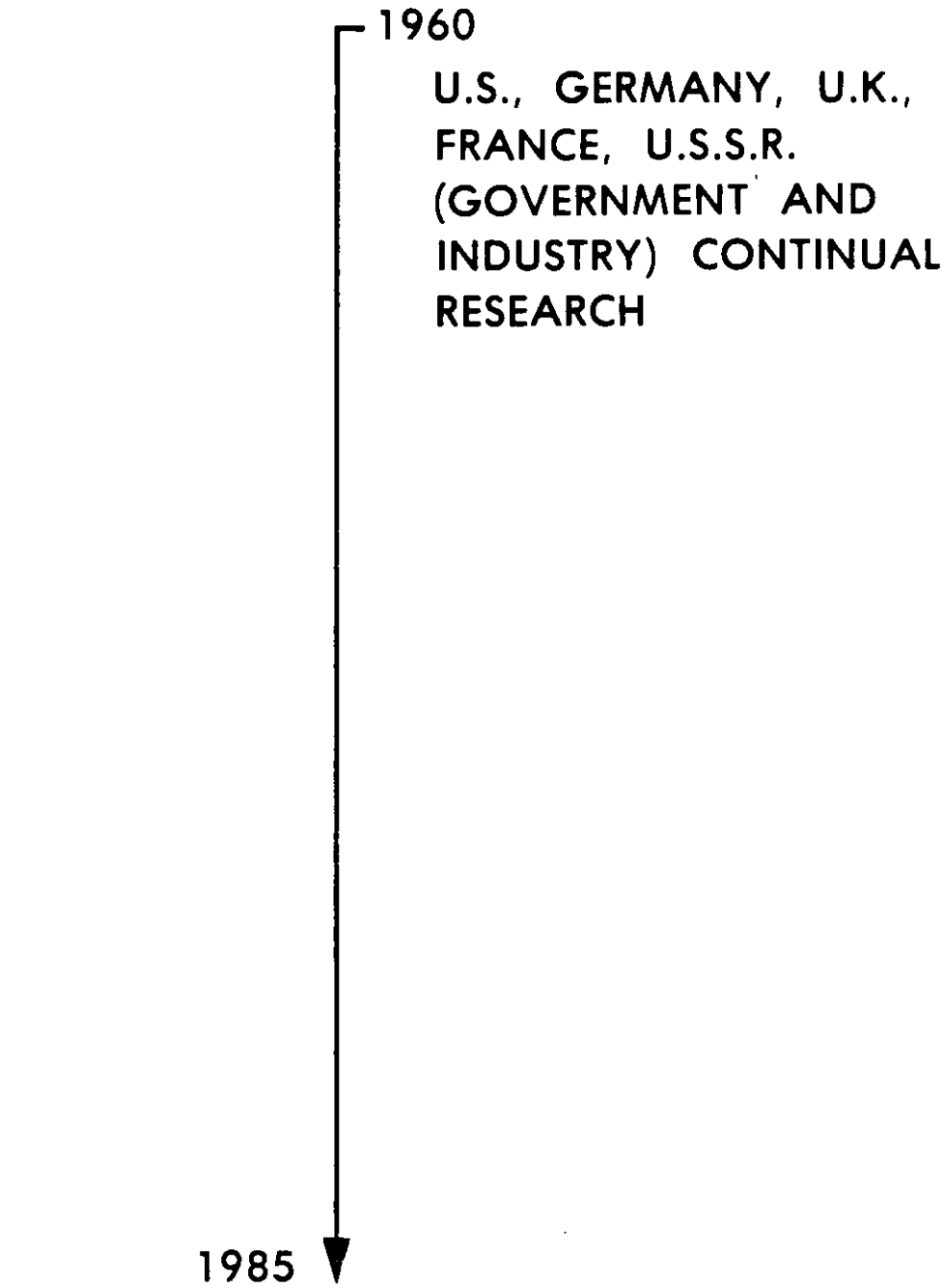

TIME LINE 1960-TO DATE

IV. Introduction to Shaped-Charges

The directional penetration effect observed when a hollow charge is detonated in contact with a steel plate is graphically depicted in Figure 1. The crater depth is about one-half of the diameter of the hollow of the conical cavity. The cavity is produced by high pressure, high velocity gas erosion (the Munroe effect). When the hollow cavity is lined with a thin hollow metallic or glass cone, the lined charge results in a much deeper crater. Furthermore, when the lined cavity charge is displaced from the target block some distance (known as the standoff) the penetration increases even more. Figure 1 depicts these three cases.

The increase in penetration resulting from the lined shaped-charge is due to the plastic deformation of the liner material under the intense pressures and temperatures generated by the detonation of the high explosive. The mechanism of jet formation for metallic conical liners with a semi-angle (one-half of the conical apex angle) less than 60° is as described below.

Figure 2 shows a typical shaped-charge warhead like that described above. Note that the explosive charge is not cylindrical, but tapered. This removal of some of the explosive weight is termed "boattailing" and does not affect the jet collapse mechanism. We need only that the detonation wave front be plane and perpendicular to the longitudinal axis-of-symmetry.

When the detonator is fired, the detonation wave propagates through the explosive with the detonation velocity of the particular explosive used. When the detonation front reaches the conical liner, the liner is subjected to the intense pressures and high temperatures of the front and begins to collapse. The collapse is depicted in Figure 3 for the conical lined shaped-charge shown in Figure 2. For the position of the detonation wave front shown in Figure 3, the upper (apex) region of the cone has collapsed and collided on the axis-of-symmetry. This collision results in plastically deformed liner material under tremendous pressure being extruded along the axis-of-symmetry [4,40,51]. This extruded material is called the jet. When the pressures generated exceed the yield strength of the liner material, the liner behaves approximately as an inviscid, incompressible fluid. The cone collapses progressively from apex to base under point initiation of the high explosive. A portion of the liner flows into a compact slug which is the large, massive portion at the rear of the jet.

A rough analogy can be drawn to the effect produced when a sphere is dropped into water. During impact and downward motion in the water, the cavity formed moves outwards around the sphere and then reverses to collide along the axis-of-symmetry. On collision, vertical jets are formed which squirt upwards and downwards [40,52].

Crude "rules of thumb" were established by Evans [40] in 1950. Namely, about 20% of the inner surface of the metal of the cones is used to form the jet. The jet diameter is about one twentieth of the diameter of the cone. The jet tip velocity is of the order of the detonation velocity of the explosive. The jet velocity decay is a nearly liner function down to about one quarter of the detonation velocity at the tail (rear) of the jet. The velocity of the slug is of the order of one tenth of the jet tip velocity. These estimates are only crude order-of-magnitude estimates and are only for

moderate apex angle, copper, conical liners. As we will see, there are techniques available to provide more accurate estimates of the jet and slug parameters. Also note that the jet formation is strongly dependent on the liner geometry, liner material, high explosive geometry, confinement geometry and material (if confinement is present), the type of high explosive used and the mode of initiation. These factors will be addressed later. In any case, the goal is to direct and concentrate energy in the axial direction to enhance the damage resulting from the hollow charge.

For any liner design, a proper match between the charge to mass ratio (explosive charge mass to liner mass ratio) is critical. If the liner is too thick, the energy losses resulting from internal friction and heating of the liner walls during the collapse and the energy losses due to spallation of the thick liner will reduce the collision velocity below the value necessary for jet extrusion. Also, if the liner wall thickness is too thin, directed flow is not achieved due to the loss of structural integrity of the liner. If the wall is extremely thin, the liner material may undergo vaporization upon collision.

Shaped-charges with wide angle cones or hemispherical liners show a radically different collapse pattern. Hemispherical liners invert (or turn inside out) from the pole and as the detonation wave progresses toward the base of the liner, the hemispherical liner approximates a conical liner and the inverted collapse pattern reverts to that of a cone. In general, the hemispherical and large angle conical liners usually result in larger diameter, but lower velocity gradient jets. No massive slug, per se, is formed.

Of course, jet effects or controlled fragmentation are not limited to conical or hemispherical liners. Extensive use has been made of other liner designs (discussed later) as well as linear and circular charges. The liner cross sections for linear and circular charges are wedges and semicircular configurations, respectively. The jet produced by a linear charge is in the form of a thin ribbon and in the case of a torus (semi-circular) charge a tubular spray [28].

The collapse mechanism of various shaped-charge liners has been verified via flash radiography. These novel experimental results lead to the formulation of fundamental jet collapse theories. These theories will be discussed later.

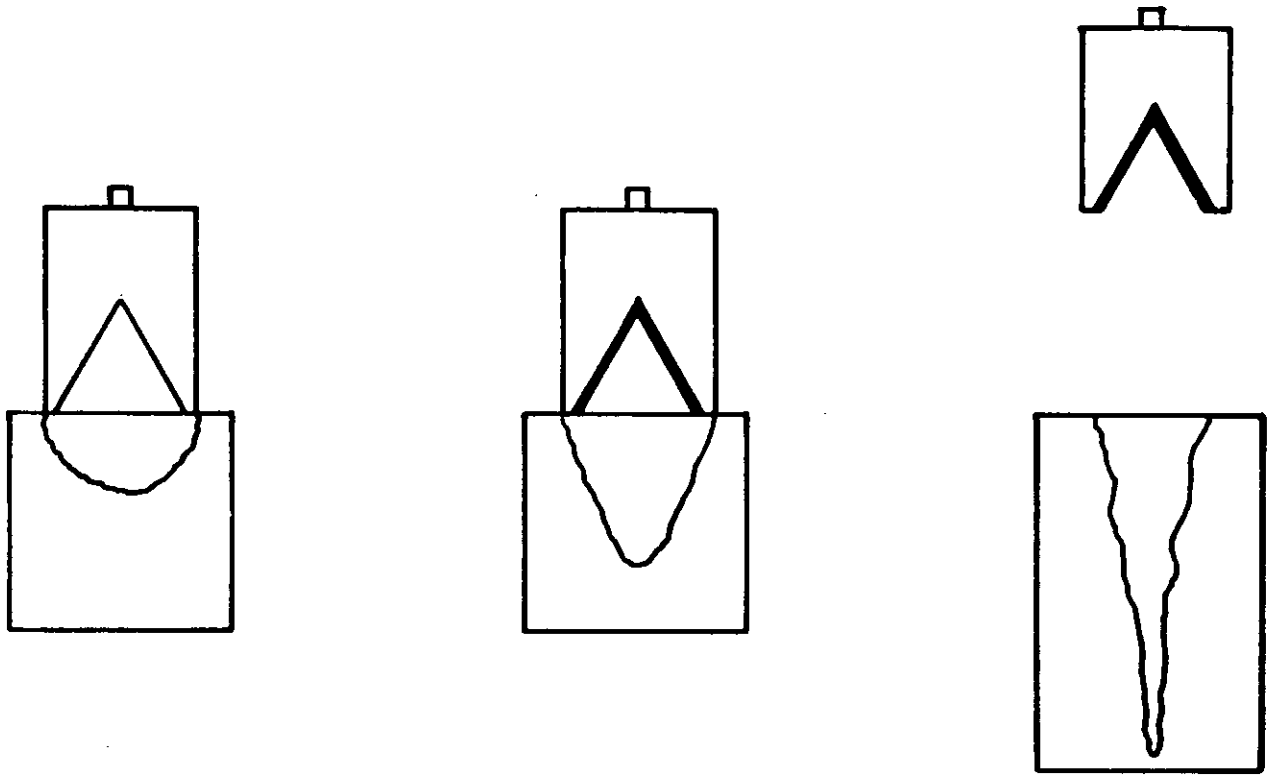

Figure 1. The Lined Cavity Effect.

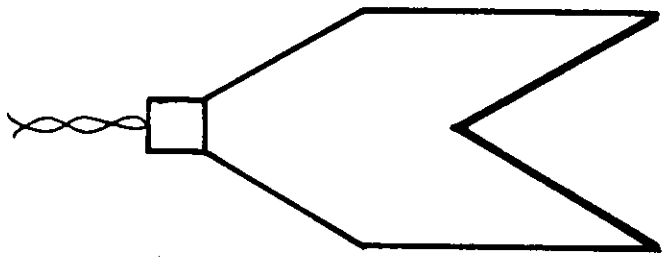

Figure 2. Typical Shaped-Charge Configuration.

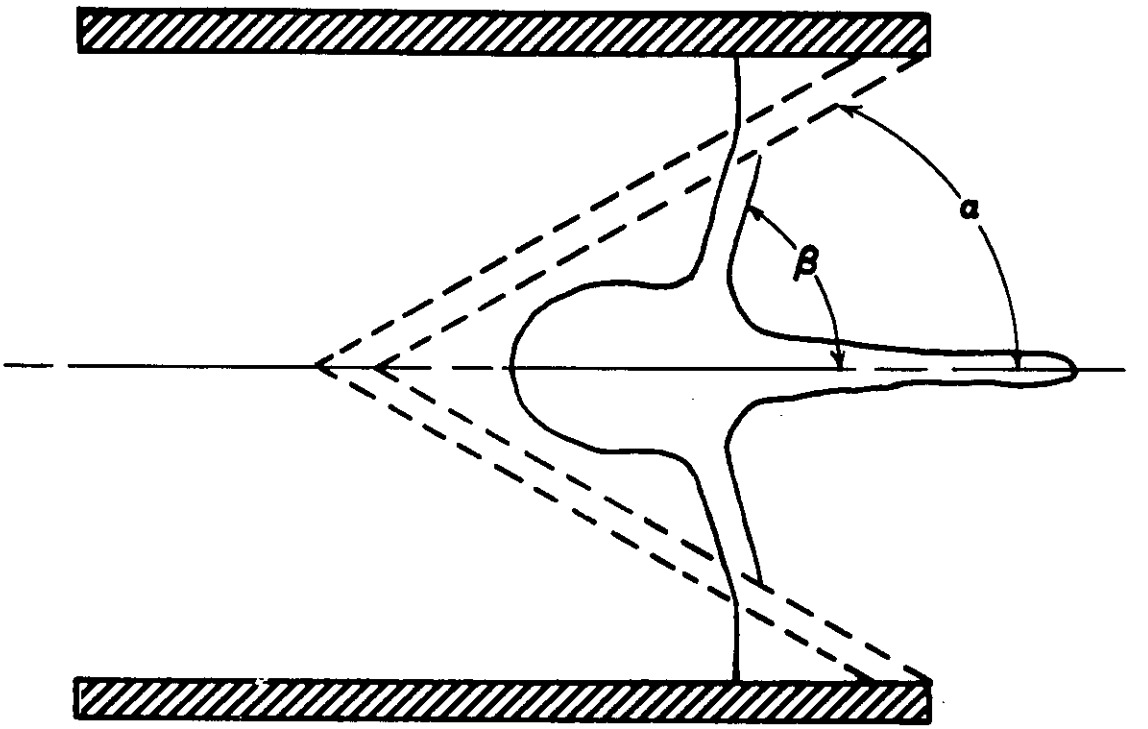

Figure 3. Schematic Collapse of a Typical Shaped-Charge.

V. APPLICATIONS

Shaped-charges are extremely useful when an intense, localized force is required for the purpose of piercing a barrier. The main application is in the military arena including torpedos, missiles, high explosive anti-tank (HEAT) rounds including hand held (bazooka type) rounds, gun launched (e.g., rifle grenades) cannon launched and various bombs. The targets are armors, bunkers, concrete or geological fortifications and vehicles. Attacks against aircraft and spacecraft are possible. Underwater applications (torpedos) are possible with the design such that water does not enter the hollow charge area. In fact, most warheads of the type described above contain an ogive to cover the liner. This ogive acts as an aerodynamic (or hydrodynamic) shield while the projectile is in flight, it can provide a housing for impact fuzes or guidance, stability and control electronics, and it provides a built-in standoff designed to improve performance. Figure 4 illustrates the concept of standoff distance and other nomenclature we will use. The standoff is the distance from the base of the charge (or liner) to the target in question. Figure 5, from Mohaupt [28] shows an old HEAT artillery projectile.

The largest shaped-charge application was known as the Beethoven Apparatus or Mistel (mistletoe) project [2,53]. The Mistel technique used a fighter aircraft mounted piggyback on the top of a large bomber aircraft. The unmanned bomber carried a large warhead in its nose. The warhead consisted of a 2 m (6 foot) diameter, wide angle, conical shaped-charge. The liner probably had a 120° apex angle, was about 30 mm thick, and made of either mild steel or aluminum. The warhead weighed 3500 kg (7700 lbs) and the explosive alone weighed 1720 kg (3800 lbs). The fighter pilot flew the combination to the target, aimed it, released it, then returned to his base. The Germans developed this device near the end of WW II and most of them were captured intact.

A shaped-charge with an aluminum liner was used in an attempt to place certain identifiable man-made materials into orbit. According to Kennedy [2], a 35° included angle aluminum shaped-charge was installed on a multistage rocket assembly. The craft was fired into near-space and the warhead was detonated in an attempt to project hypervelocity fragments into earth orbit. These tests were conducted at Holloman Air Force Base in 1955-56. It was never established whether or not any aluminum particles were detected.

Along the same line, a colleague of mine, S. K. Golaski of the Ballistic Research Laboratory and the old Firestone Tire and Rubber Company (now, a part of Physics International), developed shaped-charge meteor simulators for NASA [54,55]. The objectives of these studies were to obtain the luminous efficiency of a meteor like body of known mass, composition and speed during re-entry into the earth's atmosphere. The luminous efficiency is the percent of kinetic energy of the body which is converted into visible light as observed by photographic study of the visible re-entry tail. The study was designed to obtain the required mass, composition and speed from pellets generated by a specific shaped-charge design flown on a solid state propellant vehicle. The vehicle was used to achieve the necessary velocities. Nickel and iron were the shaped-charge liner materials. The rocket engines were designed to carry the shaped-charge liner above the atmosphere, turn, and

allow the detonated shaped-charge to accelerate at hyper-velocity through the earth's atmosphere (re-entry). The intent was to simulate a body (meteor) re-entering the earths' atmosphere. A specialized shaped-charge liner design was required along with a specialized bi-explosive waveshaping device [55].

Many other specialized shaped-charge applications have been pursued by the Departments of Defense of several nations. These specialized designs included confinement or tamping of the explosive fill, varying the geometry and material used for the confinement, varying the geometry or type of explosive used, altering the mode of initiation, using explosive lenses or more than one type of explosive or an explosive-non-explosive barrier or gap, waveshaping or shaping the detonation wave (usually done to insure a uniform wave with a short head height, see Figure 4 for definition of head height), or varying the standoff distance. Also, significant effects can be achieved by varying the liner material (including the use of non-metals such as glass), varying the liner thickness, varying the liner diameter, tapering (or causing a gradual wall thickness variation either continuously or discontinuously) or varying the liner geometry. The liner geometry variation may utilize the same basic geometry, e.g., varying the conical apex angle, or may employ a radically different liner configuration. Other useful liner geometries are hemispheres, truncated (from the equator) hemispheres, disc or dish shaped (SFF like) devices, tulips, trumpets, dual angle cones, or a combination of the above such as hemi-cones or tandem devices. In fact, any arcuate device may be used. Also, spin compensated liners may be used, especially when associated with spinning warhead applications. Spin compensation (i.e., causing the jet to spin enough to compensate for the spin of the warhead) may be achieved by metallurgical spin compensation or by the use of fluted liners (fluted liners contain raised ridges either on the outside or inside surface of the liner to allow the jet to form with a given angular momentum to compensate for the rotation of the warhead in flight). Without spin compensation, a jet formed from a spinning, detonated warhead will exhibit radial instabilities (if the rotation speed is high enough) and dispense radially, thus reducing the effective penetration capability. Spin and spin compensation will be covered in more detail in a later section.

A unique shaped-charge warhead design was developed by Kennedy and others in 1967 to 1970 as reported by Kennedy [2]. This particular missile design used a two-stage, tandem liner designed to produce a precursor or pre-jet to remove the guidance and control package located in the ogive of the missile. Otherwise, the main jet would have to penetrate the seeker package at a short (non-optimum) standoff distance. Alignment difficulties in the tandem configuration made it necessary to blend the precursor liner, its standoff tube and the main conical liner into a single piece. The result was the trumpet design configuration which is used today. This design showed improved penetration with a relatively small standard deviation in penetration.

There exists numerous other tales of warhead development, the point being that most of the warhead concepts being pursued today are not original concepts. Other warhead/liner designs will be discussed later.

Another application of shaped-charges is in demolition work. This area has both military and industrial application. Buildings, bridges and other structures are the common demolition targets. Usually demolition charges are

hand placed. Demolition charges are sometimes constructed and placed in sites using a plastic explosive and a collection of liners. This technique allows for more flexibility and adjustment to the conditions at hand than a collection of fixed charges. Of course, experience on the part of the blaster is required and this technique (the adjustment of the charge to the task) has delayed bulk charge production and research towards this particular application. The shaped-charge principle is also used in construction work to break, crack or drill holes in rock. A technique known as mudcapping is sometimes used to break rock and usually utilizes an unlined hollow charge. Shaped-charges are also used in construction as earth movers, in tunneling, or to assist in well drilling.

Hollow charges are also used as a source of earth waves for geophysical prospecting and seismic exploration. Other applications occur in mining (surface or underground), submarine blasting, timber cutting, breaking log jams, breaking ice jams and steel mill furnace tapping.

A jet tapper is a shaped-charge with a conical metal or glass liner. The steel mill furnance tapping problem is depicted in Figure 6 [37]. The tapping problem requires a means of starting the flow of molten steel once the tap hole has been plugged. Steel mill jet tapping is sometimes called salamander blasting since salamander is the term used to describe the large mass of iron deposited at the base of the blast furnance after it has been in operation for some time. The tap hole is dug out as far as possible and jet tapper is inserted into the tap hole using a loading pole. The jet tapper is then detonated, clearing the plug, usually with a high rate of success [37]. A commercial, DuPont type jet tapper is schematically illustrated in Figure 7. The shaped-charge assembly may be aligned on axis or offset up to 10^{o}, as shown in Figure 7, to reduce the line-of-sight thickness of the plug that must be perforated.

Another industrial application of the shaped-charge is in the internally coned end of certain detonators. This indented, lined cavity acts to concentrate the effect along the axis, recall Bloem [15].

Cook [56] used the original Munroe effect to engrave or stencil letters onto metal plates.

Other examples are in the oil well industry where large diameter, but extremely short, lined shaped-charges are used to penetrate various geological formations to increase the flow of oil. Oil well perforation problems present extremely difficult design problems due to the minimal amount of allowable space available in the well, the short standoff distances required and the hostile environment within the well [57].

Linear (wedge shaped, V-shaped or W-shaped) shaped-charges are also used as cutting charges. They generate a ribbon shaped jet used to cut metals and other materials. Commercial cutting charges are available from such places as Ensign-Bickford, Explosive Technology, DuPont and others. For cutting charge applications, it is sometimes advantageous to use homemade cutting charges which can be optimized to the particular problem on hand. Cutting charges and hollow charges are also used as explosive separation devices, as bolt cutters and for other applications. The shaped-charge effect is used on systems for

separation, deployment, safety destruct and similar spacecraft components. Garcia [58], Brown [59] and Sewell [60] provide additional data on the linear cutting charge concept. Leidel [61] presents a discussion of the design of a annular cutting charge.

An interesting paper by Jones [62], discusses the perforation of artic sea-ice by large, demolition type, shaped-charges. The following table was extracted from Reference [62] and illustrates the charge sizes used as well as the penetration depth achieved in various targets.

General references on application are found in Kennedy [2], Cook [5], The Blaster's Handbook [37], and Bawn and Rotter [63]. Certain specific applications of interest are found in Cook [56], on engraving; Torrey [64] on a review of shaped-charge weapons of WW II; Huttl [65] on underground blasting; Clark [66] on concrete fragmentation; Lawrence [67], and Austin, et al, [68,69,70] on boulder breaking, drilling and seismic exploration; Draper, et al, [71] on drilling; and Davidson and Westwater [72] on cratering and boulder breaking. Excellent overviews are available in Murphy [73] and Baum, et al. [74]. Extensive studies are currently underway in cratering (earth removal), boulder breaking, and penetration of concrete and geological formations at several installations, notably the Waterways Experimental Station, Vicksburg, Mississippi. The demolition and cratering work performed at the Waterways Experimental Station is too extensive to cover here, but their studies cover many of the applications cited earlier. See Joachim [75] as one example.

Additional applications relating to explosive metal interactions, and which require an understanding of the jet formation phenomena, are explosion welding, explosion calding, or explosion forming of metal parts. The principles of explosive welding are beyond the scope of this text. Basically, the technique involves using explosives to form bimetallic or trimetallic parts. A tremendous savings in material usage is thus possible because a thin layer, of an often costly material, can be applied to a cheaper, load bearing substrate. The thin noble and expensive material is usually used to provide an inert or corrosion resistance barrier to the substrate material. Applications occur in chemical vessels, heat exchanges, desalination plant piping and other areas where caustic environments exist. With explosive welding techniques even metallurgically incompatible metals and immiscible metal combinations can be bonded, as well as compatible metal systems. References [76, 77 and 78] provide an excellent introduction to the various aspects of explosion welding. Later a brief discussion of this important field will be provided.

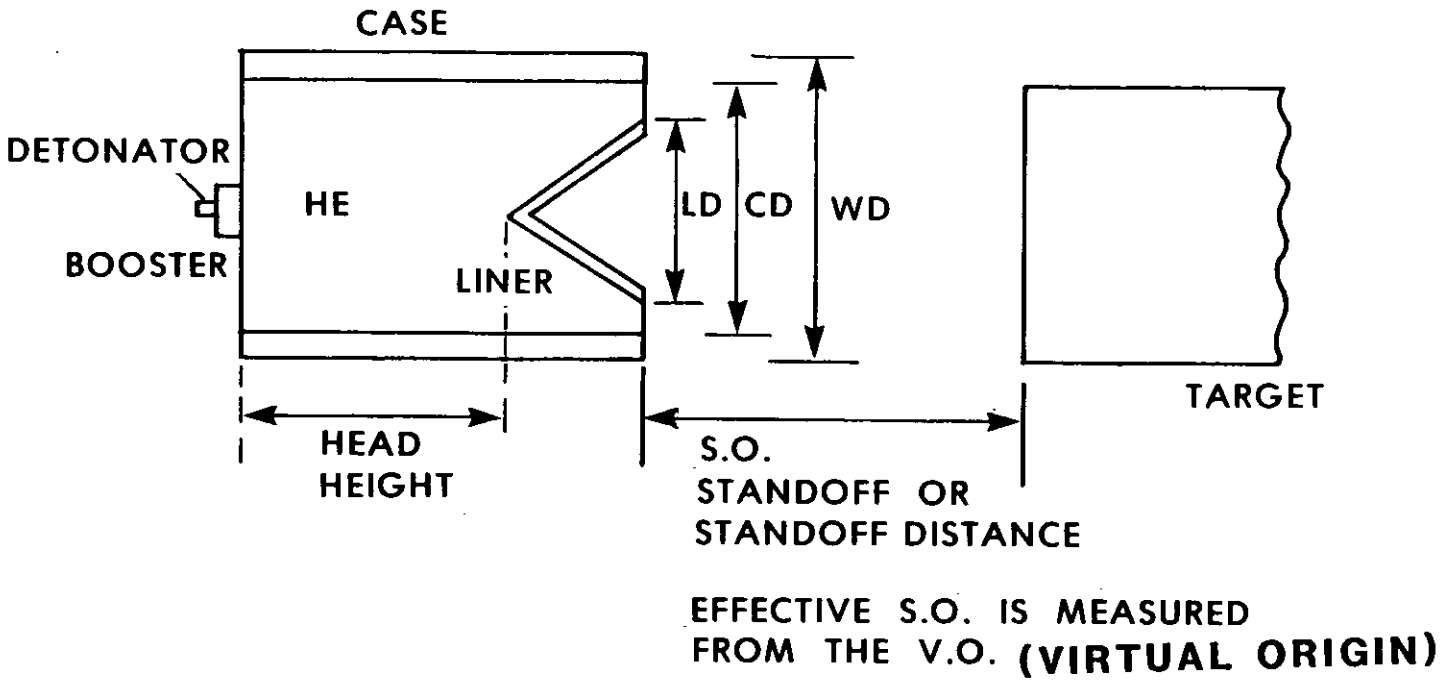

Figure 4. The Nomenclature.

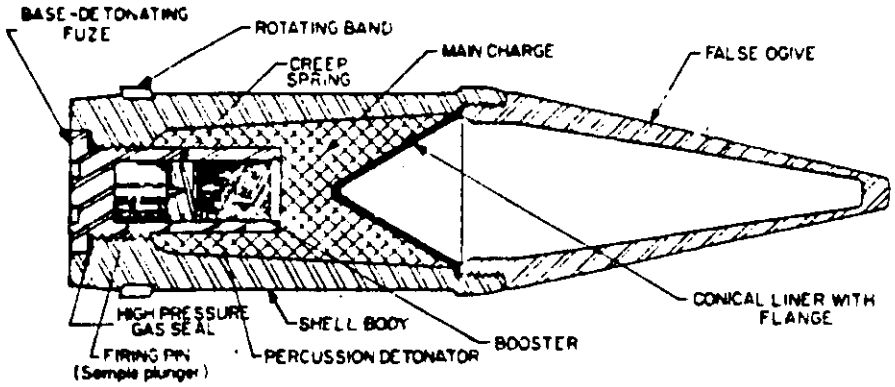

Figure 5a. High-Explosive Antitank Artillery Projectile, HEAT [28].

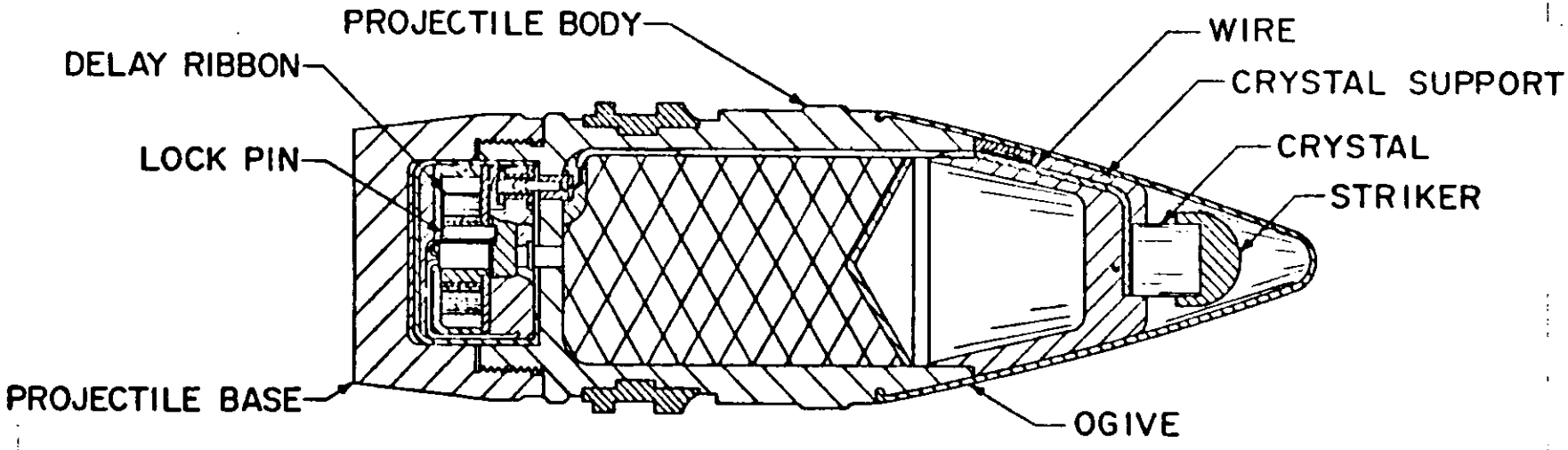

Figure 5b. HEAT (High Explosive Antitank) Projectile.

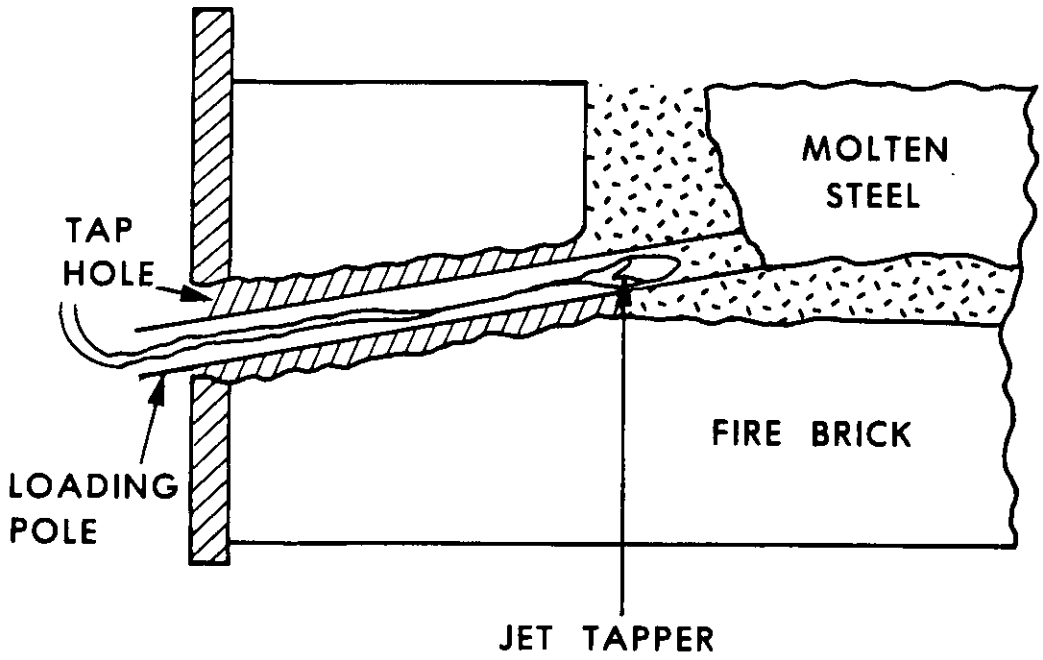

Figure 6. Steel Mill Furnace Tapping [37].

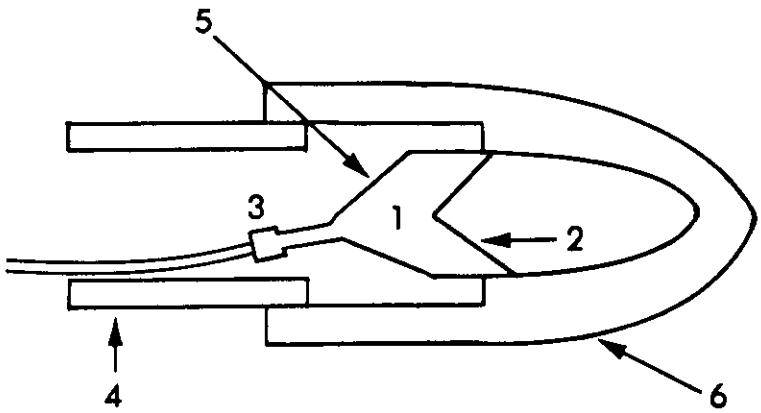

1. EXPLOSIVE
2. COPPER CONICAL LINER
3. ELECTRIC BLASTING CAP
4. LOADING POLE
5. PLASTIC CASE
6. INSULATING OGIVE

Figure 7. The Jet Tapper Charge (Offset) [37].

TABLE I.
FROM J. M JONES [62]

DESIGN AND PERFORMANCE DETAILS OF STANDARD DEMOLITION SHAPED CHARGES.

	No. 1, 6 in.	No. 11, 30 lb.	M2A3	M3
Total weight (lb.) approx.	10	50	15	40
Explosive weight (lb.)	6.7	27.5	11.5	30
Charge diameter (in.)	6.0	12	6.0	9.5
Charge length (in.)	7.5	11.75	9.44	15.5
Design Standoff (in.)	5.7	19.0	5.5	15.0
Casing material	steel	steel	fibre	steel
Cone diameter (in.)	6.0	12.0	4.88	9.0
Cone angle (deg.)	80	60	60	60
Cone material	steel	steel	glass	steel
Cone thickness (in.)	.140	.225	.350	.150
Cone weight (lb.)	-	-	1.7	5.6
Penetration				
Armour depth (in.)	6	-	12	20 +
Average diameter (in.)	-	-	1.5	2.5
Mild steel depth (in.)	9	-	-	-
Concrete depth (in.)	30	72	30	60
Entrance diameter (in.)	-	6 - 8	3.5	5
Minimum diameter (in.)	2	-	2	2
Fresh water ice depth (in.)	-	-	72	144
diameter (in.)	-	-	3.5	6
(standoff 42 in.)				
Permafrost depth (in.)	-	-	72 (30 in. standoff)	72 (50 in. standoff)
diameter (in.)	-	-	6 - 1.5	8 - 5
Crater diameter at design standoff (in.)	-	-	28	28

REFERENCES
(Sections I - V)

1. P. C. Chou and W. J. Flis, "Recent Developments in Shaped Charge Technology," Private correspondence, April 1984 (Manuscript prepared for M. Held, MBB, Germany, and presented at MBB Schrobenhausen, West Germany, September 1983).

2. D. R. Kennedy, "The History of the Shaped Charge Effect, The First 100 - Years," presented at MBB Schrobenhausen, West Germany, September 1983.

3. R. Eather and Neill Griffiths, "A U. K. Note on the History of Shaped Charges," Royal Armament Research and Development Establishment Report, August 1983, presented September 1983 at MBB, Germany.

4. Donald R. Kennedy, "The Infantryman VS the MBT," National Defense, ADPA, pp. 27-34, March 1985.

5. Melvin A. Cook, The Science of High Explosives, American Chemical Society Monograph Series, Reinhold Publishing Corp., NY, 1958.

6. Max von Foerster, "Versuche mit Komprimirter Schiessbaumwolle," 1883, Mittler and Son, Berlin.

7. Max von Foerster, "Experiments with Compressed Gun Cotton," Van Nostrand's Engineering Magazine, Vol. 31, July - December 1884, pp. 113-119.

8. Charles E. Munroe, "On Certain Phenomena Produced by the Detonation of Gun Cotton," Newport Natural History Society, Proceedings 1883-1888, Report No. 6, 1888.

9. Charles E. Munroe, "Wave-like Effects Produced by the Detonation of Gun Cotton," American Journal of Science, 36, 1888, pp. 48-50.

10. Charles E. Munroe, "Modern Explosives,'" Scribner's Magazine, Vol. 111, NY, January - June 1888, pp. 563-576.

11. C. E. Munroe, Executive Document No. 20, 53rd Congress, 1st Session, Washington, DC, 1894.

12. Charles E. Munroe, "The Applications of Explosives," Popular Science Monthly, in 2 parts pp. 300-455, Vol. 56, 1900.

13. "Verfahren zur Herstellung von Sprengkorpern," Westfolisch - Anhaltische Sprengstoffe A. G., patent DRP - Anmelding W 36269, December 14, 1910 in Zeitschrift fur das Gesamte Schiess und Sprengstoffwesen, 6, 1911, Pg. 358, 1910/1911.

14. "Improvement in Explosive Charges or Bodies," Patent No. 28,030 (UK) to Westfolisch - Anhaltische Sprengstoff Actien Gesellschsft (WASAG), Berlin, 12 December 1911.

15. Gustav Bloem of Dusseldorf, Prussia, Germany, "Shell for Detonating Caps," U.S. patent 342, 423 dated May 25, 1886.

16. LT H. W. Kline, "The Cavity Charge, Its Theory and Applications to the Opening of Explosive Filled Ordnance, etc.," U.S.N.R., Ordnance Investigation Laboratory, Naval Powder Factory, Indian Head, Maryland, 15 August 1945.

17. Sucharewski, Technica i Snabschenie Krasnoi Armii, 1925, No. 170, pp. 13-18, also Woina i Technica, 192, No. 253, pp. 18-24.

18. C. Lodati, "An Explanation of the Explosive Behavior of Hollow Blocks of Compressed TNT," Giornale di Chim. ind. ed. appl., Vol. 14, 1932, pp. 130.

19. Charles P. Watson for "Percussion Fuzes," 1925 U.S. Patents 1, 524, 011 and 1, 534, 012 filed 22 September 1921 and 27 August 1923, both issued on 14 April 1925.

20. R. W. Wood, "Optical and Physical Effects of High Explosives," Proceedings of the Royal Society (London), Vol. 157A, 1936, pp. 249-261.

21. Heinz Freiwald, "The History of Hollow Charge Effect of High Explosive Charges," with forward by Hubert Schardin, for German Academy of Aviation Research, 15 September 1941.

22. "High Explosive Charge," Hungarian Patent 134378 assigned to Engineers Carl Brandmayer and Franz Rudolf Thomanek, Berlin, December 9, 1943.

23. Hubert Schardin, "Development of the Shaped Charge," published in Wehrtechnische Hefte, Heft 4, 1954.

24. Franz Rudolf Thomanek, "Meine Hohlladungs - Aktivitaten," for Periods 1932-1935, 1938-1945, 1957-1969 and from 1975 to date, 10 March 1978.

25. "An Improved Explosive Projectile," Patent, Commonwealth of Australia, assigned to Berthold Mohaupt, Henry Mohaupt and Erick Kauders of France, August 1941 (date claimed for patent 9 November 1939).

26. "Projectile," U.S. Patent No. 2,419,414 assigned to Henry H. Mohaupt, April 22, 1947 originally filed October 3, 1941.

27. "Projectile," U.S. Patent No. 2,974,595 assigned to Henry H. Mohaupt, 1961, filed September 11, 1947.

28. Aerospace Ordnance Handbook, edited by F. Pollard and J. Arnold, Chapt. 11, "Shaped Charges and Warheads," H. Mohaupt, Prentice-Hall, Inc., NJ, 1966.

29. H. Kolsky, C. I. Snow and A. C. Shearman, "A Study of the Mechanism of Munroe Charges, Part I - Charges with Conical Liners," Research Supplement, 2-2, pp. 89-95, London, 1949.

30. H. Kolsky, "A Study of the Mechanism of Munroe Charges, Part II - Charges with Hemispherical Liners," Research Supplement, 2-2, pp. 96-98, London, 1949.

31. W. M. Evans and A. R. Ubbelohde, "Formation of Munroe Jets and Their Action on Massive Targets," Research Supplement, 3-7, London, 1950.

32. W. M. Evans and A. R. Ubbelohde, "Some Kinematic Properties of Munroe Jets," Research Supplement, 3-8, London, May 1950.

33. E. M. Pugh, R. V. Heine-Geldern, S. Foner and E. C. Mutschler, "Kerr Cell Photography of High Speed Phenomena," J. of Appl. Phys., Vol. 22, No. 4, April 1951, pp. 487-493.

34. W. S. Koski, F. A. Lucy, R. G. Shreffler and F. J. Willig, "Fast Jets From Collapsing Cylinders," J. of Appl. Phys., Vol. 23, No. 12, December 1952, pp. 1300-1305.

35. Franz R. Thomanek, "Die Erste Hohlladungswaffe - The First Hollow Charge Weapon," Explosivstoffe, No. 1, 1959, pp. 9-11.

36. Franz R. Thomanek, "Die Entwicklung der Ausgekleiden Hohlladung - The Development of the Lined Hollow Charge," Explosivstoffe, No. 8, 1960, pp. 177-179.

37. The Blaster's Handbook, E. I. du Pont de Nemours and Co., Wilmington, DE, 16th Edition, 1980.

38. G. Birkhoff, D. MacDougall, E. Pugh, G. Taylor, "Explosive with Lined Cavities," J. of Appl. Physics, Vol. 19, No. 6, June 1948.

39. E. Pugh, R. Eichelberger and N. Rostoker, "Theory of Jet Formation by Charges with Lined Conical Cavities," J. of Appl. Physics, Vol. 23, No. 5, May 1952.

40. W. M. Evans, "The Hollow Charge Effect," Bulletin of the Institution of Mining and Metallurgy, No. 520, March 1950.

41. Joseph E. Backofen, "The Weaponization of Shaped Charge Technology," Proceedings of the 4th International Symposium on Ballistics, 17-19 October 1978.

42. J. E. Backofen, "Shaped Charges Versus Armor," Armor, July-August 1980.

43. J. E. Backofen, "Shaped Charges Versus Armor - Part II," Armor, September - October 1980.

44. J. E. Backofen, "Shaped Charges Versus Armor - Part III," Armor, November - December 1980.

45. J. E. Backofen and L. W. Williams, "Antitank Mines," Armor, July - August 1981.

46. J. E. Backofen and L. W. Williams, "Antitank Mines - Part II," Armor, September - October 1981.

47. J. E. Backofen and L. W. Williams, "Antitank Mines - Part III," Armor, November - December 1981.

48. "Annotated Bibliography of NDRC Technical Reports and Memorandums of Division 2, including pertinent division 8 Reports," May 1, 1945, NRDC (National Defense Research Council) Memorandum No. A-106M, OSRD Report No. 4830B.

49. Hill, Mott and Pack, A.R.D. Theoretical Research Report No. 2/44 (January 1944) and 13/44 (March 1944).

50. "Protection Against Shaped Charges," Carnegie Institute of Technology, NDRC Report No. A-384 and OSRD Report No. 6384, February 1946.

51. Marvin E. Backman, "Terminal Ballistics," Naval Weapons Center Technical Publication 5780, China Lake, CA, February 1976.

52. A. M. Worthington, A Study of Splashes, Longmans Green, London, 1908.

53. R. Coles and P. L. Rickson, "Mistletoe - The Deadly Parasite," Air Classics Quarterly Review, Vol. 4, No. 3, pp. 38-47, 86-99, Fall 1977.

54. "Development and Testing of Advanced Shaped Charge Meteoritic Simulators Part II - Calibration of Flight Guns," R. L. Woodall and E. L. Clark, Firestone Tire and Rubber Company, NASA CR-66216, November 1966.

55. "Design, Development and Testing of Bi-Explosive Shaped Charge Meteoritic Simulators," The Firestone Tire and Rubber Company, NASA CR-66615, April 1968.

56. M. Cook, Research, 1948, 1, pp. 474.

57. J. S. Reinhart and R. D. Cocanower, "Concerning the Design of an Effective Shaped Charge for Oil Well Perforating," J. Appl. Phys., Vol. 30, pp. 680- 682, May 1959.

58. M. A. Garcia, "The End-Initiated, Linear Shaped Charge: An Analytical Model," Naval Missile Center, TM-67-64, December 1967.

59. G. E. Brown, "A New Optimization Theory for the End-Initiated Linear Shaped Charge," M. S. Thesis, Naval Postgraduate School, October 1969.

60. Robert G. S. Sewell, "Effects of Velocity and Material Properties on Design Limits for Linear Shaped Charges," NOTS Technical Publication 3894 and NAVWEPS Report 8793, August 1965.

61. David J. Leidel, "A Design Study of an Annular - Jet Charge for Explosive Cutting," Doctoral Dissertation, Drexel University, Philadelphia, PA, June 1978.

62. J. M. Jones, "The Design of a Large Shaped Charge Suitable for the Perforation of Artic Sea-Ice," Defense Research Establishment, Valcartier Report, DREV TN-1907/71, PROJ D97-01-19, May 1971, (AD 913074).

63. Science of Explosives, edited by C. E. H. Bawn and G. Rotter, Part I, Ministry of Supply, London, 1956, (AD 127695).

64. Torrey, Explosives Engineer, 1945, 23, p. 160.

65. Huttl, Eng. Min. Jour., 1947, 147, p. 58.

66. Clark, Amer. Inst. Min. Met. Eng., Tech. Pubs. 2157, 2158, 1947.

67. Lawrence, Explosives Engineer, 1947, 25, p. 171.

68. C. F. Austin, "Lined Cavity Shaped Charges and Their Use in Rock and Earth Materials," Bulletin 59, New Mexico Inst. Min. and Tech., State Bureau of Mines and Mineral Research, 1959.

69. C. F. Austin and J. K. Pringle, "Detailed Response of Some Rock Targets to Jets from Lined Cavity Charges," J. Petroleum Tech., January 1964.

70. C. F. Austin, "Lined Cavity Shaped Charge and Its Use as a Drilling Tool," Trans. AIME, Vol. 220, p. 123, 1961.

71. Draper, Hill and Agnew, U.S. Bur. of Min., R.I., 4371, 1948.

72. Davidson and Westwater, Mine and Quarry Eng., May 1949.

73. Michael J. Murphy, "Shaped Charge Penetration in Concrete: a Unified Approach," Doctor of Engineering Dissertation, University of California - Davis, January 1983, also Lawrence Livermore National Laboratory Report UCRL-53393, 1983.

74. F. A. Bawn, R. P. Stanykovich, and B. I. Skekter, Physics of an Explosion, (AD 400151), New York, Research Information Service, 546, 1949.

75. Charles E. Joachim, "Application of Shaped Charges to Rapid Atomic Demolition Munition (ADM) Emplacement," U.S. Army Engineer Waterways Experimental Station Miscellaneous Paper SL-83-20, December 1983.

76. "Explosive Welding" Mechanical Engineering, May 1978.

77. John S. Rinehart and John Pearson, Explosive Working of Metals, Macmillan Company, NY, 1963.

78. T. Z. Blazynski, (editor), Explosive Welding, Forming and Compaction, Applied Science Publishers, NY, 1983.

VI. The Generalized Equations

The general conservation equations of mass, momentum and energy may be expressed as

$$\frac{\partial \rho}{\partial t} = - \frac{\partial}{\partial x_i} (\rho u_i) \quad ,$$

$$\rho \frac{Du_j}{Dt} = \frac{\partial}{\partial x_i} (\sigma_{ij}) \quad ,$$

and

$$\rho \frac{DE_T}{Dt} = \frac{\partial}{\partial x_i} (\sigma_{ij} u_j) \quad ,$$

where

$$\sigma_{ij} = S_{ij} - \delta_{ij} P, \text{ or}$$

the stress tensor equals the stress deviator tensor plus the hydrostatic stress. Also,

$$E_T = 1/2 \ (u_i \ u_i) + E_I \quad \text{or}$$

the total energy equals the kinetic energy plus the internal energy.

The substantial derivative, $\frac{D}{Dt}$,represents

$$\frac{D}{Dt} = \frac{\partial}{\partial t} + u_i \frac{\partial}{\partial x_i} \quad .$$

Thermal energy terms do not appear in the energy equation since for the micro-second time scale involved, there is no time to radiate or conduct heat.

These equations constitute the basis of the hydrocodes. We need to relate the stress tensor to hydrostatic pressures and/or strains and strain rates. Then the strains and/or strain rates must be related to the velocities and/or the velocity gradients. The equations required for this step are known as the constitutive relationships which are intended to convert the stress tensor to a pressure and velocities and material properties (e.g., viscosity, shear modulus, etc.). These material properties are hopefully known, or expressible in terms of known quantities.

Next, it is necessary to specify the appropriate initial and boundary conditions for the partial differential equations. It is also necessary to establish explosive burn routines and provide algorithms to couple the burn routine to the liner, for example, or to couple two complete sets of conservation equations such as for a penetrator and a target. Finally, a numerical solution technique and a stability criterion are required. This is obviously a complex procedure, but satisfactory results have been obtained from several available hydrocodes. Note that accurate metal and explosive

equations of state and accurate constitutive equations and associated material properties are prerequisite to a good solution. Assuming this information is available, a few limiting assumptions will be made. First, the following equations are available for, say, the behavior of a metal undergoing explosive loading. A method to treat the explosive is assumed.

Equation Description	Number of Equations	Unknowns
Continuity	1	4 - ρ, u_i $i = 1, 2, 3$
Momentum	1 for each spatial direction	5 - ρ, u_i, P $i = 1, 2, 3$
Energy	1	5 - ρ, u_i, E_I $i = 1, 2, 3$
Equation of State	1	3 - ρ, P, E_I

Thus, for a general, three dimensional problem there are six equations: 1 continuity, 3 momentum, 1 energy and 1 equation of state. There are also six unknowns: 3 velocity components, the density, pressure and internal energy. Various simplifying assumptions change the situation as shown below:

Case	Equations	Unknowns
3-D	6	6 (ρ, P, E_I, u_i) $i = 1, 2, 3$
2-D (axisymmetric)	5 (one less momentum equation)	5 (ρ, P, E_I, u_i) $i = 1, 2$
Incompressible, 2-D	3 (continuity and 2 momentum equations; ρ = constant)	3 (P, u_i) $i = 1, 2$
Incompressible, 2-D, steady-state	3 (continuity and 2 momentum equations; ρ = constant)	3 (P, u_i) $i = 1, 2$ No initial conditions required, one less independent variable.

The axisymmetric case is the most commonly used, since this is usually a valid assumption for explosive-metal interactions. Note that a tremendous simplification is possible for an incompressible flow assumption. However, an incompressible flow implies a low Mach number flow and the complete absence of shock physics. This, of course, is not realistic. It may, though, provide approximate answers as will be seen.

Equation Description	Number of Equations	Unknowns
Continuity	1	4 : ρ, u_i $i = 1, 2, 3$
Momentum	1 for each spatial coordinate	5: ρ, u_i, P $i = 1, 2, 3$ Add P
Energy	1	5 : ρ, u_i, E_I $i = 1, 2, 3$ Add E_I
Equation of State	1	3 : ρ, P, E_I Close System

The point to be made here is that the generalized explosive-metal interaction is extremely complex. The governing equations are complicated; sufficient boundary and initial conditions must be specified; the constitutive relationships and material properties under the intense dynamic conditions encountered are not well known; equations of state must be accurately specified; and numerical algorithms and solution techniques must be accurately developed.

Next, further simplications will be presented which lead to analytical models for the collapse of the shaped-charge liner. The next section starts with the one-dimensional hydrodynamic equation, i.e., the Bernoulli equation.

Case	Equations	Unknowns	
3-D	6	6 (ρ, P, E_I, u_i) $i = 1, 2, 3$	
2-D (axisymmetric)	5	5 (ρ, P, E_I, u_i) $i = 1, 2$	Need 1 less momentum equation.
Incompressible, 2-D	3 Continuity & 2 momentum.	3 (P, u_i) $i = 1, 2$	ρ = constant. No energy or EOS needed.
Incompressible, 2-D, steady-state	3 As Above	3 As Above	No initial conditions required, one less independent variable.

DEFINITION OF TERMS

x_i - spatial coordinate

t - time

ρ - density

u_i - velocity components

σ_{ij} - stress tensor

S_{ij} - stress deviator

δ_{ij} - Kronecker delta

P - pressure

E_T - total energy

E_I - internal energy

VII. The Bernoulli Concept

One of the most basic equations in shaped-charge jet collapse (and in jet penetration) is Bernoulli's equation. Due to the repeated application of this equation, and in order to clearly understand the assumptions inherent in Bernoulli's (and modified Bernoulli's) equation, it will be derived using several methods. The intent here is not to prove "Theorems" or even to introduce rigor in our methods, but to establish assumptions inherent to Bernoulli's and similar equations.

1. The Energy Equation

Define a portion of fluid between sections (1) and (2) as shown below,

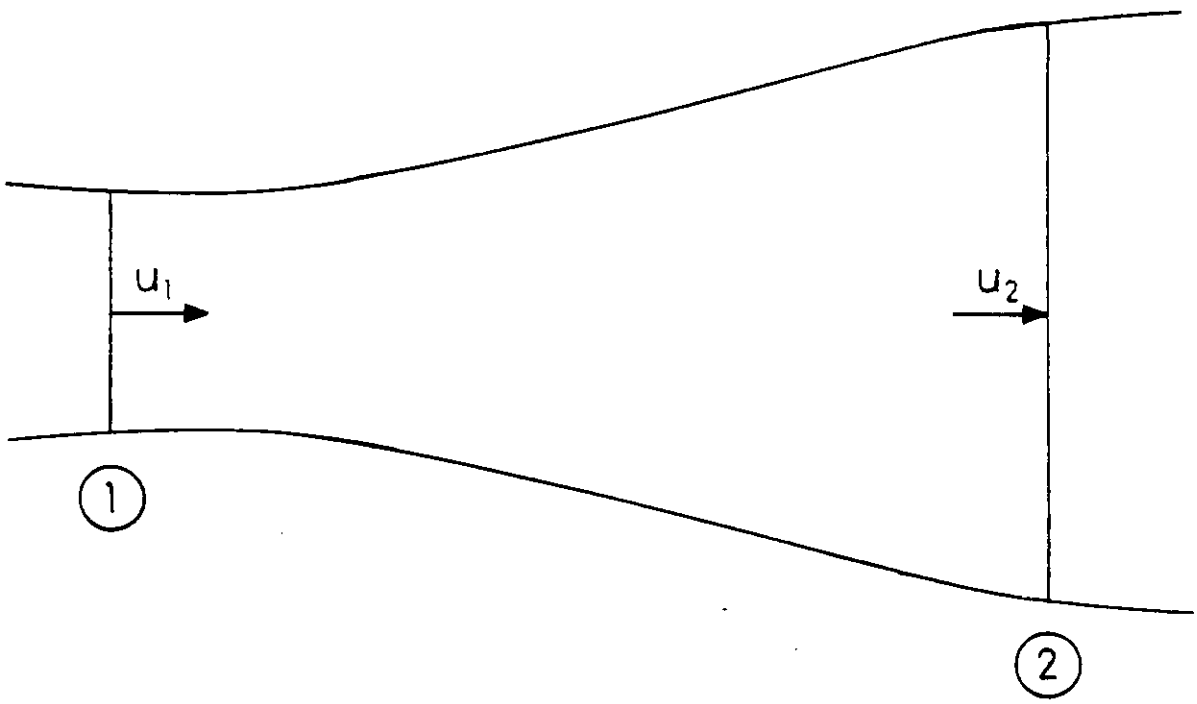

u being the velocity. We assume one dimensional (1-D) flow and follow standard fluid texts such as Liepmann and Roshko [1].

This fluid portion can be considered to be bounded by pistons at (1) and (2) instead of a fluid. These pistons are equivalent to the fluid they replace, and help to clarify the work done on the system which consists of a definite mass of fluid.

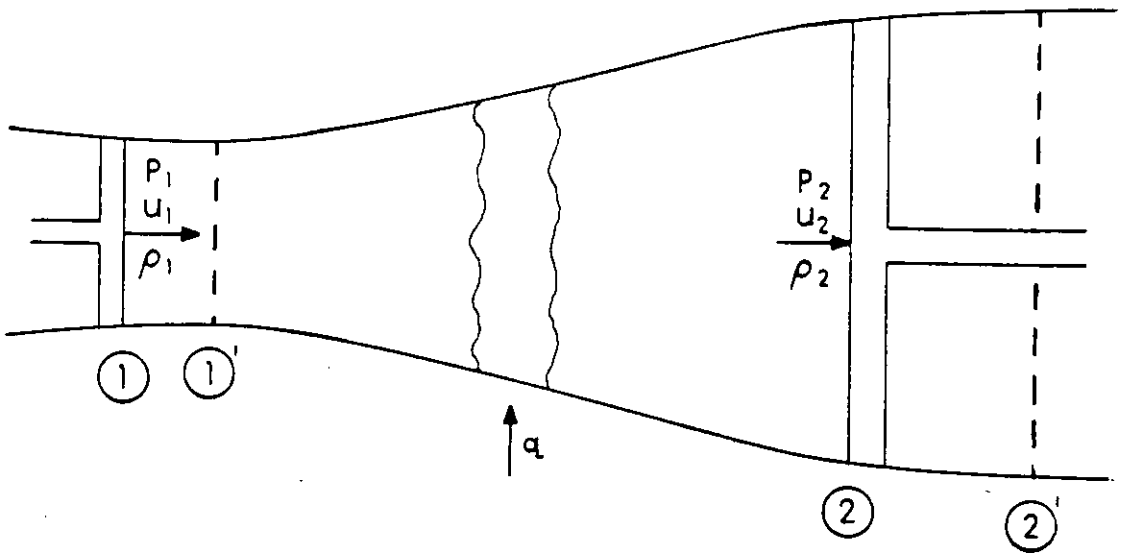

During the small time interval in which the fluid is displaced to the position (1)' - (2)', a quantity of heat q may be added, (as external heat).

Tne energy law yields,

q + work done = increase in energy,

and interpret the work done and the change (increase) in energy as;
Work done: The volume displaced at (1) is the specific volume (per a unit mass) v_1. For <u>steady flow</u> the displacement at (2) is also a unit mass, or specific volume, v_2. The work done by the pistons during this displacement is

$$P_1 v_1 - P_2 v_2 \quad ,$$

<u>neglecting any external work</u> between (1) and (2).

Change in energy: The flowing fluid has internal energy e and kinetic energy $1/2\ u^2$, per unit mass. After the displacement, there has been an increase of energy, $e_2 + 1/2\ u_2^2$ corresponding to the displacement between (2) and (2)' and a decrease of energy, $e_1 + 1/2\ u_1^2$ from (1) to (1)'.

Therefore, increase of energy = $(e_2 + 1/2\ u_2^2) - (e_1 + 1/2\ u_1^2)$.

For steady flow, the energy equation becomes

$$q + P_1 v_1 - P_2 v_2 = e_2 - e_1 + 1/2\ (u_2^2 - u_1^2)$$

or for q = o, the <u>adiabatic</u> energy equation yields

$$P_1 v_1 + e_1 + 1/2\ u_1^2 = P_2 v_2 + e_2 + 1/2\ u_2^2 \quad .$$

This equation relates conditions at two equilibrium states (1) and (2) of the flow. They are valid even if viscous stresses, heat transfer, or any nonequilibrium conditions exist between (1) and (2). However, (1) and (2) themselves must be equilibrium states.

If equilibrium exists all along the flow (at every station), the equilibrium condition is valid continuously and

$$P\,v + e + 1/2\,u^2 = \text{Const.}$$

Further, if the internal energy does not vary,

$$e_1 = e_2 = e_i \ .$$

Then

$$P\,v + 1/2\,u^2 = \text{const.},$$

and if the density is constant $\left(v = \frac{1}{\rho}\right)$,

$$P + 1/2\,\rho\,u^2 = \text{const.},$$

which is Bernoulli's equation derived from thermodynamic and conservation of energy considerations.

2. Euler's Equation

Now apply Newton's law to a flowing fluid, where

$$F = ma \ .$$

Now view the flow in an Eulerian sense, i.e., observe the flow of a fluid particle as it encounters the various conditions in the tube through which it accelerates.

The acceleration is in two parts:

Since conditions vary along the tube, there is a velocity gradient in the direction of the flow, $\frac{\partial u}{\partial x}$. The rate of change of velocity is proportional to this gradient and the speed at which a particle moves through it. Thus, the acceleration due to convection through the velocity gradient is

$$u\,\frac{\partial u}{\partial x} \ .$$

Also, conditions at a given station may be changing due to nonsteady (nonstationary) effects or

$$\frac{\partial u}{\partial t} \ .$$

Then,

$$a_x = \frac{\partial u}{\partial t} + u \frac{\partial u}{\partial x} \quad .$$

Next, it is necessary to determine the force on a fluid element as shown below:

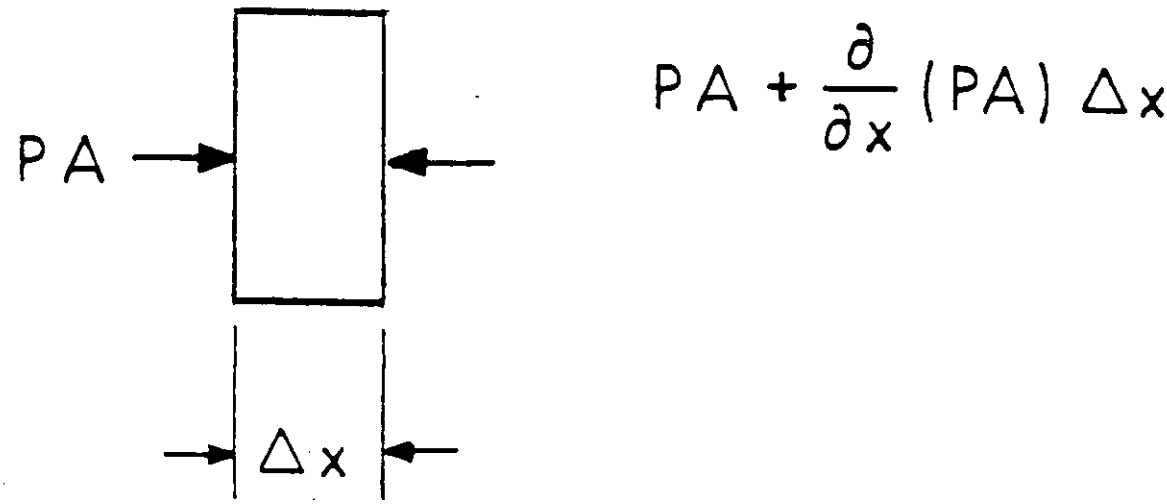

The force $-\frac{\partial P}{\partial x}$ (Δx A), and dividing by the volume of the element, AΔx, and dividing through by the density ρ gives the force per unit mass or

$$F_x = -\frac{1}{\rho}\frac{\partial P}{\partial x} \quad .$$

This result is valid for a particle (element) or any shape,

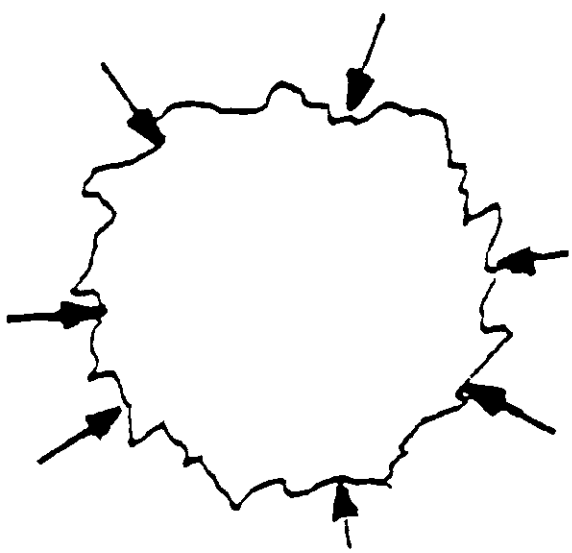

converging, diverging or whatever. The proof is standard (e.g., [1]) using Gauss's law. Note that the force term neglects all viscous terms. Then,

$$\frac{\partial u}{\partial t} + u \frac{\partial u}{\partial x} = - \frac{1}{\rho} \frac{dp}{dx} \quad ,$$

which is Euler's equation.

For steady flow, $u \frac{du}{dx} + \frac{1}{\rho} dp = 0$, since $u = u(x)$, $P = P(x)$, and for 1-D, steady flow.

For incompressible flow, $(\rho = \rho_o)$ and

$$\rho_o \frac{u^2}{2} + p = \text{const.},$$

which is the classic derivation of Bernoulli's equation. Now consider the momentum equation and the flow through a control surface, where

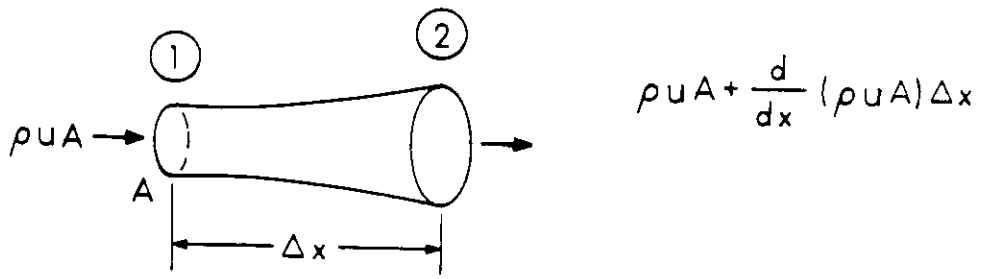

$$\rho A \frac{\partial u}{\partial t} + \rho u A \frac{\partial u}{\partial x} = - A \frac{\partial P}{\partial x} \quad \text{(Euler's equation x } \rho A)$$

and

$$u \frac{\partial}{\partial t} (\rho A) + u \frac{\partial}{\partial x} (\rho u A) = 0. \quad \text{(continuity equation x } u)$$

Adding these equations and with algebraic manipulation, we have

$$\frac{\partial}{\partial t} (\rho u A) + \frac{\partial}{\partial x} (\rho u^2 A) = - A \frac{\partial P}{\partial x} = - \frac{\partial}{\partial x} (PA) + P \frac{\partial A}{\partial x} \quad ,$$

for 1-D flow.

Integrating between any two stations (1) and (2), yields

$$\frac{\partial}{\partial t} \int_1^2 (\rho u A)\, dx = \rho_2 u_2^2 A_2 - \rho_1 u_1^2 A_1 = \rho_1 A_1 - P_2 A_2 + \int_1^2 P\, dA \quad , \text{ and}$$

$$\int_1^2 P da = P_m (A_2 - A_1), \text{ defining a mean pressure } P_m.$$

The integral momentum equation is very general in that it is valid even when there are frictional forces and dissipation regions inside the control volume, provided they are absent at the reference stations 1 and 2. The integration of the differential momentum equation corresponds to a summation of the forces on adjacent fluid elements, and of the flow into them:

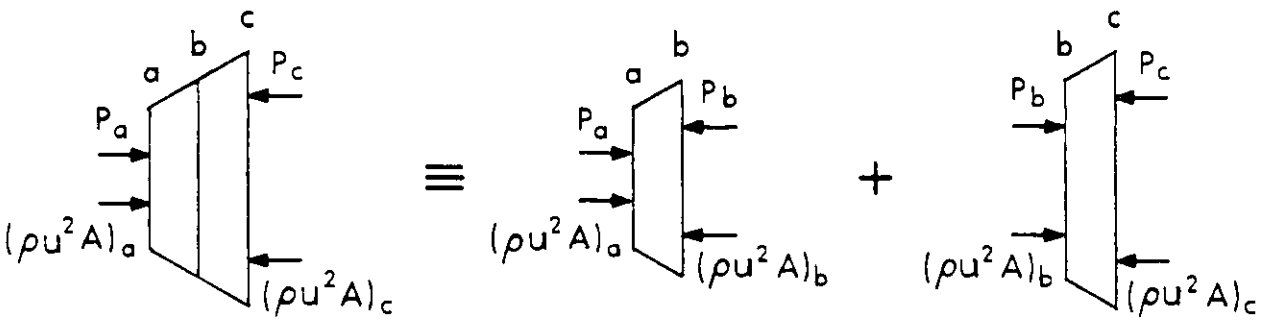

The forces on adjacent internal faces are equal and opposite, and thus cancel. Similarly, the inflows and outflows through adjacent faces cancel, leaving only the force and flux at the control space boundaries. If there is a non-equilibrium region inside the control space, it does not effect the integral result.

For steady flow in a constant area duct ($A_1 = A_2$),

$$\rho_2 u_2^2 + P_2 = P_1 + \rho_1 u_1^2$$

which, sans the factor of 1/2, is similar to Bernoulli's equation.

Harlow and Pracht [2] commented on the momentum conservation and the Bernoulli principle when considering jet penetration. They observed that the conservation of momentum principle, assuming the jet and target to be of the same width, was nearly the same equation as derived from the Bernoulli principle where the target is effectively infinite in width.

3. Euler's Equation Extended

Euler's equation can be found in any standard text, e.g., Shapiro [3]. Euler's Equations of motion in 3-D cartesian coordinates (as derived above for a 1-D case) are in general:

$$-\frac{1}{\rho}\frac{\partial P}{\partial x} = \frac{\partial u}{\partial t} + u\frac{\partial u}{\partial x} + v\frac{\partial u}{\partial y} + w\frac{\partial u}{\partial z} = \frac{Du}{Dt}\quad , \tag{1}$$

$$-\frac{1}{\rho}\frac{\partial P}{\partial y} = \frac{\partial v}{\partial t} + u\frac{\partial v}{\partial x} + v\frac{\partial v}{\partial y} + w\frac{\partial v}{\partial z} = \frac{Dv}{Dt}\quad , \tag{2}$$

and

$$-\frac{1}{\rho}\frac{\partial P}{\partial z} = \frac{\partial w}{\partial t} + u\frac{\partial w}{\partial x} + v\frac{\partial w}{\partial y} + w\frac{\partial w}{\partial z} = \frac{DW}{Dt} \quad . \tag{3}$$

Consider 2 cases:

1. Integration along a streamline (steady flow) [3]. A streamline is defined by the condition that at each instant the velocity vector is tangent to the streamline. Thus,

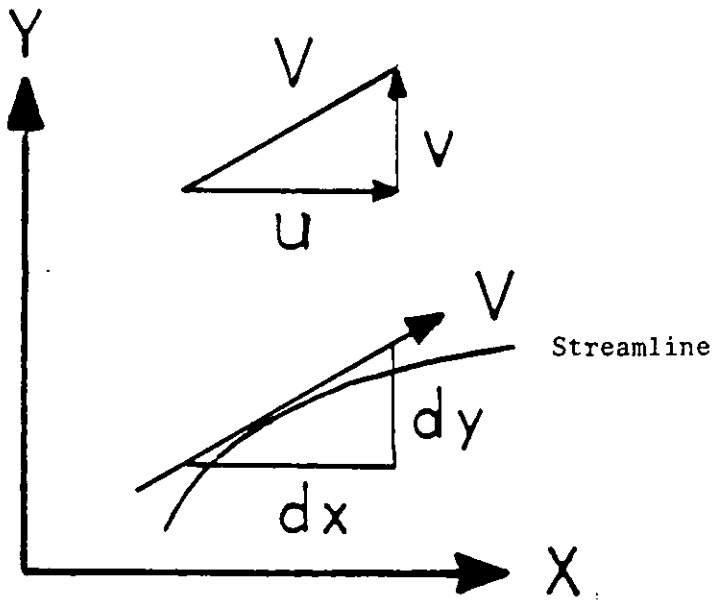

$$\frac{dy}{dx} = \frac{v}{u} \; , \; \frac{dz}{dy} = \frac{w}{v}$$

$$\text{and } \frac{dx}{dz} = \frac{u}{w}$$

Now multiply equation (1) by dx, equation (2) by dy and equation (3) by dz, assume steady flow ($\frac{\partial}{\partial t} = 0$) and for a particular streamline (using equations (4),

$$-\frac{1}{\rho}\frac{\partial P}{\partial x}\,dx = u\frac{\partial u}{\partial x}\,dx + v\frac{\partial u}{\partial y}\,dx + w\frac{\partial u}{\partial z}\,dx \quad ,$$

from equation (1), and similiar expressions result from equations (2) and (3). Then, adding the resulting equations and noting that

$$dP = \frac{\partial P}{\partial x}\,dx + \frac{\partial P}{\partial y}\,dy + \frac{\partial P}{\partial z}\,dz,$$

and

$$du = \frac{\partial u}{\partial x}\,dx + \frac{\partial u}{\partial y}\,dy + \frac{\partial u}{\partial z}\,dz, \text{ etc}$$

yields,

$$-\frac{1}{\rho}\,dP = udu + vdv + wdw = d\left(\frac{u^2 + v^2 + w^2}{2}\right) = d\,\frac{V^2}{2}$$

V being the resultant velocity.

Thus,

$dP = -V\,dV$ and for incompressible flow,

$P + \rho\frac{V^2}{2}$ = constant along a streamline = Bernoulli constant of the streamline.

This equation is only valid from point to point on a given streamline. Thus, the Bernoulli constant may vary from one streamline to another. Of course, if all the streamlines originate in a uniform flow region, the same Bernoulli constant would prevail over the entire flow field.

2. Integration for Steady, Irrotational flow [3]. We abandon the restriction that only points along the same streamline are considered and assume only irrotational, steady flow. This means,

$$\frac{\partial v}{\partial x} - \frac{\partial u}{\partial y} = 0 \quad ,$$

$$\frac{\partial w}{\partial y} - \frac{\partial v}{\partial z} = 0 \quad , \text{ and}$$

$$\frac{\partial u}{\partial z} - \frac{\partial w}{\partial x} = 0 \quad .$$

Now, multiple equation (1) by dx, equation (2) by dy, and equation (3) by dz and use the irrotationality assumption, which yields

$$-\frac{1}{\rho}\frac{\partial P}{\partial x}\,dx = u\frac{\partial u}{\partial x}\,dx + v\frac{\partial u}{\partial y}\,dx + w\frac{\partial u}{\partial z}\,dx = u\frac{\partial u}{\partial x}\,dx + v\frac{\partial v}{\partial x}\,dx + w\frac{\partial w}{\partial x}\,dx \quad ,$$

etc., and adding the equations,

$$\frac{\partial}{\partial x}\left(\frac{u^2 + v^2 + w^2}{2}\right) = \frac{\partial}{\partial x}\left(\frac{V^2}{2}\right) \quad ,$$

etc., and finally

$$-\frac{1}{\rho}\,dp = d\left(\frac{V^2}{2}\right)$$

which is identical to the Bernoulli equation obtained before. Thus, for steady, continuous, frictionless and irrotational flow the Bernoulli constant is the same for all streamlines and relates any two points in the flow field.

The constant has a particular value for each streamline except for irrotational flow in which case thc constant is the same for all streamlines.

4. Navier-Stokes Equation

We begin by investigating the derivation of the Navier-Stokes equations following, e.g., Schlichting [4].

These equations represent the equations of motion of a compressible, viscous, Newtonian fluid in three dimensional flow. The flow field will be specified by the velocity vector $\vec{V} = ui + vj + wk$ and the equation of motion (Newton's Second law) is

$$\frac{D\vec{V}}{Dt} = \vec{F} + \vec{P} ,$$

where $\frac{D\vec{V}}{DT}$ is the substantial or Eulerian derivative of the velocity vector V.

$\vec{F}$ represents the body forces (forces acting through the mass of the body) e.g., gravity, and

$\vec{P}$ represents the surface forces, stresses, shears, friction, and pressure forces.

We ignore $\vec{F}$.

The surface forces, P, depend on the strain rate of the fluid. The stress is related to the rate of strain via an isotropic, Newtonian fluid assumption. This means that the relation between the components of stress and the rate of strain is the same in all directions (isotropic) and this relationship is linear (Newtonian). However, shear stresses (viscous effects) will be ignored.

To obtain the surface forces consider the fluid volume shown below.

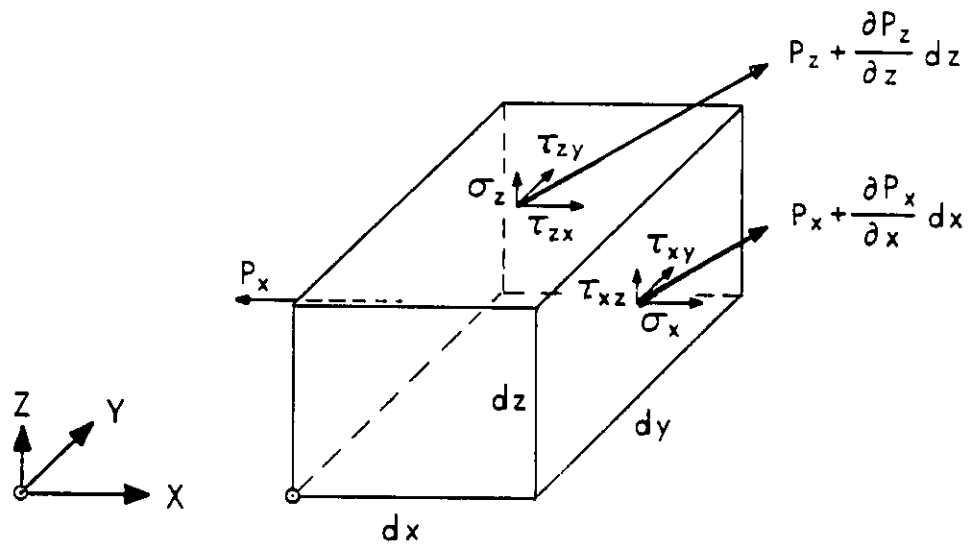

Vol. = dx dy dz

The x (plane to x) net surface force component is $\frac{\partial \bar{P}_x}{\partial x}\, dx\, dy\, dz$ for a one dimensional (1-D) case. The resultant surface force per unit volume is

$\bar{p} = \frac{\partial \bar{P}_x}{\partial x}$ where

$\bar{P}_x = \sigma_x \hat{i} + \tau_{xy} \hat{j} + \tau_{xz} \hat{k}$, after resolving P into normal stresses (σ) and shear stresses (τ).

For a 1-D case and ignoring the shear,

$$\bar{p} = \hat{i} \frac{\partial \sigma_x}{\partial x} ,$$

and neglecting body forces

$$\rho \frac{Du}{Dt} = \frac{\partial \sigma_x}{\partial x} .$$

Hydrostatic stress systems (fluid pressure) will not be considered, Stokes hypothesis will not be invoked, but deformations and rate of deformation will be neglected. Thus, the normal stress will not be related to pressure, velocities or velocity gradients as done in the classic Navier-Stokes derivation.

Instead consider a uniform stress field acting on the fluid element at rest (assume a negative σ_x) somewhat analogous to a thermodynamic pressure.

Then, expanding the substantial derivative and for incompressible flow

$$\rho \left(\frac{\partial u}{\partial t} + \frac{\partial u}{\partial x}\right) = - \frac{\partial \bar{\sigma}_x}{\partial x}$$

for a 1-D flow, (recall $\frac{Du}{Dt} = \frac{\partial u}{\partial t} + u \frac{\partial u}{\partial x} + v \frac{\partial u}{\partial y} + w \frac{\partial u}{\partial z}$).

Then, for a 1-D, steady state system

$$\rho \frac{d}{dx} \left(\frac{u^2}{2}\right) + \frac{d\sigma_x}{dx} = 0 ,$$

or

$$\rho \frac{u^2}{2} + \sigma = \text{const.},$$

with interpreted as a uniform normal stress. This result is analogous to a "Bernoulli equation with strength" which with the basic Bernoulli equation is frequently cited in penetration and shaped-charge jet collapse and formation discussions. Of course, the full Navier-Stokes equations relax to Euler's

equations under the specified assumptions, which in turn lead to the classic Bernoulli equation as shown earlier.

We conclude by remarking that the Bernoulli equation can represent a conservation of energy or a conservation of momentum depending on how it is derived. We also note that the "Bernoulli with strength" type equation, or the "modified Bernoulli equation" has some theoretical justification.

References
(Sections VI and VII)

1. H. W. Liepmann and A. Roshko, Elements of Gas Dynamics, John Wiley & Sons, Inc., London, 1957.

2. F. H. Harlow and W. E. Pracht, "Formation and Penetration of High-Speed Collapse Jets", Physics of Fluids, Vol. 9, No. 10, Oct. 1966.

3. Ascher H. Shapiro, The Dynamics and Thermodynamics of Compressible Fluid Flow, Vol. 1, Ronald Press, N.Y., 1953.

4. H. Schlichting, Boundary Layer Theory, McGraw-Hill, N.Y., 6th Edition, 1968.

VIII. The Gurney Velocity Approximation

The motion of a metal driven by an explosive was studied in the 1940's to early 1950's in a series of papers by Gurney, Sterne and Thomas [1,2,3,4,5] as applied to the motion of fragments resulting from the detonation of an adjacent high explosive [6]. This simple, approximate analysis assumes that the potential (or chemical) energy of the explosive charge before detonation is converted directly to the kinetic energy of the metal after detonation and to the expansion of the explosion products. The gas detonation products are assumed to expand uniformly and with constant density.

The so-called Gurney approximation is based on the conservation of momentum and energy. The results represent excellent engineering approximations, within 10%, of the experimental results or detailed numerical results. The Gurney method may be applied to any one-dimensional explosive-metal interaction system. The amazing accuracy of the relatively simple Gurney formulae, over a wide range of metal mass (M) to explosive mass (C) ratios ($0.1 \leq M/C \leq 10.0$), is apparently due to offsetting errors. These errors are caused by ignoring rarefaction waves passing through the detonation product gases, which causes the calculated velocity to be too high, and assuming an initial constant density distribution of the detonation product gases rather than a distribution with a peak at the surface of the charge caused by the detonation wave, which causes the calculated velocity to be too low [6]. Based on references [6,7,8] the Gurney formulae will be derived.

1. Open-Faced Sandwich

From Kennedy [8*], a specific energy (energy per unit mass) characteristic of a given explosive is assumed to be converted from chemical energy in the initial state to kinetic energy in the final state. The final kinetic energy is partitioned between the driven metal and the detonation product gases by an assumed linear velocity profile in the gases.

Figure 1 illustrates the open faced sandwich. It consists of a slab of explosive confined by a metal on one side only. This configuration is often used in experiments to obtain constitutive properties of materials or when it is necessary to impact a large target surface. The metal plate is termed the slapper or driver. The motion of the metal is obtained from momentum and energy conservation. For the open faced sandwich, Figure 2 illustrates the assumed liner velocity distribution. From this linear distribution,

$$V_{GAS}\ (Y) = (V_o + V)\ \frac{Y}{Y_o} - V. \tag{1}$$

The y coordinate is interpreted to be Lagrangian or identified with a material particle. A given material particle is assumed to move at constant speed at all times for the purpose of constructing momentum and energy balances. The initial thickness and density of the explosive are y_o and ρ_e, respectively. The energy and momentum balances follow:

$$CE = \frac{1}{2} Mv^2 + \frac{1}{2} \rho_e \int_o^{Y_o} \left[(V_o + V)\ \frac{Y}{Y_o} - V \right]^2 dy\ , \tag{2}$$

---

*Note that this is J. E. Kennedy, not the Don Kennedy referenced earlier.

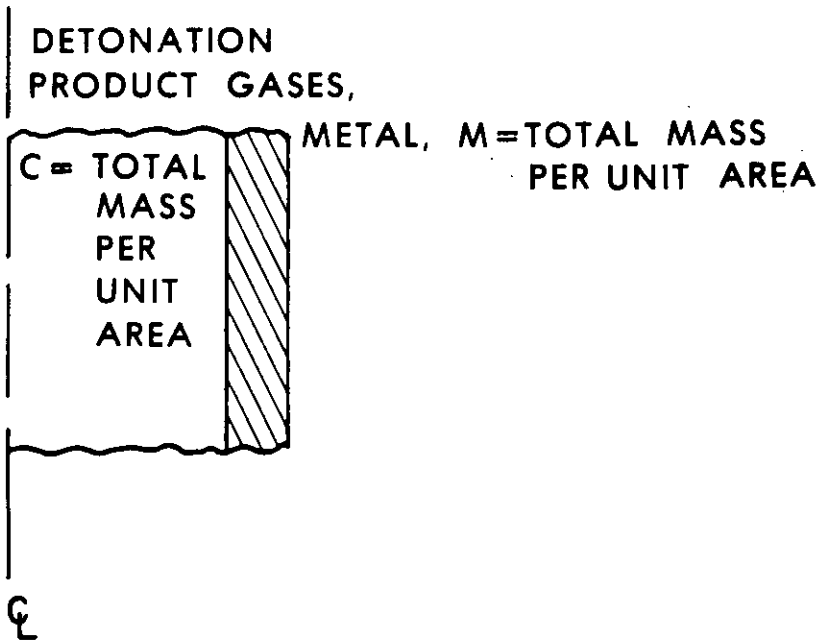

Figure 1. Open-Faced Sandwich.

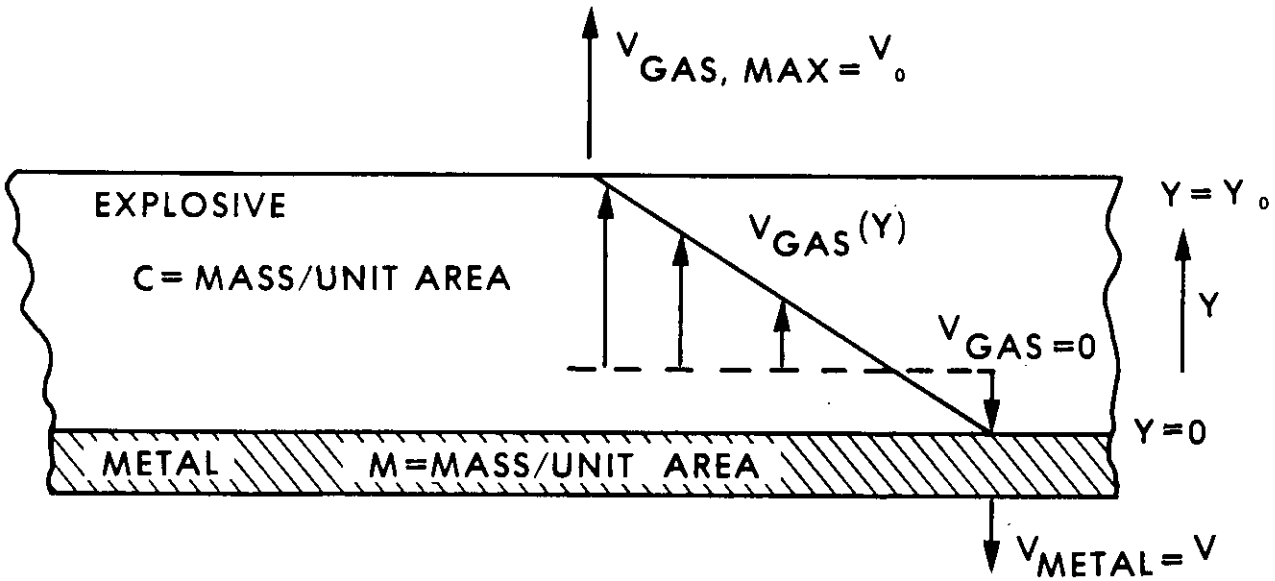

Figure 2. Linear Velocity Distribution for the Open-Faced Sandwich Configuration [8].

where

$C = Y_o \rho_e$

E = Specific explosive energy

$M = \rho_m t$

t = metal thickness, and

$$0 = - MV + \rho_e \int_o^{Y_o} \left[(V_o + V) \frac{Y}{Y_o} - V \right] dy \ , \tag{3}$$

and finally

$$V = \sqrt{2E} \left[\frac{(1 + 2 \frac{M}{C})^3 + 1}{6(1 + \frac{M}{C})} + \frac{M}{C} \right]^{-1/2} \ , \tag{4}$$

and

$$\frac{V_o}{V} = 2 \frac{M}{C} + 1 \quad . \tag{5}$$

Henry [6] provides additional mathematical details. Also, Henry presents a complete review of the Gurney formulae. The equations for some common symmetric and asymmetric configurations are presented in Figures 3, 4 and 5.

Figure 3 depicts two asymmetric configurations, namely a flat sandwich and a cylinder. M denotes the metal mass and C denotes the explosive mass. These terms are obtained as the product of the density and thickness of the material in question. Thus, M and C are really masses per unit area. The term V is the resultant metal velocity. The quantity $\sqrt{2E}$ occurs in all Gurney equations. It has the units of velocity and is termed the Gurney characteristic velocity for a given explosive. Gurney characteristic velocities have been tabulated for certain explosives by Kennedy [8], Henry [6], Jones et al [7], and many others, notably Dobratz [9]. Several explosives are tabulated from Reference [9] with their density, detonation velocity and Gurney characteristic velocity or Gurney constant. Note that two Gurney constants are given, one for warheads in which confining cases rupture at small expansions (prompt) and the other for warheads in which more ductile case materials are used which expand further before rupturing (terminal).

The tabulated densities are the actual density of the explosive used to determine the Gurney energy. The detonation velocities sometimes correspond to a different explosive density than that given in the table. It is recommended that the explosive of interest be accurately identified and the appropriate parameters be taken directly from Dobratz and the references

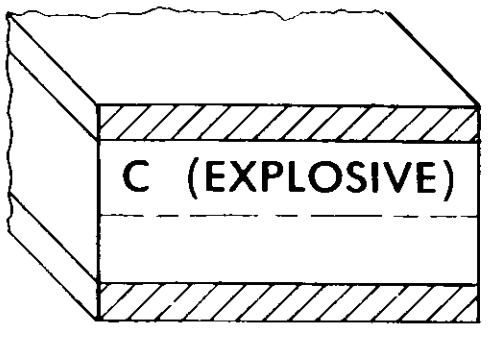

$\frac{M}{2}$ (METAL)

$\frac{M}{2}$

FLAT SANDWICH

$$V = \sqrt{2E}\left[\frac{M}{C} + \frac{1}{3}\right]^{-\frac{1}{2}}$$

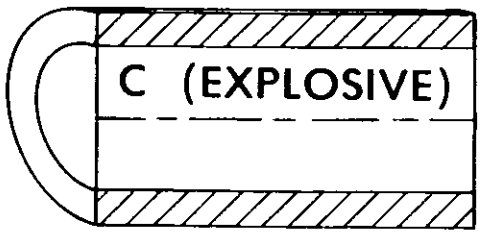

M (METAL)

CYLINDER

$$V = \sqrt{2E}\left[\frac{M}{C} + \frac{1}{2}\right]^{-\frac{1}{2}}$$

Figure 3. The Flat Sandwich and Cylindrical Configurations.

therein, or any other suitable source such as Meyer [10] or Reference [11]. La Rocca [12] presents a simple method for accurately predicting the Gurney constant and the relative power of any explosive.

Figure 4 presents the spherically symmetric case and Figure 5 shows two asymmetric configurations, an open faced sandwich and an asymmetric sandwich which has two metal plates, one being a tamper. The derivation of these equations is relatively straightforward using the assumptions stated along with elementary calculus and algebra. Derivations are given in Kennedy [8], Jones, et al [7] and Henry [6]. Henry [6] considers a few additional explosive/metal geometries. The ratio of $V/\sqrt{2E}$ or the ratio of the metal velocity to the Gurney characteristic velocity is an explicit function of M/C or the metal to charge mass ratio. For the asymmetric sandwich where the second metal plate may be considered to be a tamper, $V/\sqrt{2E}$ is also a function of N/C, where N/C is the mass to charge ratio of the tamper plate. The velocity expression given is that of the metal plate, M. The velocity ratio $V/\sqrt{2E}$ is plotted as a function of M/C in Figure 6 for all the non-tampered cases presented. Since values of $\sqrt{2E}$ have been tabulated for certain explosives, estimates of the metal velocity can be obtained for a given M/C for the geometries considered here.

Figure 7 plots the metal velocity as a function of M/C for an open faced sandwich and a few values of the Gurney constant, $\sqrt{2E}$, corresponding to PBX-9404, TNT and Comp B. This plot allows easy interpolation or extrapolation to other values of the Gurney constant.

The range of applicability of the Gurney formulae is restricted due to the simplifying assumptions in the derivation. These restrictions, according to Kennedy [8], Jones, et al [7] and Henry [6] are listed and discussed in the following tables. The Gurney assumption of a linear velocity profile of constant density detonation product gases greatly deviates from conventional gas dynamic theory. This assumption introduces the largest error in configurations involving a free explosive surface such as the open faced sandwich, for which the Gurney method may overestimate the metal velocity and impulse. Henry [6] used a parabolic pressure profile in the detonation products to remove the assumption that the gas density was constant at any given time. A simple gas equation of state was also used. Henry concluded that the additional mathematical complexity, inconsistent with the basic simplicity of the Gurney method, was not worthwhile based on the small improvement obtained in accuracy. Other extensions of the Gurney method are given in Reference [13].

Explosive	Density	D	$\sqrt{2E}$, km/s	
	gm/cm^3	km/s	Prompt	Terminal
			5 - 7 mm	19 - 26 mm
Comp A-3	1.61	8.47	2.402	
	1.59			2.63
Com B	1.71			2.70
	1.717	7.89	2.35	2.756 - 2.821
	1.717			2.71
Cast	1.68		2.402	
	1.62		2.32	
Pressed	1.59		2.335	
Comp C-4	1.52	8.37	2.176	
Comp C-3	1.60	7.63		2.68
Cyclotol 75/25	1.754	8.2 - 8.3		
Cast	1.69		2.286	
Pressed	1.64		2.362	
DATB	1.68	7.52	1.975	
Explosive D	1.50	6.85	1.942	
HBX-1	1.70	7.31	2.213	

Explosive	Density	D	$\sqrt{2E}$, km/s	
	gm/cm^3	km/s	Prompt	Terminal
			5 - 7 mm	19 - 26 mm
HBX-3	1.81	6.9 - 7.1	1.984	
HMX	1.89	9.11		2.97
LX-14	1.835	8.83		2.80
NM	1.14	6.35		2.41
NQ	1.44	7.65	1.896	
Octol 75/25	1.81	8.48		2.58
	1.821			2.83
DETASHEET C (DuPont)	1.48	6.8		2.1 - 2.3
(BRL)		7.0		2.8

Explosive	Density	D	$\sqrt{2E}$, km/s	
	gm/cm^3	km/s	Prompt	Terminal
			5 - 7 mm	19 - 26 mm
PBX-9011	1.77	8.5	2.82	
PBX-9404	1.84	8.8		2.90
PBX-9502	1.885	7.71		2.377
Pentolite 50/50				
Cast	1.64	7.52	2.301	
Pressed	1.57		2.317	
PETN	1.76	8.26		2.93
RDX	1.59	8.25	2.451	
	1.77	8.70		2.93
TACOT	1.61	7.25		2.12
Tetryl	1.63	7.5	2.274	
	1.62			2.50
TNT	1.63		2.039	2.419 - 2.505
	1.63			2.37
Cast	1.61	6.73	2.097	
Pressed	1.54	6.93	2.103	

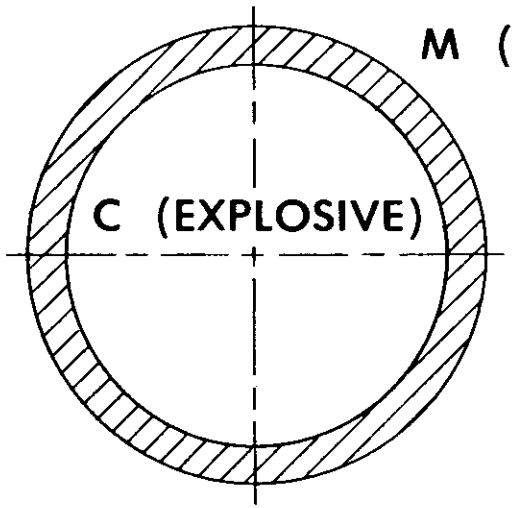

SPHERE

$$V = \sqrt{2E}\left[\frac{M}{C} + \frac{3}{5}\right]^{-\frac{1}{2}}$$

Figure 4. The Spherical Configuration.

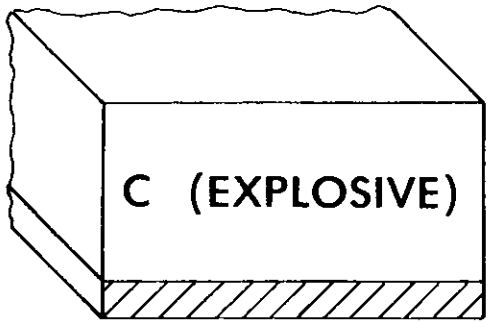

OPEN FACED SANDWICH

$$V = \sqrt{2E}\left[\frac{\left(1+2\frac{M}{C}\right)^3+1}{6\left(1+\frac{M}{C}\right)}+\frac{M}{C}\right]^{-\frac{1}{2}}$$

ASYMMETRIC SANDWICH

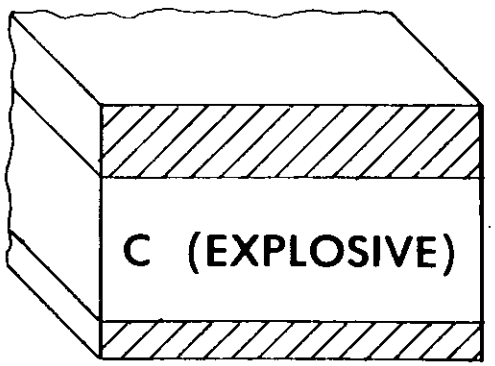

$$V_M = \sqrt{2E}\left[\frac{1+A^3}{3(1+A)}+\frac{N}{C}A^2+\frac{M}{C}\right]^{-\frac{1}{2}}$$

$$V_N = AV_M$$

$$A = \frac{1+2\frac{M}{C}}{1+2\frac{N}{C}}$$

Figure 5. Asymmetric Configurations.

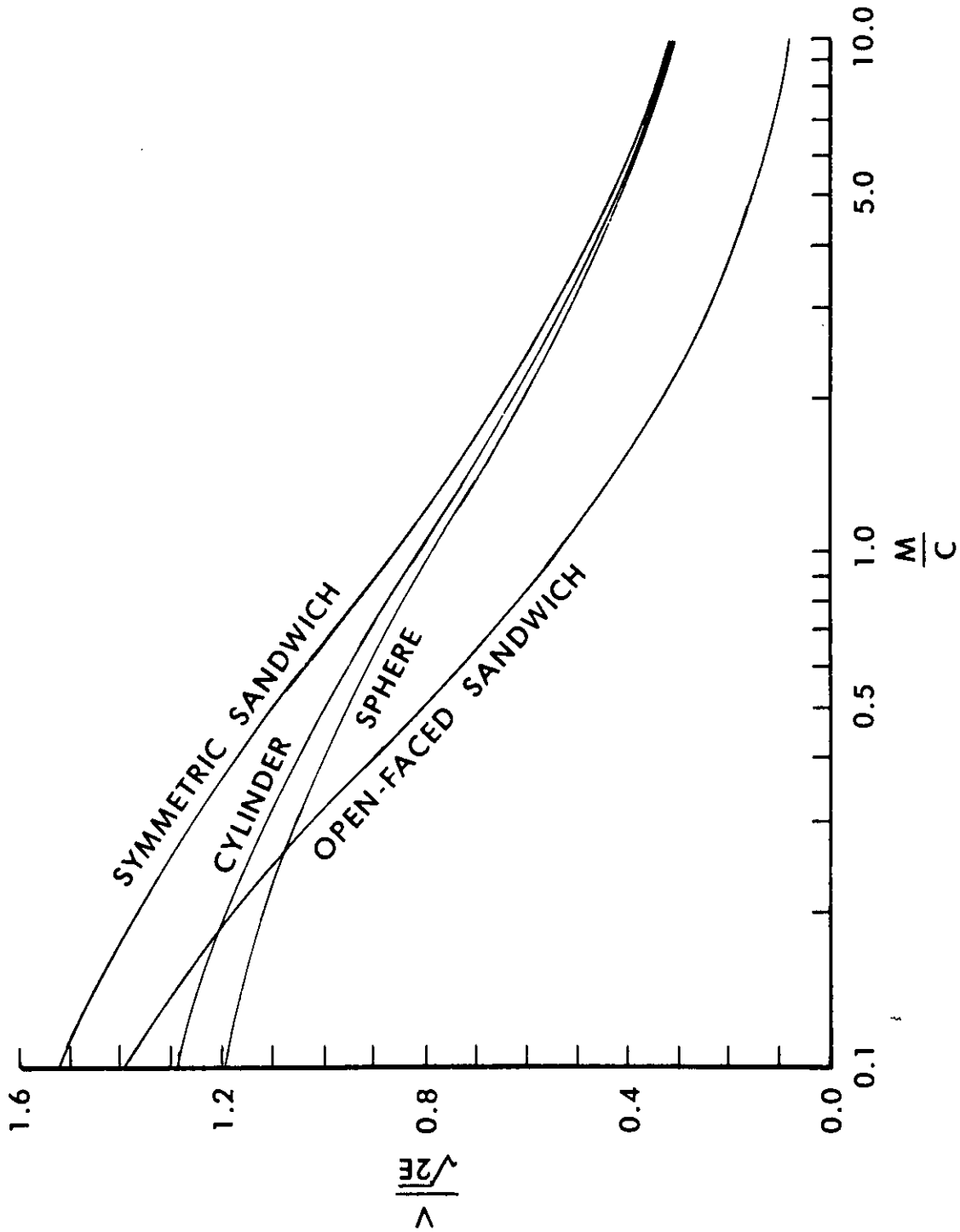

Figure 6. $V/\sqrt{2E}$ Versus M/C, Kennedy [8].

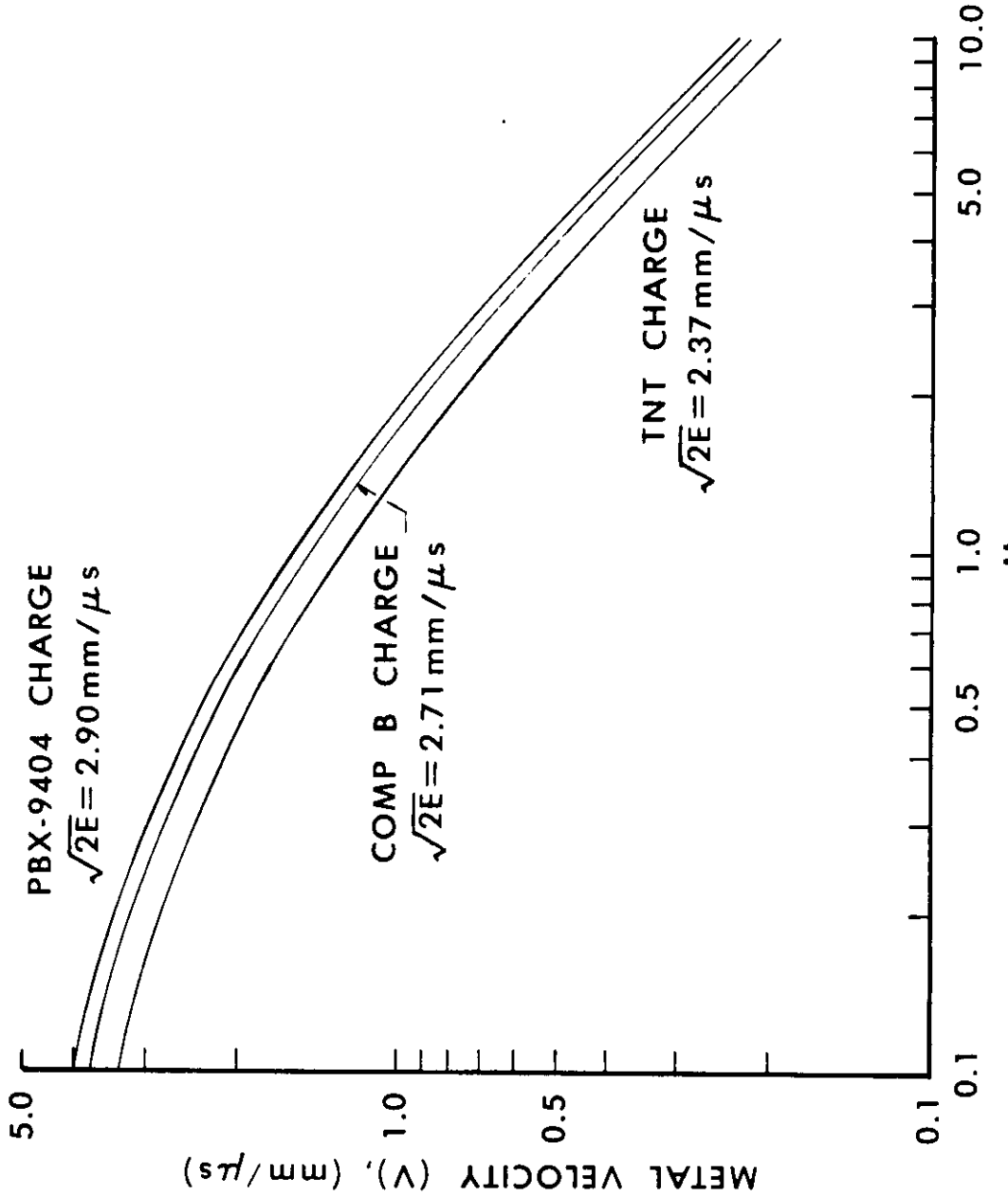

Figure 7. V Versus M/C for an Open-Faced Sandwich, Kennedy [8].

RESTRICTIONS ON THE GURNEY MODEL

Restriction	Remarks and Recommendations
Range of M/C ratio	Henry [6] claims accuracy for $0.1 < M/C < 5$ and Kennedy [8] states a range of $0.2 < M/C < 10$ for velocity calculations. Impulse calculations are usually acceptable for $M/C > 0.2$.
Acceleration Phase	The Gurney method in its basic form is not capable of analyzing motion during acceleration. However, Henry [6] and Jones, et al [7], used the assumption of a liner velocity profile in the uniformly dense gases in conjunction with an equation of state of the gases to yield acceleration solutions for flying metal plates. The detonation product gases must be allowed to expand sufficiently to complete the acceleration. The flying metal will reach its calculated velocity only if no external forces (or interactions) are applied during the initial acceleration phase.
Direction of Detonation Propagation	The detonation of the HE drives the metal at a given velocity (approximately) for a given M/C regardless of the angle between the detonation front and the metal. The direction in which the metal is driven will vary slightly with the angle (see Taylor angle discussion).
Gas Velocity Profile Assumption	The assumed linear velocity profile and constant density gas expansion are major assumptions. Ignoring effects of both rarefaction waves and of pressure peaks near the metal surface would seem to be cancelling errors. However, these assumptions are inherent to the simplicity of the Gurney method.

RESTRICTIONS ON THE GURNEY MODEL

Restriction	Remarks and Recommendations
One-Dimensional Motion	The Gurney approach is not valid for the estimate of variations in local velocity of a plate driven by a charge with a tapered thickness (or a tapered metal thickness). In this case, an average value of M/C could be used to estimate the final velocity of the entire plate.
Metal Strength Effects	Forces exerted by the metal to oppose deformation are not considered, other than inertia. Hoop stresses in cylinders and spheres can reduce the metal velocity in explosions and the strength effect is greater in implosions.
Metal Spallations	Metal spallation may occur when $M/C < 2$ for high density explosives and metals. Spallation can, in come cases, be avoided by introducing an air gap of a few millimeters between the explosive and the metal. This results in a small decrease in metal velocity.
Early Case Fracture	The leakage of the detonation product gases through fractures in the metal case can decrease the final metal velocity perhaps significantly depending on the nature and extent of the leakage.

The specific impulse delivered by the explosive can be calculated as the total momentum imparted to the metal body divided by the total explosive charge mass or

$$I_{sp} = \frac{Mv}{C} \quad . \tag{6}$$

The specific impulse, I_{sp}, will now be derived for an unconfined surface charge. Explosive may be detonated directly on the surface of a massive metal body in order to deliver a desired impulse for testing pruposes. If the loaded body is considered to be rigid, all detonation product gases will flow away from the surface and a maximum specific impulse will be delivered to the body. For a very large metal body mass to explosive mass ratio, M/C >> 1, the open faced sandwich velocity, equation (4), reduces to

$$V \sim \sqrt{2E}\sqrt{\frac{3}{4}}\ \frac{C}{M} \quad , \tag{7}$$

then $I_{sp} \sim \sqrt{\frac{3E}{2}}$, from equation (6).

Also since

$V_o = V\left[2\frac{M}{C} + 1\right]$ from equation (5) and for M/C >> 1,

$V_o = 2V\ M/C$ and with V given by equation (7),

$V_o = 2\sqrt{\frac{3}{4}}\ \sqrt{2E}$ or

$$V_o = \sqrt{6E} \tag{8}$$

for the maximum free gas velocity.

The impulse delivered to a body by the explosive can be increased by tamping or confining the explosive with an outer layer of metal. Tamping acts to hold back the detonation gases, keep the pressures high and force the detonation gases to do useful work against the body. A tamping and a confinement are analogous. The Gurney method can be used to estimate the change in impulse as a function of the tamper areal density. If the heavy metal body sandwich is considered to be rigid, it resembles the plane of symmetry in the symmetrical flat sandwich configuration shown in Figure 3. The velocity of the tamper plate is then given by the flat sandwich of Figure 3 with the tamper to explosive mass ratio N/C, used instead of M/C or

$$V + \sqrt{2E}\ \left[\frac{N}{C} + \frac{1}{3}\right]^{-1/2} \quad . \tag{9}$$

The effective specific impulse of the explosive for a tamping ratio of N/C follows from the equation for the asymmetric sandwich of Figure 5, namely,

$$V_m = \sqrt{2E}\left[\frac{1 + A^3}{3(1 + A)} + \frac{N}{C} A^2 + \frac{M}{C}\right]^{-1/2} . \qquad (10)$$

Assuming M/C >> 1 and with $A = \frac{1 + 2\ M/C}{1 + 2\ N/C}$, the specific impulse becomes

$$I_{sp},\ \text{tamped} = \sqrt{2E}\ (N/C + 1/2)\ /\ (N/C + 1/3)^{1/2} . \qquad (11)$$

Note that when N/C = 0, i.e., no tamper, equation (11) reduces to

$I_{sp} \sim \sqrt{\frac{3E}{2}}$ as derived earlier.

The acceleration of explosively driven metal plates can also be determined by using the Gurney assumption of a liner velocity profile in uniformly dense gases in conjunction with an equation of state for the gases. Acceleration calculations showing the displacement as a function of time or speed are important when estimating the effects of venting in a perforated casing. Henry [6] and Jones, et al [7], calculate the acceleration of the casing for various sandwich configurations. These same authors also extended the Gurney analysis by considering the pressure gradients within the gas in order to remove the assumption that the gas density is constant at any given time. These results however, complicate the simple Gurney model.

The Gurney model yields explicit algebraic relationships for estimating the velocity imparted to a metal in contact with a detonating explosive. The model can be used for several simple geometric metal/explosive configurations. The specific impulse of an explosive can also be obtained for these geometries and is directly related to the Gurney energy of the explosive. Thus, the Gurney method can be directly and simply applied to a multitude of explosive/metal interaction problems. Design and parametric studies can be readily performed. Applications include warhead and fragmentation design, the study of the efficiency of conversion of the high explosive chemical energy to the kinetic energy of the plate, explosive initiation by the impact of an explosively driven plate, the launching of a dielectric plate by electrical detonation of a metal foil, and the calculation of layers of metal fragments in conjunction with shock wave physics.

Note that the Gurney method does not consider the propagation of shock waves through metals, but only the terminal effect of the shock propagation. Duvall [14] provides an excellent description of shock wave propagation, transmission and reflection. He describes a plane wave lens, a plane wave generator and methods of forming oblique shock waves. He also states the

pressure levels attained by the various methods of shock wave generation. Duvall's article [14] explains shock wave phenomena without recourse to advanced mathematical concepts. Thus, Reference [14] is an excellent introductory article for the layman. Courant and Friedrichs [15] provide an excellent mathematical treatment of shock wave physics. Shock wave propagation through solid media is an important aspect of explosive/metal interaction, but is beyond the scope of this introductory report.

An extension of the Gurney method was given recently by Chanteret [16]. Chanteret developed an analytical model for symmetrical geometries with energy partitioning during expansion. This model allows a calculation of the Gurney energy as a function of the expansion ratio. The expansion ratio is $(R/R_o)^n$ where R is the current value of the radius of the explosive-metal interface and R_o is the undetonated radius of the explosive-metal interface. The constant n depends on the geometric configuration (n = 1 for symmetrical plane sandwiches and n = 2 for cylinders with a constant wall thickness). Chanteret's results can be used in conjunction with the classical Gurney formulae to obtain the entire velocity-time curve for all symmetrical steady-state configurations. Also Chanteret extended the Gurney model to include imploding cylinders by introducing a fictitous rigid boundary in the explosive cylinder. The results are claimed to agree well with available experimental data and two-dimensional hydrocode results.

The Gurney method and extensions of this method are useful analytical tools. The flyer plate velocity depends only on the M/C ratio and the Gurney constant or Gurney characteristic velocity, $\sqrt{2E}$. This constant is available for several explosives (as we have seen), but when the Gurney constant is not available, Kennedy [8] recommends that $E \sim 0.7\ H_D$ be used when H_D is the heat of detonation. This recommendation follows from the fact that $0.61 < EH_D < 0.76$ for most explosives. Another option is to use La Rocca's method [12] to calculate the Gurney constant.

The Gurney method ignores rarefaction effects and the shock characteristics of metals. Thus, we can expect errors to occur when these effects are important. An example would be a short open ended cylinder which will deviate from the Gurney prediction near its ends. Also, the difference in shock impedance between different metals will alter the energy coupling and as a result, the same M/C ratios with different metals but with the same explosive will yield different velocities. The applicable range of M/C values is $0.2 < M/C < 10$ as discussed earlier. Note that as M/C decreases, e.g., when adding HE to a given metal slab, the velocity cannot increase indefinitely as predicted by the Gurney method.

Finally, the Gurney equations assume that the metal moves in a direction normal to its surface. This is true when the detonation wave encounters the metal at normal incidence. It is not true when the detonation wave encounters the metal plate at a grazing incidence. The grazing incidence is treated by another model known as the Taylor angle approximation.

Before investigating the Taylor angle approximation, a few Gurney type formulae relating to flat plates and imploding devices will be discussed.

For shaped charges, a popular formula for a single flat plate backed by slab of explosive is given by [17], where $\mu = M/C$, and V_o is the liner collapse velocity, and

$$V_o = \sqrt{2E}\left[\frac{3}{4\mu^2 + 5\mu + 1}\right]^{1/2} \tag{12}$$

For this same configuration, with the detonation wave (of velocity D) propagating in a direction tangent to the liner, Duvall and Erkman [18, 19] used hydrodynamic theory to obtain the collapse velocity formula

$$V_o = D\left[1 + \frac{27\mu}{16}\left(1 - \sqrt{1 + 32/(27\mu)}\right)\right] \quad . \tag{13}$$

Kleinhanss [20] also presented equation (13) and credited Trinks with another formula based on semi-empirical data related to the explosive launching of plates,

$$V_o = 0.36D \arctan\left(\frac{2}{3\mu}\right) \quad . \tag{14}$$

These formulae were developed for flat plates, and although they are quite accurate, they do not account for the effect of curvature such as in implosive geometries, e.g., a conical shaped charge. Kleinhanss [20], in experiments with imploding cylindrical charges, showed a strong dependence of the liner collapse velocity (V_o) on its radius. He obtained the semi-empirical formula

$$V_o = D\left[\frac{r_i - \sqrt{\varepsilon(2r_i - \varepsilon)}}{r_i - \varepsilon} \cdot \frac{1}{(C_o + \varepsilon f(b))}\right] \quad , \tag{15}$$

where ε is the metal thickness, $b = r_o - r_i$, r_o and r_i being the outer and inner explosive radii, respectively, and thus b is the explosive thickness. C_o and $f(b)$ are empirical constants that depend on the type of explosive and metal being used. Other studies on implosive geometries were given by Chanteret [16] as discussed earlier, Chou et al, [21] and Hennequin [22]. All of these studies provide improved results over the basic Gurney model for implosive geometries.

Other formula are available for plate acceleration and are often used in shaped charge liner collapse and explosive welding models. For example, Singh

[23] considers the velocity of the casing of a thin walled cylinder filled with explosive and detonated at one end. The velocity of the casing at the time of fracture is given by

$$\frac{V_o}{D} = \frac{1}{4}(1 + \sin\alpha) \tag{16}$$

where each element of the casing subtends an angle α with the axis of propagation of detonation.

Deribas [24] gives

$$\frac{V_o}{D} = 1.2\left\{\frac{\sqrt{1 + \frac{32\eta}{27}} - 1}{\sqrt{1 + \frac{32\eta}{27}} + 1}\right\}, \tag{17}$$

where η is the charge to mass ratio.

Shushko, et al [25], gives

$$\frac{V_o}{D} = 0.61\left[\frac{\eta^2 + 12\eta + 18 - 6\sqrt{2\eta^2 + 12\eta + 9}}{\eta(\eta + 6)}\right]. \tag{18}$$

Mikhailov and Dremin [26] provide several frequently used expressions for the plate speed. They are:

$$\frac{V_o}{D} = \frac{\sqrt{1 + \frac{32\eta}{27}} - 1}{\sqrt{1 + \frac{32\eta}{27}} + 1}, \tag{19}$$

$$V_o = \frac{0.602\eta}{2 + \eta}, \text{ and} \tag{20}$$

$$\frac{V_o}{D} = 1 - \frac{\Theta - 1}{\Theta\gamma} - \frac{H\theta}{Dt}, \tag{21}$$

where $\gamma = \frac{16}{27}\frac{1}{\eta}$, $\Theta = 1 + 2\gamma\left[(1 - \frac{H}{Dt}\right]^{-1/2}$, t is the time taken to travel the flight distance or the length of the driver plate, and H is the height of the explosive charge.

Smith, et al [27] used formulae analogous to equations (12) and (17) to determine the terminal velocity of flyer plates used in plate acceleration experiments. Smith, et al [27] also calculated the flyer plate terminal bend angle which will be discussed shortly. Both the bend angles and flyer plate terminal velocities are in agreement with the experimental values obtained for three different explosives.

Explosive-metal interaction models are also useful in fragmentation calculations. Fragmentation, of course, does not always result from an explosive-metal interaction. For example, fragments are generated when gas pressurized pipes or vessels fail. The velocity of the fragments following a gas pressurized system failure is necessary in order to determine the damage to neighboring equipment on structures. Fragment velocities resulting from a pressurized pipe or vessel failure are usually predicted by the Moore equation [28]. The Moore equation is semi-empirical based on experimental data from the velocity of explosively generated fragments (i. e., Gurney data).

Another method for estimating the fragmentation velocity from ruptured pipes or vessels follows from the theoretical model of Baum [29].

Of course, other Gurney like models are also available. The section on explosive welding and the sections on jet formation provide references to other metal acceleration models. Walters [30] and Walters and Harrison [31] provide several references (mostly Soviet), related to the acceleration of metals by high explosives. Dehn [32], recently published a report containing an overview of Gurney type velocity approximation models as well as the Taylor angle (grazing incidence) models. Dehn provides additional historical information and correctly analyzes geometric configurations in this report such as the Jelly Roll, the Dagwood and similar explosive-metal multilayer arrangements.

In conclusion, care must be taken in comparing the various explosive-metal interaction formulae. Many authors use M/C (ratio of the mass of metal to the explosive mass) as a key parameter. Other authors prefer C/M as the parameter.

Next, grazing detonation waves will be investigated.

THE TAYLOR ANGLE APPROXIMATION

The Taylor approximation [33] is shown in Figure 8, which depicts a grazing (parallel) incidence of the detonation wave to the metal surface. The plate is deflected at an angle θ from its initial position. Acceleration of the metal to its final velocity is assumed to be instantaneous. For this steady-state condition, the metal plate is assumed to undergo pure rotation, i. e., no net shear flow, or no change in length or thickness. Thus, the plate element that was at P initially will be a P' after launch and the lengths

$$\overline{OP} = \overline{OP'} \quad .$$

Construct a line from O perpendicular to $\overline{PP'}$. This line bisects the angle since OPP' is an isosceles triangle. If the time, t, is measured from the time when the detonation wave passes point P, then:

$$\overline{OP} = Dt,$$

$$\overline{PP'} = Vt$$

and
$$\sin \frac{\Theta}{2} = \frac{\overline{PP'}/2}{\overline{OP}} = \frac{Vt}{2Dt} = \frac{V}{2D} \quad . \tag{1}$$

An estimate of the direction in which the metal plate is projected is the angle $\Theta/2$ which can be determined from equation (1) with V known from the Gurney method and D determined from the specified explosive. As the plate moves, it will be tilted an an angle θ from its initial position, and by assumption, will not be rotating.

When using a streak camera located perpendicular to the initial charge axis, a component of the velocity, namely Va, the apparent velocity, was measured by Kury, et al [34]. This velocity can be related to V by the geometry or

$$Va = D \tan \theta \, , \tag{2}$$

then

$$\frac{V}{Va} = \frac{2D \sin \theta/2}{D \tan \theta} = \frac{2 \sin \theta/2}{\frac{\sin \theta}{\cos \theta}} = \frac{\cos \theta \, (2 \sin \theta/2)}{2 \sin \frac{\theta}{2} \cos \frac{\theta}{2}} \tag{3}$$

or $\frac{V}{Va} = \frac{\cos \theta}{\cos \theta/2}$.

Hoskin, et al [13] expressed their results in terms of the velocity component V_N, the velocity component normal to the flight plane of the plate,

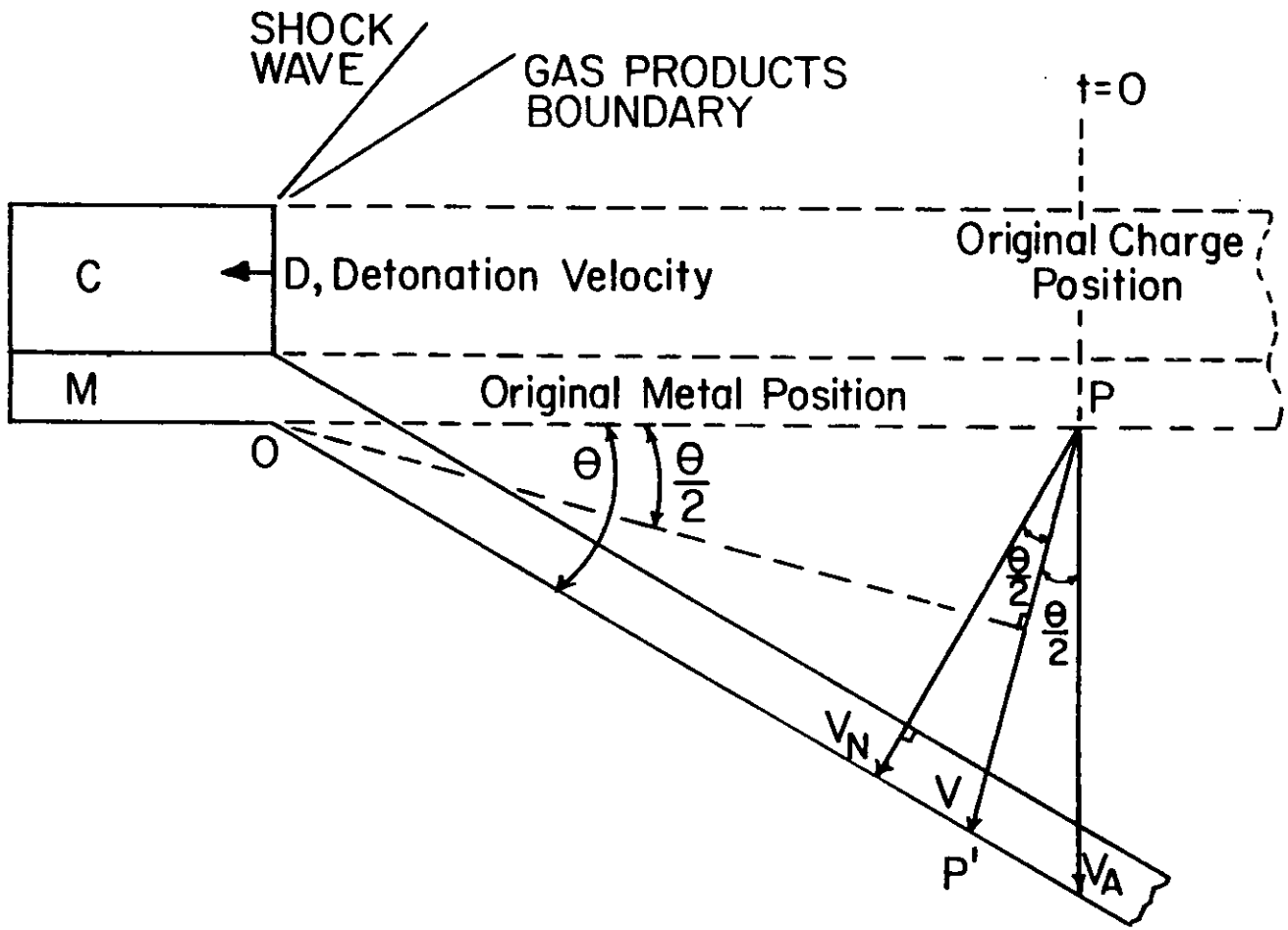

Figure 8. Direction of Metal Projection By a Grazing Detonation Wave.

since this velocity is of interest when the flying plate is used in impact studies. Since the angle between V_A and V_N is θ, we can write

$$V_N = D \sin \theta, \text{ and} \tag{4}$$

$$\frac{V}{V_N} = \frac{2D \sin \theta/2}{D \sin \theta} = \frac{1}{\cos \theta/2} = \sec \theta/2 \quad . \tag{5}$$

The difference between V, V_N and V_A is usually only a few percent. Also, the term V/2D is approximately the same for many explosives. Thus, θ is approximately constant. If we fix the mass of the plate (its thickness) being driven, we observe that increasing the detonation velocity of the explosive implies an increase in the plate velocity such that V/2D is approximately constant. These concepts will be used to study jet formation theory.

REFERENCES
(Section VIII)

1. R. W. Gurney, "The Initial Velocities of Fragments from Bombs, Shells and Grenades," BRL Report 405, September 1943.

2. R. W. Gurney, "Fragmentation of Bombs, Shells and Grenades," BRL Report 635, March 1947.

3. T. E. Sterne, "A Note on the Initial Velocities of Fragments from Warheads," BRL Report 648, September 1947.

4. T. E. Sterne, "The Fragment Velocity of a Spherical Shell Containing an Inert Core," BRL Report 753, March 1951.

5. L. H. Thomas, "Theory of the Explosion of Cased Charges of Simple Shape," BRL Report 475, July 1944.

6. I. G. Henry, "The Gurney Formula and Related Approximations for the High-Explosive Deployment of Fragments," Hughes Aircraft Company, Culver City, CA, Report No. PUB-189, April 1967, (AD 813398).

7. G. E. Jones, J. E. Kennedy and L. D. Bertholf, "Ballistics Calculations of R. W. Gurney," Am. J. Phys. 48 (4), pp. 264 - 269, April 1980.

8. J. E. Kennedy, "Gurney Energy of Explosives: Estimation of the Velocity and Impulse Impacted to Driven Metal," Sandia Laboratories, SC-RR-70-790, December 1970.

9. B. M. Dobratz, "LLNL Explosives Handbook. Properties of Chemical Explosives and Explosive Stimulants," LLNL Report UCRL-52997, March 1981, with Errata dated January 1982.

10. Rudolf Meyer, Explosives, Verlag Chemie, Weinheim and New York, 1977.

11. "Properties of Chemical Explosives," University of California, Lawrence Radiation Laboratory, UCRL-14592, December 1965.

12. E. W. La Rocca, "Advances in Predicting the Relative Power of High Explosives and the Correlation with Fragment Velocity," General Dynamics, TM-6-348-1.13-4, October, 28, 1980.

13. N. E. Hoskin, J. W. S. Allan, W. A. Bailey, J. W. Lethaby and I. C. Skidmore, "The Motion of Plates and Cylinders Driven by Waves at Tangential Incidence," The Fourth Symposium on Detonation Preprints, Vol. I., NOL, MD., October 1965.

14. George E. Duvall, "Shock Waves In Solids," International Science and Technology, April 1963.

15. R. Courant and K. O. Friedrichs, Supersonic Flow and Shock Waves, Interscience Publishers, Inc., N.Y., 1948.

16. P. Y. Chanteret, "An Analytical Model For Metal Acceleration by Grazing Detonation," Proceedings of the Seventh International Symposium on Ballistics, The Hague, Netherlands, April 1983.

17. P. C. Chou and W. J. Flis, "Recent Developments in Shaped Charge Technology," Private Correspondence, April 1984, (Manuscript prepared for M. Held, MBB, Germany and presented at MBB, Schrobenhausen, West Germany, September 1983.)

18. G. E. Duvall and J. O. Erkman, Technical Report No. 1, Stanford Research Institute, No. GU-2426, 1958.

19. G. E. Duvall, J. O. Erkman and C. M. Ablow, "Explosive Acceleration of Projectiles," Israel J. Tech., Vol. 7, No. 6, pp. 469 - 475, January 1969, AD # 709810.

20. H. R. Kleinhanss, "Experimentelle Untersuchungen Zum Kollapsrozess bei Hohlladungen," Proc. 3rd Int. Symp. on Military Application, FRG, September 1971 and FSTC-HT-23-794-73, March 1973.

21. P. C. Chou, et al, "Improved Formulas for Velocity, Acceleration and Projection Angle of Explosively Driven Liners," Proc. 6th Int. Symp. on Ballistics, Orlando, FL, 27 - 29 October 1981.

22. E. M. Hennequin, "Analytical Model of the Shaped Charge Liner Collapse," Proc. 7th Int. Symp. on Ballistics, The Hague, Netherlands, 19 - 21 April 1983.

23. Sampooran Singh, "Spatial Distribution of Fragments of Explosively Loaded Thin-Walled Steel Cylinders," Proc. Phys. Soc., London, V. B 69, pp. 1089 - 1094, 1956.

24. A. A. Deribas, Physics of Explosive Work-hardening and Welding, Nauka, Novosibirsk, 1972.

25. L. A. Shushko, B. I. Shekhter and S. L. Krys'kov, "Bending of a Metal Strip by a Sliding Detonation Wave," Fizika Goreniya i Vzryva, Vol. 11, No. 2, pp. 264 - 274, March - April 1975.

26. A. N. Mikhailov and A. N. Dremin, "Flight Speed of a Plate Propelled by Products From a Sliding Detonation," Fizika Goreniya i Vzryva, Vol. 10, No. 6, pp. 877 - 884, November - December 1974.

27. E. G. Smith, Jr., D. Laber and V. D. Linse, "Explosive Plate Acceleration Studies Using a Dual-Channel Flash X-Ray Technique," The Third International Conference of the Center for High Energy Forming, Vail, Colorado, July 1971.

28. C. V. Moore, Nuclear Engineering and Design, Vol. 5, pp. 81 - 97, 1967.

29. M. R. Baum, "The Velocity of Missile Generated by the Disintegration of Gas-Pressurized Vessels and Pipes," J. of Pressure Vessel Technology, Trans of the ASME, Vol. 106, November 1984, pp. 362 - 368.

30. W. P. Walters, "Influence of Material Viscosity on the Theory of Shaped-Charge Jet Formation," BRL Memorandum Report, ARBRL-MR-02941, August 1979.

31. W. P. Walters and J. T. Harrison, "Modeling of the Shaped-Charge Jet Formation" Proceedings of the Army Symposium on Solid Mechanics, 1980 - Designing for Extremes: Environment, Loading and Structural Behavior, AMMRC MS 80-4, September 1980.

32. James T. Dehn, "Models of Explosively Driven Metal," BRL Technical Report, BRL-TR-2626, December 1984.

33. G. I. Taylor, "Analysis of the Explosion of a Long Cylindrical Bomb Detonated at One End," Paper written for the Civil Defense Research Committee, Ministry of Home Security in 1941, available in The Scientific papers of Sir Geoffrey Ingram Taylor, Vol. III, G. K. Batchelor, ed., The University Press, Cambridge, 1963.

34. J. W. Kury, H. C. Hornig, E. L. Lee, J. L. McDonnel, D. L. Ornellas, M. Finger, F. M. Strange and M. L. Wilkins, "Metal Acceleration by Chemical Explosives," The Fourth Symposium on Detonation Preprints, Vol. I, NOL, MD, October 1965.

IX. JET FORMATION

Birkhoff, Mac Dougall, Pugh and Taylor [1] formulated the first theory of conical shaped charge jet formation assuming that the detonation wave produces such large pressures during the collapse process that the material strength of the liner may be neglected. In fact, the liner is treated as an inviscid, incompressible fluid. The conical liner is modeled as a wedge, and a steady state collapse model is assumed. Thus, the liner elements are instantaneously accelerated to their final collapse velocity. The steady state model predicted a jet with a constant length equal to the slant height of the cone. It has been observed however, that shaped charge jets possess a velocity gradient with the tip traveling much faster than the tail, causing the jet to stretch and eventually break up. This steady-state theory was later modified by Pugh, Eichelberger and Rostoker [2] to include the jet velocity gradient. The modified "non-steady" theory is based on the same principles as the original theory except that the velocities at which the various liner elements collapse is not constant, but depends on the original position of the element in the liner. We begin with an examination of the Birkhoff, et al [1] steady state model.

As the detonation wave impacts the liner the pressure on all sides of the liner is assumed to be equal and the liner walls are assumed to collapse inward at a constant velocity, say V_o. The angle 2β between the moving walls is greater than the original apex angle 2α, because of the finite time required for the detonation wave to sweep the liner surface from apex to base. Figure 1 describes the geometry of the collapse process. The conical liner is symmetric so α represents one half of the liner apex angle and β represents the collapse angle. The liner assumes a velocity, V_o, which bisects the angle APP' of Figure 1. To show this consider a coordinate system having a constant velocity such that the origin moves from point P to P' in a unit time. In this coordinate system steady state conditions exist at the origin and the liner moves inward along P'P and flows outward along the path PA. The velocity of the liner passing through this region changes its direction but not its magnitude, because the pressure forces are everywhere perpendicular to the motion. P'P and P'B represent the entering and emerging velocities, respectively, of the liner in the moving coordinate system. P'B is constructed parallel to PA and P'P and P'B are equal in magnitude. Since the velocity in the moving coordinate system is PP' the velocity of the collapsing liner in the stationary system is the vector sum

$$PP' + P'B = PB = V_o \ .$$

Since P'P = P'B, the triangle BPP' is isosceles and since P'B is parallel to PA, angle BPP' = angle PBP' = angle BPA. Call these angles θ. Thus, V_o bisects angle APP'.

The walls of the collapsing liner are two planes moving inward. The junction of these planes moves from A to B with a velocity V_1,

$$V_1 = V_o \cos\left(\frac{\beta - \alpha}{2}\right) / \sin \beta \ . \qquad (1)$$

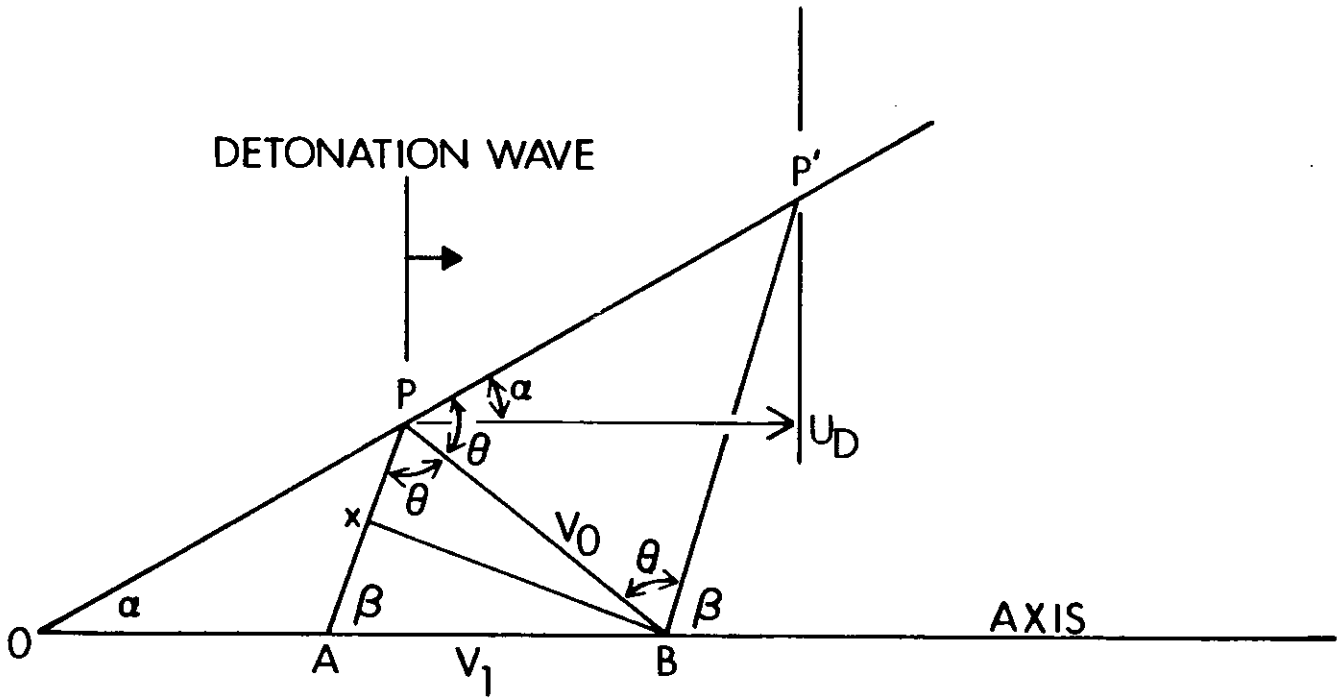

Figure 1. Birkhoff et al, Geometry of the Collapse Process.

From Figure 1, the angle OPA = ϕ follows from the fact that $\alpha + \phi + 180 - \beta = 180$ or $\phi = \beta - \alpha$, i.e., the sum of the angles of a triangle equals 180°. Next, consider the triangle PXB where $180 = 90 + \theta + (\sphericalangle XBP = \gamma)$ or $\gamma = 90 - \theta$. In triangle XAB, $180 = 90 + \beta + \sphericalangle ABX$ or $\sphericalangle ABX = 90 - \beta$. Then along the line OPP', $2\theta + \phi = 180$ or $\theta = 90 - \phi/2 = 90 - \left(\frac{\beta - \alpha}{2}\right)$, from above. Then since $\gamma + \theta = 90$, $\gamma + 90 - \left(\frac{\beta - \alpha}{2}\right) = 90$ or $\gamma = \left(\frac{\beta - \alpha}{2}\right)$. Angle PP'B = ϕ since in triangle PP'B we have $2\theta + \sphericalangle PP'B = 180$ or $180 - \phi + \sphericalangle PP'B = 180$ or $\sphericalangle PP'B = \phi$. This establishes the geometry of Figure 1. Now for some trigonometry.

In triangle APB by the law of sines, $V_1/\sin\theta = V_o/\sin\beta$ or $V_1 = V_o \sin\theta/\sin\beta$. The $\sin\theta = \sin\left(90 - \left(\frac{\beta - \alpha}{2}\right)\right) = \cos\left(\frac{\beta - \alpha}{2}\right)$ and

$$V_2 = V_o \cos\left(\frac{\beta - \alpha}{2}\right)/\sin\beta = V_o \cos(\phi/2)/\sin\beta \ . \tag{2}$$

A moving observer positioned at A would observe any point P in the upper plane approaching him with a velocity $V_1 \cos\beta + V_o \cos\theta$. This velocity, V_2, becomes $V_2 = V_1 \cos\beta + V_o \cos\left(90 - \left(\frac{\beta - \alpha}{2}\right)\right) = V_1 \cos\beta + V_o \sin\left(\frac{\beta - \alpha}{2}\right)$, and from equation (2),

$$V_1 = V_o \left[\cos\left(\frac{\beta - \alpha}{2}\right)/\tan\beta + \sin \right. \tag{3}$$

Also $U_D = U \cos\alpha$ where U is along PP' and using the law of sines for triangle PBP', $\frac{V_o}{\sin(\beta - \alpha)} = \frac{U}{\sin\theta}$ or

$$U = \frac{V_o}{\sin(\beta - \alpha)} \sin\ 90 - \left(\frac{\beta - \alpha}{2}\right) = \frac{V_o \cos\left(\frac{\beta - \alpha}{2}\right)}{\sin(\beta - \alpha)} \ ,$$

then

$$\frac{U_D}{\cos\alpha} = \frac{V_o \cos\left(\frac{\beta - \alpha}{2}\right)}{\sin(\beta - \alpha)} \ . \tag{4}$$

Returning to V_2 from equation (3) the observer sees a "jet" moving to his right and a "slug" moving to his left, as in Figure 2. Also, as viewed by this observer, the whole process appears to be unchanged by the lapse of time, or steady state motion exists. This, with the earlier assumptions of inviscid, incompressible and one-dimensional flow allows the use of the Bernoulli equation or

$$P = \tfrac{1}{2} \rho_o U^2 = \text{constant}, \tag{5}$$

which relates the pressure and the corresponding velocity U. The pressure at any point in the liner determines the velocity at that point. Assume the liner moves away from the detonation so fast that the pressure of the surface decreases rapidly and the pressure on all surfaces of the collapsing liner is constant. This allows free streamlines, i.e., the boundary streamlines are at constant pressure and density (and hence velocity). As viewed by the observer, the jet and slug will appear to recede with exactly the same speed, V_2, as the walls approach as in Figure 1.

Returning to the stationary system of coordinates, it is seen that the jet, traveling to the right in Figure 2, has a velocity

$$V = V_1 + V_2,$$

while the slug, traveling to the left in the moving system of Figure 2, has a velocity to the right given by

$$V_s = V_1 - V_2.$$

To further visualize this process consider that the point P (fixed in the upper plane) travels to point B (fixed in space) in unit time, the material from the inner surface of the upper plane included between PA and AB moves into the jet, and the front of the jet moves to the right a distance PA + AB in the same time, forming a high velocity jet. This jet velocity is $V = V_1 + V_2$ and from equations (2) and (3):

$$V = V_o \left\{ \frac{\cos\left(\frac{\beta - \alpha}{2}\right)}{\sin \beta} + \frac{\cos\left(\frac{\beta - \alpha}{2}\right)}{\tan \beta} - \sin\left(\frac{\beta - \alpha}{2}\right) \right\}. \tag{6}$$

Also, the outer surface of each plane forms a slug moving with the lower velocity, $V_s = V_1 - V_2$ or

$$V_s = V_o \left\{ \frac{\cos\left(\frac{\beta - \alpha}{2}\right)}{\sin \beta} + \frac{\cos\left(\frac{\beta - \alpha}{2}\right)}{\tan \beta} - \sin\left(\frac{\beta - \alpha}{2}\right) \right\}. \tag{7}$$

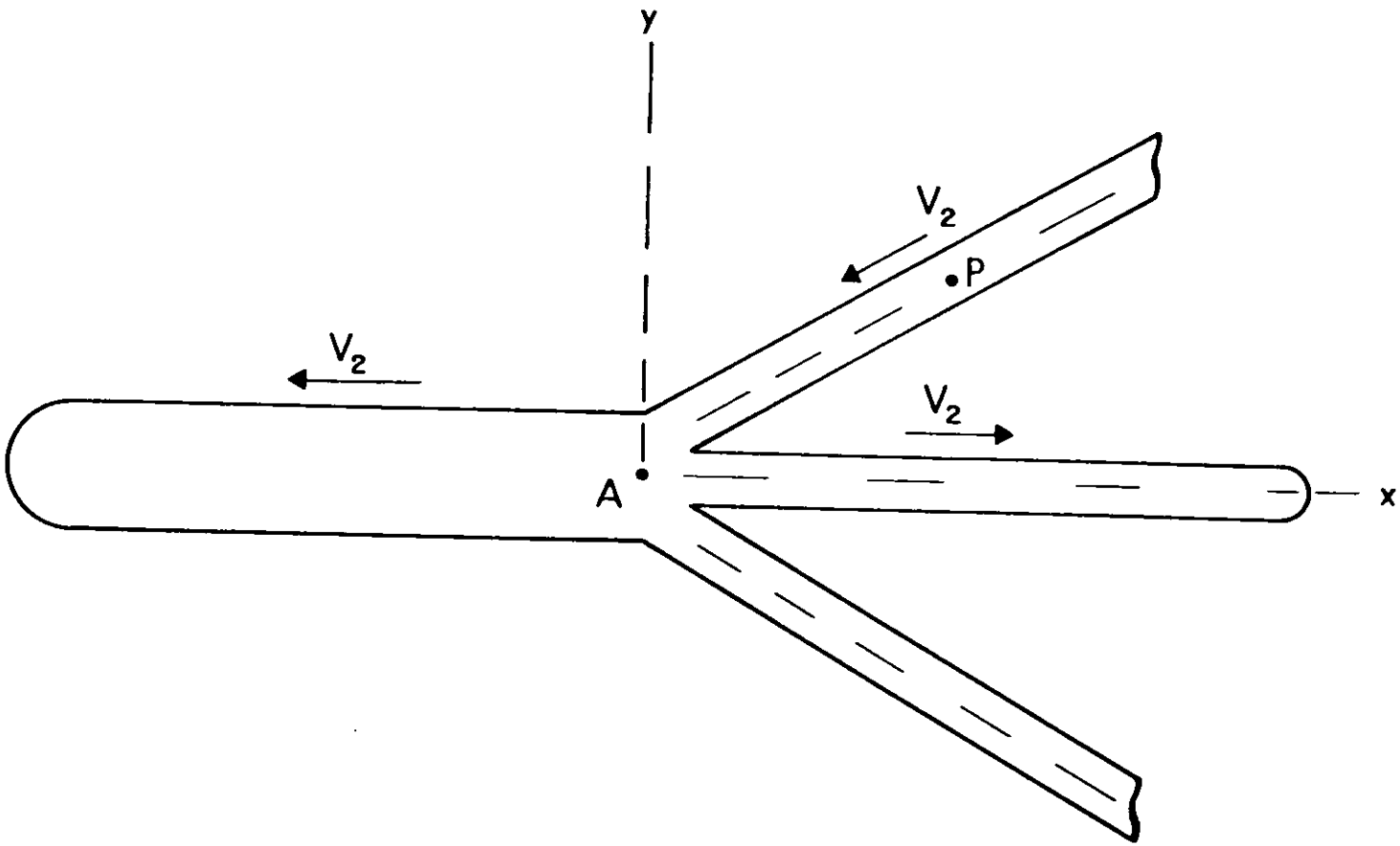

Figure 2. Birkhoff, et al, The Formation of a Jet and Slug by a Wedge from the Point of View of an Observer Stationed at the Moving Junction at A.

Conservation of momentum dictates the division of material between the jet and the slug. Let m be the total liner mass per unit length of the two collapsing planes (sides of the wedge) approaching the junction. Let m_j represent that part of the liner mass entering the jet and m_s represent that part entering the slug, so

$$m = m_j + m_s \quad . \tag{8}$$

Equating the horizontal momentum components entering and leaving the junction A of Figure 2 in the moving coordinate system yields

$$m V_2 \cos \beta = m_s V_2 - m_j V_2 \quad . \tag{9}$$

Solving equations (8) and (9) simultaneously gives

$$m_j = (m/2)\ (1 - \cos \beta) \ , \tag{10}$$

and

$$m_s = (m/2)\ (1 + \cos \beta) \quad . \tag{11}$$

According to this model, the velocities of the jet and slug and their cross-sectional areas are constant.

The analysis assumed a wedge configuration. A conical liner may be treated in the same way. In the conical case, the walls converge on the axis from all sides. The moving observer must travel at the same rate as in the case of the wedge. In order for the process to appear stationary to him, the total mass per unit distance along the axis must be constant. This is approximately true for a constant wall thickness liner. In reality, the liner wall thickness would have to be tapered to be inversely proportional to the distance from the apex.

For the detonation wave traveling parallel to the axis with speed U_D, as in Figure 1, equations (6) and (7) become, from equation (4),

$$V = \frac{U_D}{\cos \alpha} \sin (\beta - \alpha) \left\{ \csc \beta + \operatorname{ctn} \beta + \tan \left(\frac{\beta - \alpha}{2} \right) \right\} \ , \tag{12}$$

and

$$V_S = \frac{U_D}{\cos \alpha} \sin (\beta - \alpha) \left\{ \csc \beta + \operatorname{ctn} \beta + \tan \left(\frac{\beta - \alpha}{2} \right) \right\} \ , \tag{13}$$

The jet velocity, V, increases as α decreases, since β also decreases. The jet velocity approaches a maximum as $\alpha \to 0$, or $V = U_D$ {1 + cos + tan $\beta/2$} or $\beta \to 0$ as $\alpha \to 0$ so $V = 2\ U_D$, which means that the jet velocity cannot exceed

twice the detonation velocity. Also, as $\alpha \to \beta \to 0$, $V_S \to 0$. Note that as $\alpha \to 0$ the conical liner approaches a cylinder. Cylindrical lines are capable of generating high velocity (and low mass) jets.

For the hypothetical case of a conical wave front moving perpendicular to the surface of a conical liner such that the wave strikes all surfaces at the same time, $\beta = \alpha$ and the velocities of the jet and slug from equations (6) and (7) this time, become:

$$V = \frac{V_o}{\sin \alpha} (1 + \cos \alpha), \text{ and } \quad V_S = \frac{V_o}{\sin \alpha} (1 - \cos \alpha) .$$

With this type of wave front the jet velocity could be increased indefinitely by decreasing α. However, as $\alpha \to 0$, $V_o \to 0$, $m_j \to 0$ and the jet momentum

$$m_j V = \frac{m V_o}{2} \sin \alpha \to 0.$$

Finally, the theory of Birkhoff, et al predicts steady state jet and slug velocities as in equations (6) and (7) or equations (12) and (13) and masses as in equations (10) and (11) for conical or wedge shaped liners.

Comments on the Birkhoff, et al Solution

The steady state model provides quantitative agreement with flash radiograph experiments. The model tends to overpredict the jet velocities. Also, the jet possesses a velocity gradient from tip to tail and continues to stretch after the walls have collapsed giving a jet length greater than the slant height of the cone. The ductility of the jet under the intense pressures and dynamic collapse conditions is responsible, at least in part, for the elongation of the jet.

Important modifications have been made to the steady state theory of Birkhoff, et al notably by Pugh, Eichelberger and Rostoker [2] and Godunov, Deribas and Mali [3]. Pugh, et al, hereafter referred to as the PER theory, developed a non-steady theory based on the same concepts as Birkhoff, et al [1] except that the collapse velocities of the various liner elements are not the same for all elements but vary depending on the original position of the liner element. Thus, the collapse velocity decreases continuously from the cone apex to its base, producing significant jet elongation.

In the Soviet Union Godunov, et al [3] hereafter referred to as the visco-plastic theory, modified the steady state theory to include visco-plastic behavior, i.e., strain rate dependence.

Both of these models will be discussed in turn.

The PER Theory

The PER theory assumes a variable instead of a constant collapse velocity for the walls of the conical (or wedge) liner. This condition greatly improves the steady state theory results. The collapse velocity decreases from the apex to the base of the cone and Figure 3 illustrates the effect of these velocity variations. Note that as the collapse angle β increases, the jet velocity decreases, but the portion of the liner entering the jet increases. Figure 3 also shows how the decreasing collapse velocity increases β. As the detonation wave travels from P to Q along the conical surface APQ, the liner element originally at P collapses to J. The liner element originally at P', starts later and collapses slower than P, and arrives at M at the same time P arrives at J. The element P' would have reached N when P reached J if their collapse velocities were identical. Thus, with a constant collapse velocity, the surfaces remains conical, or QNJ is a straight line. However, since P' has a slower collapse velocity than P, the collapsing liner has the non-conical contour QMJ of Figure 3. The angle β is greater than B^+, the "steady-state" β. This assumes that each liner element is thin and not affected by its neighbors, consistent with the hydrodynamic assumption.

Next, Figure 4, which is similar to the steady state model of Birkhoff, et al, illustrates the flow situation. QJ is parallel to PA and equal in length to PQ. If the magnitudes of QP and QJ are equal to U, they represent the velocities in the moving coordinate system of the liner elements entering and leaving the region P. The vector $PJ = \vec{V}_o$ is the velocity of the collapsing liner element in a stationary system of coordinates. Thus, the arguments of Birkhoff, et al [1] are valid. The liner element does not move perpendicular to its original surface, but along a line that makes a small angle δ with the normal. This angle, from Figure 4, is

$$\sin \delta = V_o/2U \tag{14}$$

If V_o is constant, $\beta = \beta^+$ and $\delta = \left(\frac{\beta - \alpha}{2}\right)$ and all the PER results relax to the steady state model.

By the proper choice of coordinate systems, the geometric relationships at the moving junction (J) are shown in Figure 5. The axis of the cone is along JR and OJ is the element of the liner moving toward the axis. This element has a velocity $OJ = \underline{V}$ in moving coordinates. The velocity of the moving coordinate is $JR = V_1$. Using the law of sines from Figure 5 we have

$$V = V_o \cos (\alpha + \delta)/\sin \beta, \text{ and} \tag{15}$$

$$V_1 = V_o \cos (\beta - \alpha - \delta)/\sin \beta. \tag{16}$$

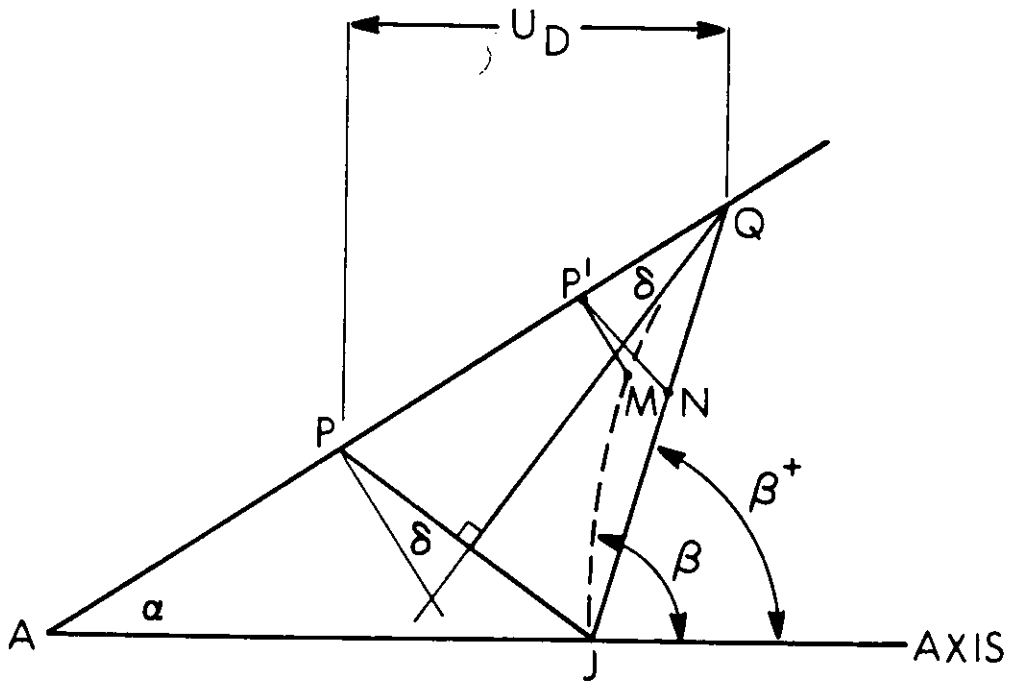

Figure 3. The Collapse Process for a Variable Collapse Velocity Liner, PER [2].

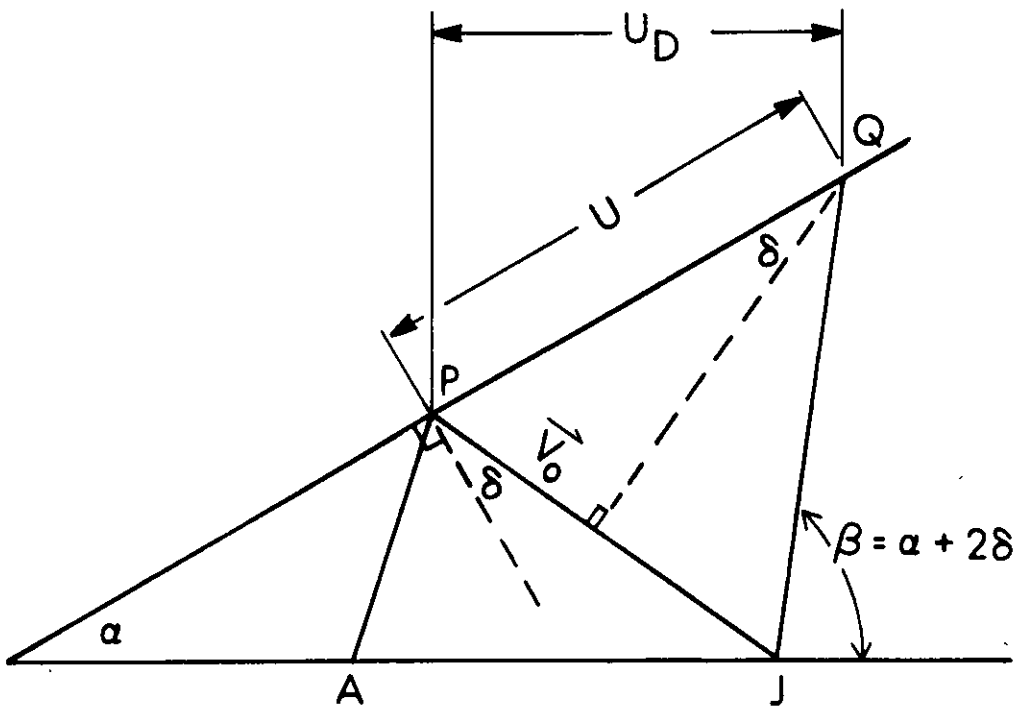

Figure 4. Velocity Vectors of a Collapsing Conical Liner Element, PER [2].

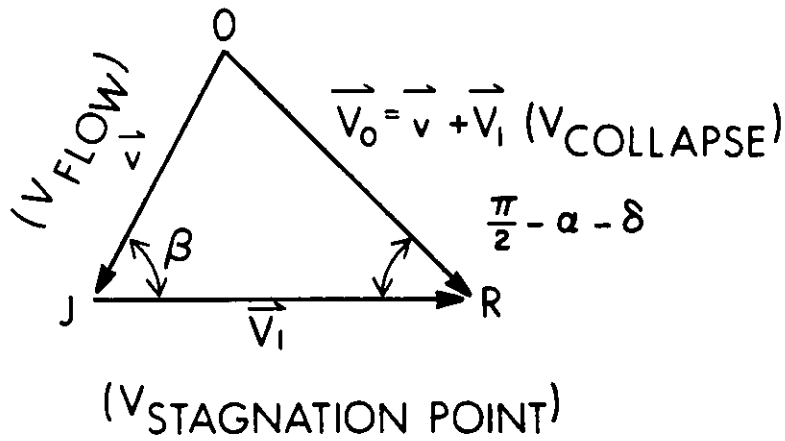

Figure 5. Relationship Between $\vec{V}_0$, The Liner Collapse Velocity, $\vec{v}$ The Collapse Velocity Relative To The Collision Point, and V_1 The Collision Point Velocity.

In fixed coordinates, the velocities of the jet and slug are $V_j = V_1 + V$ and $V_s = V_1 - V$, respectively. Using equations (15) and (16), along with some trigonometric manipulations, the jet and slug velocities become:

$$V_j = V_o \, (\csc \beta/2) \cos (\alpha + \delta - \beta/2) \text{ and} \tag{17}$$

$$V_s = V_o \, (\sec \beta/2) \sin (\alpha + \delta - \beta/2) \, , \tag{18}$$

respectively. Note that for $\beta = \beta^+ = \alpha + 2\delta$ we get the Birkhoff, et al jet and slug velocities, after some trigonometric manipulation.

We can eliminate from equations (17) and (18) using equation (14) to yield

$$V_j = V_o \, (\csc \beta/2) \cos (\alpha - \beta/2 + \sin^{-1} V_o/2u) \, , \tag{19}$$

$$\text{and } V_s = V_o \, (\sec \beta/2) \sin (\alpha - \beta/2 + \sin^{-1} V_o/2u) \, . \tag{20}$$

These equations are valid in either the steady-state case when V_o is constant or in the nonsteady case where V_o varies. In the steady state case, however, β could be expressed in terms of α, U and V_o and need not appear in the equation.

Of the four unknowns V_j, V_s, m_j and m_s we still need expressions for m_j and m_s. These equations follow from the conservation of mass and momentum, or, where m is the liner mass and m_j and m_s are the jet and slug masses respectively,

$$dm = dm_j + dm_s,$$

$$\frac{dm_j}{dm} = \sin^2 (\beta/2), \text{ and} \tag{21}$$

$$\frac{dm_s}{dm} = \cos^2 (\beta/2) \, . \tag{22}$$

Equations (21) and (22) are identical to the steady state theory, (equations (10) and (11)).

Equations (19), (20), (21) and (22) describe the mass separation and the velocities of each element of a conical liner. They depend upon the cone angle 2α and the detonation velocity $U_D = U \cos \alpha$, and on the collapse angle β and velocity V_o, both of which are variables.

From Figure 3, observe that the calculation of the angle β^+ would be more straight forward than the calculation of β, since V_o is different for each element of the liner and thus the contour of the collapsing liner is not straight but curved as line QMJ of Figure 3. Toward this end, let the cylindrical coordinates of M be (r, Z) and the coordinates of P' be (X tan α, X) in Figure 3. The coordinate directions are indicated in Figure 6. Then we have

$$Z = X + V_o\ (t - T) \sin A, \text{ and} \tag{23}$$

$$r = X \tan \alpha - V_o\ (t - T) \cos A\ , \tag{24}$$

where t is the elapsed time since the detonation wave passed the apex of the cone, $T = \frac{X}{U_D} = X/(u \cos \alpha)$ and the angle $A = \alpha + \delta$. The slope of the contour of the collapsing liner at any time t can be obtained from the $\partial r/\partial Z$ using equations (23) and (24) and some calculus. The time when a given element reaches the axis is found from equation (24) with r = 0 or

$$t - T = \frac{X \tan \alpha}{V_o \cos A}\ , \tag{25}$$

and $\partial r/\partial Z$ evaluated at r = 0 is the tan β. Using the Taylor relationship, equation (14), to simplify we have finally

$$\tan \beta = \frac{\sin \alpha + 2 \sin \delta \cos A - X \sin \alpha\ (1 - \tan A \tan \delta)\ V_o'/V_o}{\cos \alpha - 2 \sin \delta \sin A + X \sin \alpha\ (\tan A + \tan \delta)\ V_o'/V_o}\ . \tag{26}$$

Since $2\delta = \beta^+ - \alpha$ and $2A = \beta^+ + \alpha$, equation (26) may be further simplified to yield,

$$\tan \beta = \frac{\sin \beta^+ - X \sin \alpha\ (1 - \tan A \tan \delta)\ V_o'/V_o}{\cos \beta^+ + X \sin \alpha\ (\tan A + \tan \delta)\ V_o'/V_o}\ . \tag{27}$$

The term V'_o represents the partial derivative of V_o with respect to X.

The angle $\beta > \beta^+$ since $V'_o < 0$, i.e., the collapse velocity decreases from apex to base, and for cone angles (2α) which are not extremely large. Additional mathematical details and a more complete discussion can be found in Reference [2] and Eichelberger's Doctoral dissertation [4].

The reader should pay careful attention to the quadrant in which the angles calculated in equations (26) and (27) may fall. For angles in the

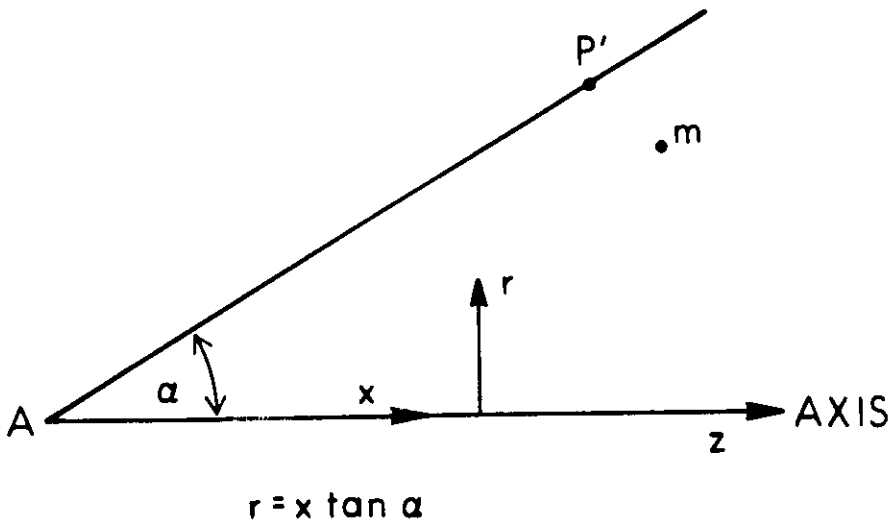

Figure 6. The Coordinate Directions.

second quadrant, minor modifications of the equation may be necessary and numerical algorithms that calculate trigonometric functions should be checked for the proper quadrant.

The PER theory provides expressions for m_j, m_s, V_j, V_s, δ and β, although the number of unknowns exceed the number of independent equations. Experimental evidence that verifies the model and the assumptions of the PER theory was given by Eichelberger and Pugh [5]. Also, Eichelberger [6] noted a systematic discrepency between the theoretical and experimental results. It was noted that the liner acceleration to the axis was assumed instantaneous in the PER model but the effect of a finite acceleration time would influence the value of β. In 1962, Allison and Vitali [7], in another classic paper, used a radioactive tracer technique and obtained excellent agreement between the PER theory and experiment.

Although Allison and Vitali obtained excellent agreement between the theory and experiment for a 42° unconfined copper cone, they were unable to get the PER theory to agree with the data from a 42° confined copper cone. Merendino and Jonas of the Ballistic Research Laboratory obtained similar data for a 60° unconfined copper cone which also failed to match the results of the PER model. G. H. Jonas recalls that Allison concluded that the PER model provides valid predictions for shallow angle, unconfined conical charges, but needs to be modified for wide angle or confined concial charges.

The PER theory constitutes the basis of all one-dimensional shaped charge jet formation models. Many extensions have been made to the PER model and auxiliary equations have been added to facilitate and extend the solution.

The plate bending angle or the Taylor angle (δ) can be determined by the formula proposed by Richter [8] and Defournaux [9]:

$$\frac{1}{2\delta} = \frac{1}{\phi_o} + \frac{\rho\,\varepsilon\,K}{e}\,, \tag{28}$$

where ρ and ε are the density and thickness of the liner wall, respectively, and e is the explosive thickness driving the liner. K and ϕ_o are constants which are determined from the type of explosive used and the angle of incidence, i, which the detonation wave makes with the liner. Equation (28) is coupled with the PER theory in the one-dimensional jet formation codes BASC [10, 11] and DESC [12] and probably others. Defournaux [9] also presents a good discussion of the liner collapse and formation which is an excellent supplement to the PER study. Kerdraon [13, 14] modified equation (28) by including terms to account for the effect of liner radius in imploding cylindrical liner charges.

The PER theory assumes the liner element is instantaneously accelerated to the axis as depicted in Figure 7(a). The first order correction is the assumption that the liner acceleration is constant over a finite period of time, as first proposed by Eichelberger [6] and used in Reference [12]. The velocity then increases linearly over a short period, as shown in Figure 7(b),

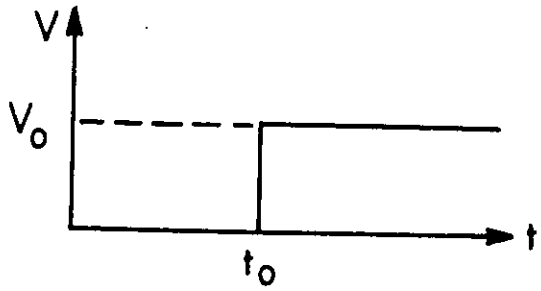

(a) Instantaneous Acceleration:

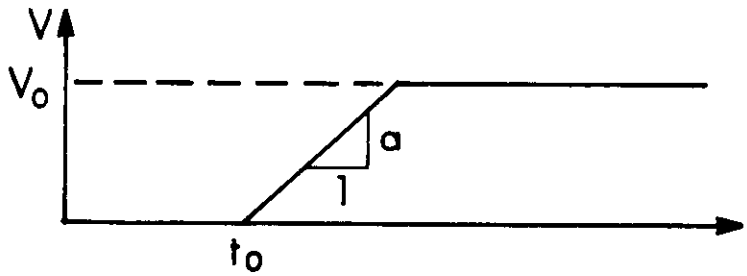

(b) Constant Acceleration:

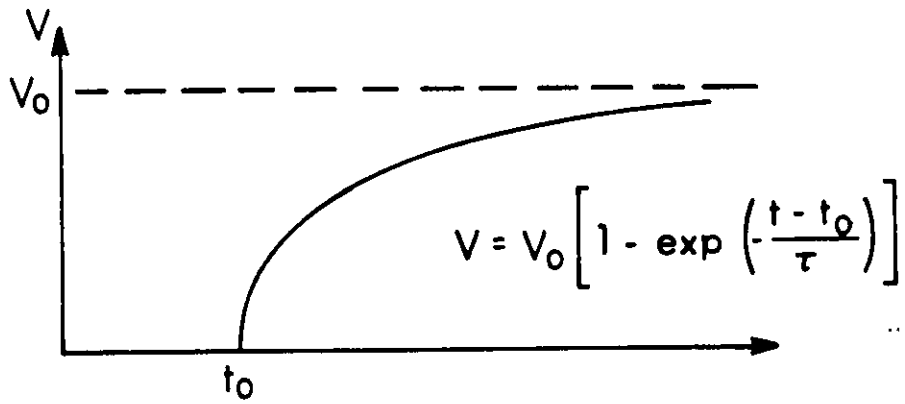

(c) Exponential Acceleration:

Figure 7. Liner Acceleration Histories, Chou and Flis [15].

until it reaches its final velocity or collapses on the axis. In Reference [12], the acceleration is given by

$$a = c \frac{P_{cJ}}{\rho \varepsilon},$$

where P_{cJ} is the Chapman-Jouguet pressure of the explosive, ρ and ε are the liner density and thickness, respectively, and c is an empirical constant. Figure 7 was taken from Chou and Flis [15].

Possibly, a more realistic form of the liner velocity history is given as an exponential form by Randers-Pehrson [16],

$$V(t) = V_o \left[1 - \exp\left(- \frac{t - t_o}{\tau} \right) \right],$$

as shown in Figure 7(c). This formula requires knowledge of the time constant, τ, for which Chou, et al [17] recommend

$$\tau = c_1 \frac{M V_o}{P_{cJ}} + c_2 ,$$

where M is the initial mass per unit area of the liner and c_1 and c_2 are empirical constants.

Considering the effects mentioned above, Chou, et al [17, 18] provide a more exact expression for the projection (Taylor)angle,

$$\delta = \frac{V_o}{2U} - \frac{1}{2} \tau V_o' + \frac{1}{4} \tau' V_o ,$$

where the prime denotes differentiation along the liner. Randers-Pehrson [16] proposed a similiar formula. Both References [16, 17, 18] show better agreement with the hydrocode results than the Taylor angle (steady state) formula for δ.

Models of this type, for acceleration to the liner axis during the collapse process, have been incorporated into the PER theory. These one dimensional computer programs use the analyses presented in this section to calculate the Taylor angle δ, the flow velocity V, the collapse velocity V_o, the stagnation point velocity V_1, the collapse velocity gradients V_o', the jet velocity V_j, the slug velocity V_s, the collapse angle β, the jet mass m_j, and the slug mass m_s. The input values consist of the complete geometry and material density of the conical liner and the explosive charge. The mode of initiation of the charge and the type of HE (high explosive) must be known to determine the HE density and detonation velocity. The mode of initiation determines the shape of the detonation wave (i.e., plane or spherical) and the angle of incidence of the detonation wave to the liner wall. Also, the

relative distribution of the kinetic energy entering the jet and slug are given as

$$\frac{dE_j}{dE} = \cos^2 (\alpha + \delta - \beta/2) \tag{29}$$

and

$$\frac{dE_s}{dE} = \sin^2 (\delta + \delta - \ /2) \tag{30}$$

respectively.

The stretching jet radius is also calculated assuming the jet to be circular in cross-section. In addition, the material near the liner apex does not have sufficient time to reach its theoretical collapse velocity and hence the earliest formed portions of the jet have lower velocities than the jet material formed behind them. This "piling up" of jet particles causes the formation of the inverse velocity gradient and this coalescence of particles is treated separately to calculate the jet tip velocity. All these effects are included in most jet formation codes such as BASC [10, 11] along with certain other parameters such as momentums, jet strains and strain rates.

To calculate the strain, jet length and jet radius, it is necessary to relate the position of a jet element back to its original position in the liner. This was done by Carleone and Chou by using a simple Lagrangian coordinate definition [19]. The coordinate x is used for the axial liner position and the coordinate ζ for the position of the jet as shown in Figure 8. The jet position is given as

$$\zeta (x, t) = Z (x) + (t - t_o) V_j (x), \tag{31}$$

where t_o is the time when the liner element first arrives at the axis, Z (x) is the location of the formation, and V_j (x) is the jet velocity. Note that V_j is a function of a liner position but ζ is a function of both liner position and time. Outside the inverse velocity gradient region, a liner element with a smaller x always proceeds (is ahead of, or has a larger ζ than) an element with a larger x. The strain rate, η, is given as

$$\eta = \lim_{x_2 \to x_1} \frac{\Delta\zeta - \zeta_o}{\Delta\zeta} = \frac{(\partial\zeta/\partial x)_t}{(\partial\zeta/\partial x)_{to}} - 1 \tag{32}$$

Equations (31) and (32), with the statements made earlier, allow the jet length and radius to be calculated.

Special techniques are necessary to calculate the jet tip velocity as discussed earlier. The PER theory indicates that the jet velocity decreases

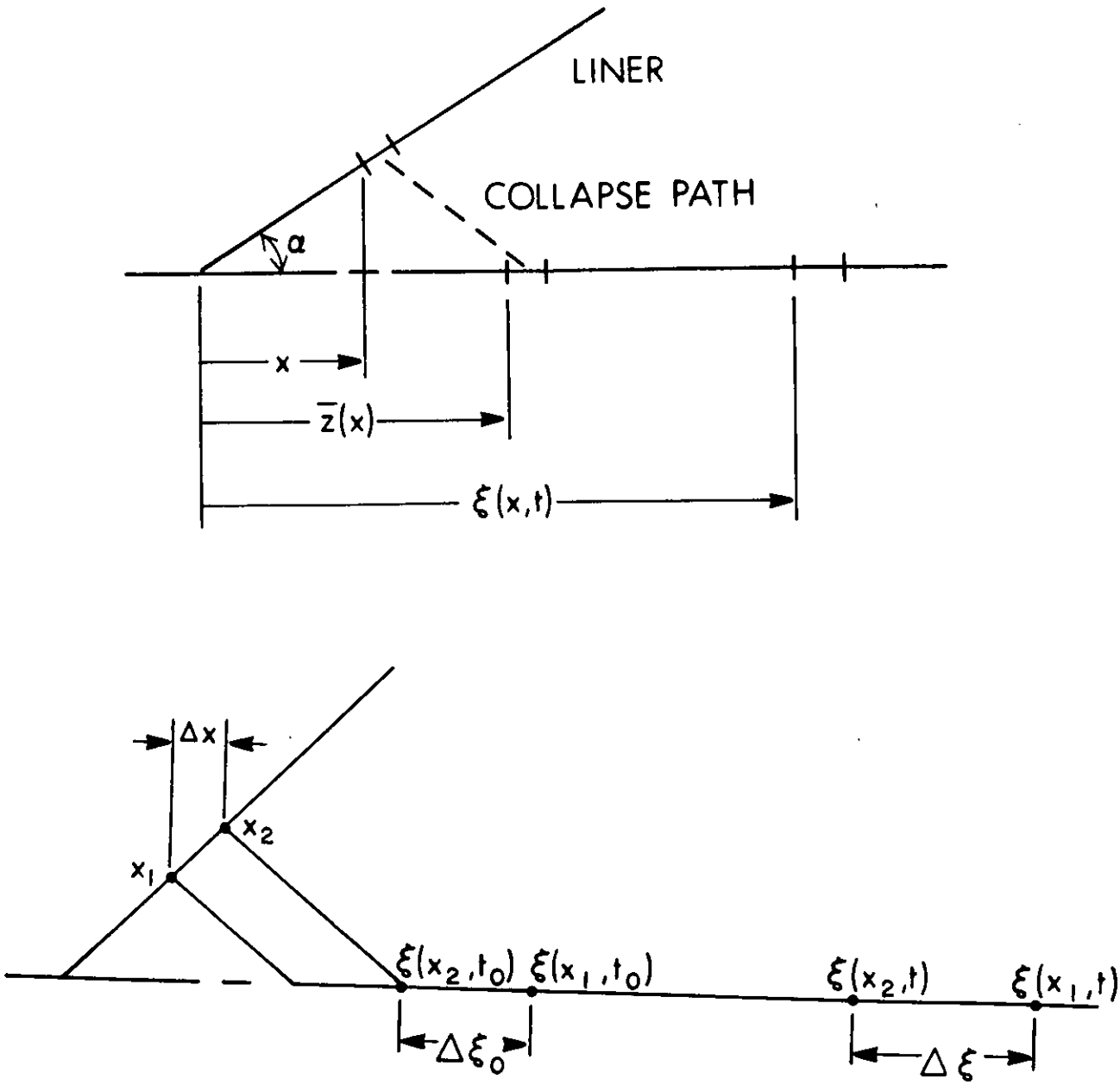

Figure 8. Relations Between the Liner Coordinate x, and the Jet Coordinate ξ Chou and Flis [15].

monotonically from tip to tail. Thus, the gradient of the jet velocity is negative with respect to the original liner position or positive with respect to the jet position. As mentioned earlier, liner elements near the apex collide on the axis before reaching their final collapse velocity, V_o. This reduced collapse velocity results in a reduced jet speed, so that the jet velocity gradient with respect to the liner position is positive. This is termed the inverse-velocity gradient [20]. In the apex region, each jet element has a higher velocity than the one ahead of it, causing a "piling-up" of jet mass. This piled up mass forms the jet tip as verified experimentally [21]. For conventional conical charges, the first 30 to 40% of the liner from the theoretical apex forms the tip of the jet. The tip has a much larger radius than the rest of the jet.

Figure 9 shows the inverse-velocity gradient with respect to X, the liner element position. The velocity of the jet tip is given as

$$V_{jo} = V_{TIP} = \frac{\int_o^{X_{TIP}} V_j \frac{dm_j}{dX} dX}{\int_o^{X_{TIP}} \frac{dm_j}{dX} dx}, \tag{33}$$

based on the conservation of momentum.

Recently, Hirsch [22] extended the PER model to include non-steady effects at the collision point (or formation point) by assuming that relative to this point, the jet and slug velocities, V_j and V_s, are not equal to the incoming liner velocity V as the PER theory assumed from the Bernoulli equation.

Other studies involve modifications or extentions of the PER theory, such as Perez, et al [23] who modified PER to account for two-dimensional effects of the flow near the collapse axis, and Hirsch [24]. Leidel [25] provides an overview of the PER model and analyzes annular cutting charges, or cookie cutter warheads as first conceived by Glass, et al [26]. Harrison [27, 28] compares the simple one-dimensional models to hydrocodes and experimental data. These methods are also related to warhead design.

Other shaped charge publications of interest include Hornemann and Senf [29] on wide angle cones, Van Thiel and Levatin [30], Trinks [31] for his shaped charge discussion and historical inferences, Rostoker [32], Simon and DiPersio [33], and the USSR studies by Novikov [34] and Titov [35]. These papers relate to jet formation and collapse and related topics pursuing the concepts we have reviewed so far. An excellent Soviet paper was published by Ivanova and Rozantseva [36] which is very long and very informative. It provides a detailed discussion and derivation of the PER theory and simple penetration models including experimental data and numerous flash radiographs or x-ray photographs of shaped charge jets. The USSR models are discussed in more detail later in the text.

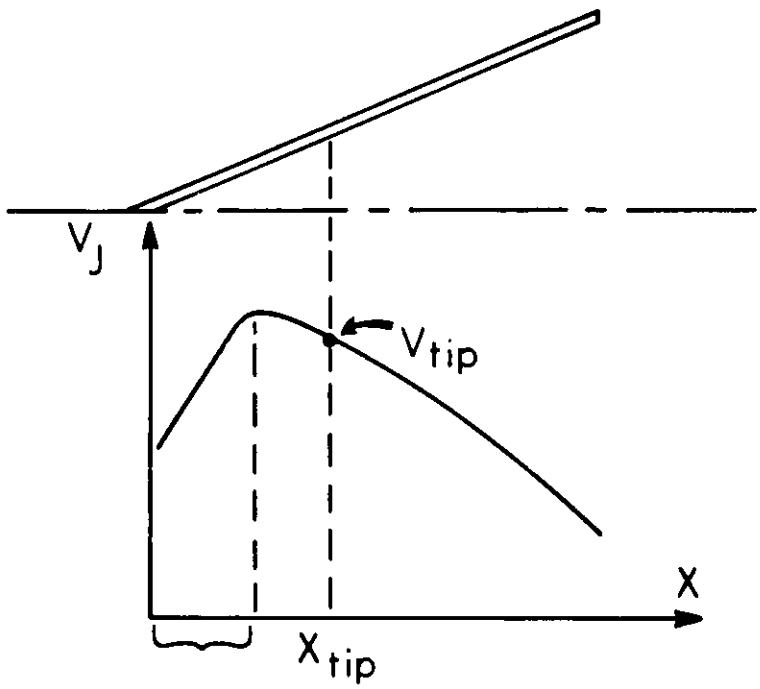

Figure 9. A Typical Jet Velocity Distribution Curve Showing That the Inverse-Velocity Gradient Region Near the Apex of the Liner Forms the Jet Tip Particle, Chou and Flis [15].

Excellent flash radiography data and analysis thereof is given by Breidenbach [37] and by Heine-Geldern and Pugh [38]. Classical papers on jets and jet formation are given by Harlow and Pracht [39] and on collapsing cylinders by Koski, et al [40].

Zernow and Simon [41], investigated the behavior of jets from several different shaped charge materials. Aseltine [42] studied the effect of several different warhead asymmetries on the behavior and performance of shaped charge jets. Merendino, et al [43] altered a shaped charge liner, i.e., inhibited the collapse of the liner to obtain a massive hypervelocity pellet in lieu of a jet. Other studies regarding shaped-charge analyses are given in the recent papers by Robinson [44, 45] and Lee [46].

Kolsky, et al [47] studied the formation and penetration of conical shaped charge liners. Kolsky [48] continued his studies regarding the formation and penetration of hemispherical shaped charge liners. The formation and collapse of hemispherical liners were also studied via hydrocodes by Kiwan and Arbuckle [49], Arbuckle, et al [50], Chou, et al [51] Aseltine, et al [52], Chou, et al [53], and Lacetera and Walters [54].

Studies on the formation of hemispherical shaped charge liners were presented by Lee [46] Singh [55], Shepherd [56] and Grace [57]. A closed form analytical expression (analogous to the PER theory for conical liners) for the collapse and formation of hemispherical shaped-charge liners does not currently exist.

REFERENCES
(Section IX)

1. G. Birkhoff, D. Mac Dougall, E. Pugh, G. Taylor, "Explosives with Lined Cavities, " J. of Applied Physics, Vol. 19, No. 6, June 1948.

2. E. Pugh, R. Eichelberger and N. Rostoker, "Theory of Jet Formation by Charges with Lined Conical Cavities," J. of Appl. Physics, Vol. 23, No. 5, May 1952.

3. S. K. Godunov, A. A. Deribas and V. I. Mali, "Influence of Material Viscosity on the Jet Formation Process During Collisions of Metal Plates," Translated from Fizika Goreniya i Vzryva, Vol. 11, No. 1, pp. 3 - 18, January - February 1975.

4. R. J. Eichelberger, "Re-examination of the Theories of Jet Formation and Target Penetration by Lined Cavity Charges," CEL Report No. 1., June 1954, (Dissertation of R. J. Eichelberger).

5. R. J. Eichelberger and E. M. Pugh, "Experimental Verification of the Theory of Jet Formation by Charges with Lined Conical Cavities," J. Appl. Phys., Vol. 23, No. 5, April 1952.

6. R. J. Eichelberger, "Re-examination of the Non-Steady Theory of Formation by Lined Cavity Charges," J. Appl Phys., Vol 26, No. 4, April 1955.

7. F. E. Allison and R. Vitali, "An Application of the Jet Formation Theory to a 105mm Shaped Charge," Ballistic Research Laboratory Report No. 1165, March 1962.

8. H. Richter, "On the Theory of Shaped Charges: Motion of Thin Layers of Plastic Material on the Surface of a Plane Explosive," Note Technique ILS No. 6a/48, 1948.

9. M. Defournaux, "Theorie Hydrodynamique des Charges Creuses," Memorial de l'artillerie Francaise, T. 44, 2e Fasc., pp. 293 - 334, 1970.

10. J. T. Harrison, "Improved Analytical Shaped Charge Code: BASC," Ballistic Research Laboratory Technical Report No. ARBRL-TR-02300, March 1981.

11. J. T. Harrison, "BASC, An Analytical Code for Calculating Shaped Charge Properties," Proc. 6th Int. Symp. on Ballistics, Orlando, FL, 27 - 29 October 1981.

12. J. Carleone, P. C. Chou and C. A. Tanzio, "User's Manual for DESC-1, A One-Dimensional Computer Code to Model Shaped Charge Liner Collapse, Jet Formation, and Jet Properties," Dyna East Corp. Technical Report No. DE-TR-75-4, December 1975.

13. A. Kerdraon, "Etude de la Projection Cylindrique Convergente," ISL Symposium, October 1975.

14. A. Kerdraon, "Study of Converging Cylindrical Projection," Proc. 3rd Int. Symp. on Ballistics, Karlsruhe, W. Germany, 23 - 25 March 1977.

15. P. C. Chou and W. J. Flis, "Recent Developments in Shaped Charge Technology," Private Correspondence, April 1984. (Manuscript prepared for M. Held, MBB, Germany, and presented at MBB Schrobenhausen, West Germany, September 1983).

16. G. Randers-Pehrson, "An Improved Equation for Calculating Fragment Protection Angle," Proc. 2nd Int. Symp. on Ballistics, Daytona Beach, FL, 9 - 11 March 1976.

17. P. C. Chou, et al, "Improved Formulas for Velocity, Acceleration, and Projection Angle of Explosively Driven Liners," Proc. 6th Int. Symp. on Ballistics, Orlando, FL, 27 - 29 October.

18. P. C. Chou, E. Hirsch, R. D. Ciccarelli, "An Unsteady Taylor Angle Formula for Liner Collapse," Ballistic Research Laboratory Contractor Report, ARBRL-CR-00461, 1981.

19. J. Carleone and P. C. Chou, "A One-Dimensional Theory to Predict the Strain and Radius of Shaped Charge Jets," Proc. 1st Int. Symp. on Ballistics, Orlando, FL, 13 - 15 November 1974.

20. A. R. Kiwan and H. Wisniewski, "Theory and Computations of Collapse and Jet Velocities of Metallic Shaped Charge Liners," Ballistic Research Laboratory Report No. 1620, November 1972.

21. P. C. Chou, J. Carleone, and R. Jameson, "The Tip Origin of a Shaped Charge Jet," Propellants and Explosives, 2, pp. 126 - 130, 1977.

22. E. Hirsch, "An Analytical Model for the Nonsteady Shaped Charge Jet Formation Junction," Proc. 7th Int. Symp. on Ballistics, Karlsruhe, W. Germany, March 1977.

23. E. Perez, C. Fauquignon and P. Chanteret, "Fundamental Studies of Shaped Charge Mechanisms," Proc. 3rd Int. Symp. on Ballistics, Karlsruhe, W. Germany, March 1977.

24. Eitan Hirsch, "A Simple Representation of the Pugh, Eichelberger, and Rostoker Solution to the Shaped Charge Jet Formation Problem," J. of Appl. Phys., Vol. 50, No. 7, July 1979.

25. David J. Leidel, "A Design Study of an Annular-Jet Charge for Explosive Cutting," Doctoral Dissertation, Drexel University, Philadelphia, Pa., June 1978.

26. C. M. Glass, S. Kronman, S. K. Golaski, "The Cookie Cutter Warhead," Ballistic Research Laboratory Report No. 1455, October 1969.

27. J. T. Harrison, "A Comparison Between the Eulerian, Hydrodynamic Computer Code (BRLSC) and Experimental Collapse of a Shaped Charge Liner," Memorandum Report ARBRL-MR-02841, June 1978.

28. J. T. Harrison and R. R. Karpp, "Terminal Ballistic Application of Hydrodynamic Computer Code Calculations," Ballistic Research Laboratory Report 1984, April 1977.

29. U. Hornemann and H. Senf, "Parameter Studies of 120° Flat-Cone Shaped Charges," Proc. 3rd Int. Symp. on Ballistics, Weil am Rhein, June 1971, FSTC-HT-23-797-73, September 1974.

30. M. Van Thiel and J. Levatin, "Jet Formation Experiments and Computations with a Lagrange Code," LLNL, UCRL-82834, September 1978.

31. Dr. Trinks, "German WW II Calculation Methods for Shaped Charges," MBB Report No. SOB-583, MWD-DEA G 1060 Meeting at ISL/Weil, FSTC 1198-76, October 1975.

32. N. Rostoker, "The Formation of Craters by High-Speed Particles," Meteoritics, Vol. 1, No. 1, pp. 11 - 27, 1953.

33. J. Simon and R. DiPersio, "Jet Formation and Utilization," Proc. of Behavior and Utilization of Explosives in Engineering Design, edited by L. Davison and J. E. Kennedy, Published by N. Mexico Section of the ASME.

34. N. P. Novikov, "High-Speed Shaped Jets," PMTF, No. 6, pp. 22 - 28, FSTC-HT-1384-82, 1962.

35. V. M. Titov, "Possible Regimes for Hydrodynamic Cumulation During the Collapse of a Casing," Doklady Academic Nauk SSSR, Vol. 247, No. 5, pp. 1082 - 1084, 1979.

36. V. Ivanova and V. Rozantseva, "Theoretical and Experimental Investigation of the Shaped-Charge Effect," Mekhanika, Sbrorniki Penevodov i Obzonov Inostrannoy Periodicheskoy Literatury, Issue 4 (2), pp. 51 - 105, FSTC-HT-426-82, 1953.

37. H. I. Breidenbach, "The Evolution of Jets From Cavity Charges as Shown by Flash Radiographs," Ballistic Research Laboratory Report No. 808, April 1952.

38. R. V. Heine-Geldern and E. M. Pugh, "The Photography of High-Speed Metallic Jets," Meteoritics, Vol. 1, No. 1, 1953, pp. 5 - 10.

39. F. H. Harlow and W. E. Pracht, "Formation and Penetration of High-Speed Collapse Jets," Physics of Fluids, Vol. 9, No. 10, October 1966.

40. W. S. Koski, F. A. Lucy, R. G. Schreffler and F. J. Willig, "Fast Jets From Collapsing Cylinders," J. of Appl Physics, Vol. 23, No. 12, pp. 1300 - 1305. December 1952.

41. L. Zernow and J. Simon, "High Strain Rate Plasticity of Liner Materials and Jet Behavior," Ballistic Research Laboratory Report No. 954, August 1955.

42. C. L. Aseltine, "Analytical Predictions of the Effect of Warhead Asymmetrics on Shaped Charge Jets," Technical Report ARBRL-TR-02214, February 1980.

43. A. Merendino, J. M. Regan and S. Kronman, "A Method of Obtaining a Massive Hypervelocity Pellet From a Shaped Charge Jet," Ballistic Research Laboratory Memorandum Report No. 1508, August 1963.

44. A. C. Robinson, "Asymptotic Formulas for the Motion of Shaped Charge Liners," Sandia Report SAND 84-1712, Unlimited Release UC-35, September 1984.

45. A. C. Robinson, "SCAP - A Shaped Charge Analysis Program - User's Manual for SCAP 1.0," Sandia Report SAND 85-0708, Unlimited Release UC-35, April 1985.

46. Wen Ho Lee, "High Explosive Modeling In 2D Euler Code for Shaped Charge Problems," Los Alamos National Laboratory Report LA-UR-85-2954, 1985.

47. H. Kolsky, C. I. Snow and A. C. Shearman, "A Study of the Mechanism of Munroe Charges, Part I - Charges with Conical Liners," Research Supplement, 2-2, pp. 89 - 95, London, 1949.

48. H. Kolsky, "A Study of the Mechanism of Munroe Charges, Part II - Charges with Hemispherical Liners," Research Supplement, 2-2, pp. 96 - 98, London, 1949.

49. A. R. Kiwan and A. L. Arbuckle, "Study of Liner Collapse, Jet Formation and Characteristics from Implosive Shaped Charge Systems," Ballistic Research Laboratory Report 2028, November 1977.

50. A. L. Arbuckle, W. P. Walters and C. L. Aseltine, "Analysis of Uniform Wall and Tapered Hemispherical Liners with Several Explosive Confinement Geometries," ARBRL-TR-02222, March 1980.

51. P. C. Chou, R. D. Ciccarelli, A. L. Arbuckle and W. P. Walters, "Jet Formation of an Implosively Loaded Hemispherical Liner," Contract Report, ARBRL-CR-00470, September 1981.

52. C. L. Aseltine, W. P. Walters, A. L. Arbuckle and J. E. Lacetera, "Hemispherical Shaped Charges Utilizing Tapered Liners," Proc. 4th Int. Symp. on Ballistics, Monterey, CA, 17 - 19 October 1978.

53. P. C. Chou, R. D. Ciccarelli and W. P. Walters, "The Formation of Jets from Hemispherical Liner Warheads," Proc. 7th Int. Symp. on Ballistics, The Hague, Netherlands, 19 - 21 April 1983.

54. J. E. Lacetera and W. P. Walters, "Theoretical and Experimental Studies of Hemispherical Shaped-Charge Liners," Transactions of the Twenty-Fifth Conference of Army Mathematicians, ARO Report 80-1, held at Johns Hopkins University, June 1979.

55. Sampooran Singh, "On the Jet Formation by Explosives with Lined Hemispherical Cavities," Research Notes, Proc. Phys. Soc., Vol. 68B, London, pp. 785 - 789, October 1, 1955.

56. W. C. F. Shepherd, "Strength of High Explosives and Effects Due to Shape," Chapter V of Science of Explosives, edited by C. E. H. Bawn and G. Rotter, Published for the Ministry of Supply, London, 1956.

57. F. I. Grace, S. K. Golaski and B. R. Scott, "The Nature of Jets from Hemispherical Lined Explosive Charges," Proc. of 8th Int. Symp. on Ballistics, Orlando, FL, Oct. 1984.

X. THE VISCO-PLASTIC THEORY

Other studies involving the collapse and formation of shaped charge liners were advanced by Soviet researchers. Returning to the collapse of conical liners or wedges, the USSR used the results of Birkhoff, or perhaps Lavrent'ev, as the basis for their studies, Lavrent'ev [1] having claimed prior discovery. In any case, the results of Birkhoff or Lavrent'ev were extended to include visco-plastic effects by Godunov, et al [2].

The visco-plastic model follows from References [1 - 7] and a detailed derivation and discussion of this model is given by Walters [8]. The basic viscoplastic theory [1 - 7] does not include transient effects. Typically, in the axisymmetric hydrocode models used at the BRL and other agencies, compressible flow is assumed and the material constitutive relationships are based on elastic-perfectly plastic, work hardening models or more sophisticated models, e.g. [9, 10]. The USSR analytical models typically assume an incompressible flow, but use a rate-dependent, visco-plastic material constitutive equation [2, 3, 11]. This equation is usually of the form $\sigma = \sigma_y + \mu\dot{\varepsilon}$, where the stress σ, is related to the strain rate $\dot{\varepsilon}$, by the yield stress σ_y and the constant dynamic viscosity coefficient, μ.

Thus, the visco-plastic models require a knowledge of the dynamic viscosity coefficient and many USSR investigators have deduced viscosity coefficients from experimental measurements under shock loading conditions. Walters [11] summarizes many of the experimental viscosity values. Additional data related to viscosity measurements and the collapse of metallic bodies by high explosives are given by References [12 - 34]. Material viscosity values have also been experimentally determined in the US [11, 35], under shock loading conditions. The viscosity values deduced from various experimental measurements depend on many parameters, primarily strain rate, pressure and temperature. Thus, the viscosity coefficient is not constant. In fact, for solid metals, the dynamic viscosity may range from typically 10 to 10^5 Pa-sec (10^2 - 10^6 poise) depending on the strain rate, pressure and temperature and the experimental method used to measure μ. Usually, the US measured viscosity values under shock loading conditions may be as much as two orders-of-magnitude lower than the USSR measured viscosity values [11 - 35]. The uncertainty in the US measured μ values is $\pm$ a factor of ten. The USSR methods may even have a greater amount of uncertainty. Experimental determination of μ in the US, as performed by Chhabildas and Asay [35], involves measurement of the shock rise time via velocity interferometry. The maximum stress is taken to be proportional to the strain rate, $\sigma \sim \mu\dot{\varepsilon}$, and the maximum stress is determined from the Rayleigh line and the shock Hugoniot pressures. The strain rate is calculated as the strain induced by the shock divided by the shock rise time, which is resolution limited. The time resolution is limited to 1 to 3 nanoseconds [35].

The USSR shaped-charge liner collapse model includes the influence of viscosity on the jet formation process. A jet formation criterion is derived which is based not on taking account of the compressibility effects or shock

effects as in References [36] or [37], or on consideration of a critical Mach number as in Reference [38], but on taking into account the viscous properties of metals.

Following Godunov, et al [2], an appropriate method is used to estimate the effect of viscosity in the plane problem (two-dimensional) of jet collisions. The fluid is incompressible, the motion irrotational and steady state, and the coefficient of viscosity is constant. Then the solutions of Euler equations automatically satisfy the Navier-Stokes equations of motion and the difference between the problems of ideal and viscous jet collisions is the conditions on the free surface of the jet. The flow fields are taken to be Newtonian. For the flow fields to agree in the ideal and viscous flow problems, some forces must be applied to the free surface in the viscous flow case [2]. Consideration of the influence of these forces on the flow resulting from the collision between jets of an ideal fluid will provide a measure of the influence of viscosity in the jet formation problem [2].

The formation of a reverse jet (slug) is possible only if the horizontal component of the viscous force, acting on the free surfaces of the reverse jet, is less that the force resulting from the symmetric collision of two plane fluid jets [2]. This inequality allows one to define a Reynolds number and a critical Reynolds number for jet formation.

The visco-plastic shaped-charge jet collapse model derived by Godunov [2] relaxes to the classical US models reviewed earlier when the dynamic viscosity is zero. Basically, the visco-plastic model yields a lower jet velocity and a lower flow velocity than the US models. However, the visco-plastic model predicts a higher slug velocity than the US models. The USSR (visco-plastic) criterion to form a coherent jet is that the Reynolds number,

$$Re = \frac{tu\sin^2\beta}{\nu\,(1 - \sin\beta)} \qquad (1)$$

be greater than two. The wall thickness is denoted by t, ν is the kinematic viscosity, 2β is the collision angle, and u is the inviscid flow velocity as given by Defourneaux or the PER model for example. The Reynolds number greater than two criterion is based on experimental observations [2, 11]. Detailed USSR formulae for the jet strain rate, jet velocity, viscid flow velocity, and slug velocity, are given in References [2, 11]. Also, by setting Re = 2 in Equation 1, an expression for the critical flow velocity as a function of β, t and ν can be obtained. If the critical flow velocity is greater than the flow velocity, a coherent jet will not form. Simonov [6] and others [11 - 14, 18, 20, 21, 24, 27, 28, 31, 32] define collapse angles for the transition from the jet regime to the jetless regime for explosive bonding applications. These USSR investigators defined collapse angles below which only incoherent jets will form and collapse angles below which no jet at all will form. Walsh, et al [36] served as the basis for many of the USSR studies.

For the transient flow (PER) case, the stagnation point velocity (V_c) is given as

$$V_c = D_a \left[\frac{\sin(\beta - \alpha)-\sin(\beta - \alpha - \phi)}{\sin\beta}\right], \tag{2}$$

where D_a is the speed of the detonation wave, 2α is the conical liner apex angle and $\phi = 2\delta$ is the plate bending angle. Equation 2 is used in both the PER and visco-plastic models. The flow velocity is given by

$$U = D_a \left[\frac{\sin(\alpha + \phi)-\sin\alpha}{\sin\beta}\right] \tag{3}$$

in the PER model. The visco-plastic flow velocity is

$$U_2 = U\ (1 - 2/Re)^{\frac{1}{2}} \tag{4}$$

from Reference [2] for $Re > 2$. Also, $U_2 = U$ when the dynamic viscosity, μ, is zero.

In the PER model, the jet velocity and slug velocity are, respectively,

$$V_j = V_c + U, \tag{5}$$

and

$$V_s = V_c - U. \tag{6}$$

In the visco-plastic model, the jet and slug velocities are

$$V_j = V_c + U_2, \tag{7}$$

and

$$V_s = V_c - U_2. \tag{8}$$

In both models,

$$V_j + V_s = 2V_c.$$

For steady state collapse, analogous formulae are available from Godunov and Birkhoff.

For both the steady state and transient version of the visco-plastic theory, the US theory can be obtained by setting the dynamic viscosity, μ, or the kinematic viscosity, $\nu = \mu/\rho$ equal to zero. Walters and Harrison [8]

discuss the PER and the visco-plastic models and comparison is made to the experimental data obtained by Allison and Vitali [39].

The strain rates calculated by the visco-plastic model [2] are of the order of 10^6/s and show little variation with liner element position. Chou and Caleone [40] calculated strain rates for a 81 mm diameter precision charge with a copper conical liner with a 42^o apex angle and a 1.9 mm wall thickness and found a larger variation of strain rate with a liner element position including liner elements in both compression and tension. The peak strain rate was 10^5/s. Experimental measurements of the strain rate of collapsing liners are not available, but Bauer and Bless [41] measured the strain rate of exploding copper tubes to be about 10^4/s and Walters deduced the strain rates of stretching jets to be of the order of 10^4/s.

Comments on Jet Coherency

The visco-plastic coherent jet or incoherent jet criterion is based on a critical Reynolds number being greater than 2 [2], or some other number [44]. The US criterion is inviscid, but compressibility effects are taken into consideration in the determination of the cohesiveness of the jet.

Walsh, et al [36] studied the compressibility effect in the jet formation process as related to the oblique impact of explosively driven plates. The symmetric plate collision as viewed from a moving coordinate system, reduces to a flow field analogous to two impinging streams. Walsh, et al [36] concluded that jetting always occurs if the fluid is incompressible or if the collision velocity in the moving coordinate system is subsonic. For supersonic flow, jetting always occurs if $\beta > \beta_c$, where β_c is the critical turning angle for an attached oblique shock wave at the collision velocity. Walsh, et al [36] did not address jet cohesiveness per se, since their primary interest was explosive bonding. Cowan and Holtzmann [45] present additional flow criteria for explosive bonding.

In the studies of Chou, et al [37, 46], jetting criteria for plane axisymmetric cases are presented along with a measure of the jet quality. From References [37] and [46], Chou states:

1. For subsonic collisions (or the collision velocity $V < C$, the material bulk speed of sound) a solid coherent jet always forms;

2. For supersonic collisions ($V > C$) jetting occurs if $\beta > \beta_c$, but the jet is not coherent. The angle β_c is the maximum angle that an attached shock wave can form at a prescribed supersonic velocity, V; and

3. For supersonic collisions ($V > C$) but $\beta < \beta_c$, a jet will not be formed.

For shaped charge applications, the major criterion for jetting is that the formation process be subsonic. Otherwise, the jet will be incoherent and spread out radially.

The speed of sound referred to is usually taken to be the bulk speed of sound of the material as opposed to a longitudinal or transverse shear speed of sound. The appropriate speed of sound, as well as its exact value under the extreme pressures and temperatures encountered in the formation region is not well known. Also, the actual flow field is compressible and two-dimensional (at least) and hence the subsonic collision condition is useful only as a general principle. In practice, it has been observed that the value of the critical Mach number based on the static bulk speed of sound is about 1.2 for conical copper liners, Harrison [38, 47], and Walters and Harrison [8]. In other words, the liner velocity divided by the bulk speed of sound, i.e., the Mach number, could be as high as 1.2 and still achieve a cohesive jet for a conical, copper liner. A flow velocity of 4.8 km/s (1.23 times the bulk speed of sound of copper) is the calculated flow velocity above which 20° copper liners have been observed to have incoherent jet tips [38]. Figure 1 shows a flash radiography photograph of a copper, coherent and incoherent jet.

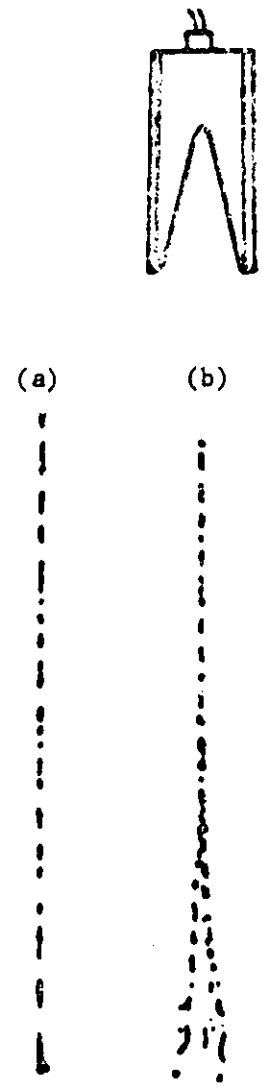

Figure 1. Radiographs of Jets From Two Typical Conical Charges.
(a) 40° Copper-lined Charge, Subsonic Collision, Coherent Jet, and
(b) 20° Copper-lined Charge, Supersonic Collision, Incoherent Jet.

REFERENCES
(Section X)

1. M. A. Lavrent'ev "A Cumulative Charge and the Principle of its Work," Usp. Mat. Nauk., V. 12, No. 4, 1957.

2. S. K. Godunov, A. A Deribas and V. I. Mali, "Influence of Material Viscosity on the Jet Formation Process During Collisions of Metal Plates," Fizika Goreniya i Vzryva, V. 11, No. 1, January - February 1975.

3. S. K. Godunov and A. A. Deribas, "Jet Formation Upon Collision of Metals," Doklady Akademii Nauk. SSSR, V. 202, No. 5, February 1972.

4. A. A. Deribas, V. M. Kudinov, F. I. Matveenkov and V. A. Simonov, "Determination of the Impact Parameters of Flat Plates in Explosive Welding," Fizika Goreniya i Vzryva, V. 3, No. 2, 1967.

5. N. P. Novikov, "Certain Properties of High-Speed Cumulative Jets," Zh. Prikladnoy Mekhaniki i Tekhnicheskvy Fiziki, No. 1, 1963.

6. V. A. Simonov, "Flows Due to an Incident Impact Wave on a Wedge Shaped Cavity," Fizika Goreniva i Vzryvs, V. 7, No. 2, April - June 1971.

7. S. K. Godunov, A. A. Deribas, A. V. Zabrodin and N. S. Kozin, "Hydrodynamic Effects in Colliding Solids," J. of Comp. Phys., V. 5, 1970.

8. W. P. Walters and J. T. Harrison, "Modeling of the Shaped-Charge Jet Formation," Proceedings of the Army Symposium on Solid Mechanics, 1980 - Designing for Extremes: Environment, Loading, and Structural Behavior, AMMRC MS 80-4, September 1980.

9. D. J. Steinberg and R. W. Sharp, "An Elastic-Viscoplastic Constitutive Model for Metals," LLNL UCRL-85086, October 1980.

10. D. J. Steinberg, S. G. Cochran and M. W. Giunan, "A Constitutive Model for Metals Applicable at High Strain Rate," J. Appl. Phys., 51 (3), pp. 1498 - 1504, March 1980.

11. W. P. Walters, "Influence of Material Viscosity on the Theory of Shaped-Charge Jet Formation," BRL Memorandum Report, ARBRL-MR-02941, August, 1979.

12. L. V. Al'tshuler, G. I. Kanel' and B. S. Chekin, "New Measurements of the Viscosity of Water Behind a Shock Wave Front," Sov. Phys. JETP, 45(2), February 1977.

13. A. A. Deribas and I. D. Zakharenko, "Surface Effects With Oblique Collisions Between Metallic Plates," Fizika Goreniya i Vzryva, V. 10, No. 3, May - June 1974.

14. Yu. A. Gordopolov, A. N. Dremin and A. N. Mikhailov, "Theory of Waves on the Interface of Metals Welded by Explosion," Fizika Goreniys i Vzryva, V. 14, No. 4, July - August 1978.

15. Yu. A. Gordopolov, A. N. Dremin and A. N. Mikhailov, "Experimental Determination of the Dependence of the Wavelength on the Angle of Collision in the Process of the Explosive Welding of Metals," Fizika Goreniya i Vzryna, V. 12, No. 4, July - August 1976.

16. L. A. Shushko, B. I. Shekhter and S. L. Krys'kov, "Bending of a Metal Strip by a Sliding Detonation Wave," Fizika Goreniya i Vzryva, V. 11 No. 2, March - April 1975.

17. V. F. Lobanov, "Numerical Simulation of Flow During Compression of Cylindrical Samples By a Glancing Detonation Wave," Zh. Prikladnoi Mekhaniki i Tekhnicheskoi Fiziki, No. 5, September - October 1975.

18. V. V. Efromov, "Oblique Impacts of Metallic Plates In an Elastic Formulation," Zh. Prikladnoi Mekhaniki i Teknicheskoi Fiziki, No. 5, September - October 1975.

19. K. A. Bezhanov, "Irregular Interaction of a Moving Shock Wave With a Tangential Discontinuity," PMM, V. 41, No. 6, 1977.

20. A. P. Pogorelov, B. L. Glushok, S. A. Novikov, V. A. Sinitsyn and A. V. Chernov, "Dependence of Recoil Impulse From A Rigid Barrier Under Sliding Conditions of Detonation of an Explosive Layer," Fizika Goreniya i Vzryva, V. 13, No. 5, September - October 1977.

21. Yu. A. Gordopolov, A. N. Dremin and A. N. Mikhailov, "Wave Formation With the High-Speed Collision of Metallic Bodies," Fizika Goreniya i Vzryva, V. 13, No. 2, March - April 1977.

22. V. V. Efremov, "Investigation of Oblique Collisions of Metal Plates in an Elastic Formulation," Zh. Prikladnoi Mekhaniki i Technicheskoi Fiziki, No. 1, January - February 1975.

23. N. S. Sanasaryan, "Explosive Viscoplastic Deformation of a Tube and its Relationship With the Properties of the Surrounding Medium," Fizika Goreniya i Vzryva, No. 4, October - December 1971.

24. N. A. Kozin, V. I. Mali and M. V. Rubtsov, "Tangential Explosion with Collapse of a Bimetallic Casing," Combustion, Explosion and Shock Waves, V. 13, No. 4, July - August 1977.

25. L. V. Shurshalov, "Calculation of Cumulative Jets," Izvestiya Akademii Nauk. SSSR, Mekhanika Zhidkosti i Gaza, No. 4, July - August 1975.

26. M. V. Rubtsov, "Deformation of Liquid Line With the Collision of Jets," Zh. Prikladnoi Mekhaniki i Tekhnicheskoi Fiziki, No. 6, November - December 1977.

27. A. N. Mikhailov and A. N. Dremin, "Flight Speed of a Plate Propelled by Products From a Sliding Detonation," Fizika Goreniya i Vzryva, V. 10, No. 6, November - December 1974.

28. S. K. Godunov, Ya. M. Kazhdan and V. A. Simonov, "Shock Wave Incidence on a V-Shaped Cavity," Zh. Prikladnoi Mekhaniki i Tekhnicheskoi Fiziki, V. 10, No. 6, November - December 1969.

29. V. A. Ivanov, "Disintegration of a Liquid Jet," Zh. Prikladnoi Mekhaniki i Tekhnicheskoi Fiziki, V. 7, No. 4, 1966.

30. A. G. Ivanov, S. A. Novikov and L. I. Kochkin, "Detonation Wave Collision on Surface of an Inert Material," Fizika Goreniya i Vzryva, V. 13, No. 4, July - August 1977.

31. M. V. Rubtsov, "Measurement of Velocity of a Cumulative Jet," Fizika Goreniya i Vzryva, V. 13, No. 6, November - December 1977.

32. E. I. Bichenkov and V. A. Lobanov, "Acceleration of Metallic Plates by Explosion," Fizika Goreniya i Vzryva, V. 10, No. 2, March - April 1974.

33. B. I. Shekhter, L. A. Shushko and S. L. Krys'kov, "Investigation of the Squeezing Process of the Lining of an Elongated Hollow-Charge Pedicle," Fizika Goreniya i Vzryva, V. 13, No. 2, March - April 1977.

34. V. I. Laptev and Yu. A. Trishin, "Increase of Initial Velocity and Pressure Upon Impact on an Inhomogenous Target," Zh. Prikladnoi Mekhaniki i Tekhnicheskoi Fiziki, No. 6, November - December 1974.

35. L. C. Chhabildas and J. R. Asay, "Rise-Time Measurements of Shock Transitions in Aluminum, Copper, and Steel," J. Appl. Phys. 50(4), April 1979.

36. J. M. Walsh, R. G. Shreffler and F. J. Willig, "Limiting Conditions for Jet Formation in High Velocity Collisions," J. of Appl. Phys., V. 24, No. 1, March 1953.

37. P. C. Chou, J. Carleone and R. R. Karpp, "Criteria for Jet Formation From Impinging Shells and Plates," J. Appl. Phys., V. 47, No. 7, July 1976.

38. J. Harrison, R. DiPersio, R. Karpp and R. Jameson, "A Simplified Shaped Charge Computer Code: BASC," DEA-AF-F/G-7304 Technical Meeting: Physics of Explosives, Vol. II, April - May 1974, Paper 13 Presented at the Naval Ordnance Laboratory, Silver Spring, MD.

39. F. E. Allison and R. Vitali, "An Application of the Jet-Formation Theory to a 105-mm Shaped Charge." BRL Report No. 1165, March 1962.

40. P. C. Chou. and J. Carleone, "Calculation of Shaped-Charge Jet Strain, Radius and Breakup Time," BRL CR 246, July 1975.

41. D. P. Bauer and S. J. Bless, "Strain Rate Effects on Ultimate Strain of Copper," AFML-TR-79-4021, May 1979.

42. R. DiPersio, W. Jones, A. Merendino and J. Simon, "Characteristics of Jets From Small Caliber Shaped Charges With Copper and Aluminum Liners," BRL MR 1866, September 1967.

43. M. Defourneaux, "Hydrodynamic Theory of Shaped Charges and of Jet Penetration," Memorial De L'art Ille'rie Francasise-T, 44, 1970.

44. V. I. Mali, V. V. Pai and A. I. Skovpin, "Investigation of the Breakdown of Flat Jets," Fizika Goreniya i Vzryva, V. 10, No. 5, September - October 1974.

45. G. R. Cowan and A. H. Holtzman, "Flow Configurations in Colliding Plates: Explosive Bonding," J. Appl. Phys., Vol. 34, No. 4 (Part 1), pp. 928 - 939, April 1963.

46. P. C. Chou, J. Carleone and R. R. Karpp, "The Effect of Compressibility on the Formation of Shaped Charge Jets," Proc. 1st Int. Symp. on Ballistics, Orlando, FL, 13 - 15 November 1974.

47. J. T. Harrison, "Improved Analytical Shaped Charge Code: BASC," Ballistic Research Laboratory, Technical Report ARBRL-TR-02300, March 1981.

XI. EXPLOSIVE WELDING, SHAPING AND FORMING

As mentioned in the first section, we will briefly address the concepts of explosive welding, explosive bonding and explosive forming.

The explosive working of metals and concepts related to explosive effects, standoff systems, contact systems, shock physics and material effects are presented in an excellent introductory book by Rinehart and Pearson [1].

An explosive forming procedure is shown in Figure 1. A die assembly holding the work piece is positioned in a tank of water. A vacumm is drawn below the work piece and an explosive charge is detonated in the water. The work piece then assumes the shape of the die (if all goes well).

A method for bulging cylindrical tubing is shown in Figure 2. The explosive charge is sealed in plastic and positioned in the cylindrical work piece filled with water. The ends are sealed to add confinement and reduce water splash. The charge is detonated within the cylinder held by a split die assembly. Figure 2 shows the bulging cylinder produced.

In explosive welding or bonding applications, two or more plates are driven together at high velocities and surface jetting occurs. This results in a bond between the two driven metals and can result in a wave interface of high strength between the welded materials. If the plate impact velocities are too high (relative to the material properties), the interface material will jet as a shaped-charge and the bonding will be poor. If the impact velocities are too low, no interaction will occur at the interface. The velocity must be such that plastic deformation occurs at the interface and local surface jetting occurs. The requirements for welding to occur are [2]:

a. the existence of a jet at the interface, and

b. an increase in pressure, associated with the rapid dissipation of kinetic energy, to a sufficient level for a sufficient time to achieve stable interatomic bonds. The pressure is determined by the impact velocity and the time available for bonding is determined by the velocity of the collision point.

The final geometry of the explosive-metal system will vary depending on the geometry and materials of the parts to be welded. The nature of the interface between the welded parts will vary depending on the materials welded and the nature of the explosive-metal interaction system.

Figure 3 shows a surface cladding test arrangement. The top plate, or flyer plate, only is driven by the explosive force in order to weld a thin sheet of material onto a heavy sheet. This technique is useful in plating a good structural material with a thin cladding to protect it from a corrosive or hazardous environment.

Explosive welding is similiar to explosive cladding, but two flyer plates are used to form an explosively welded final product. Figure 4 depicts an explosively welded sandwich or a three-layer weld.

Other examples of the explosive working of metals as well as the details associated with these processes can be found in Reference [1].

Blazynski [2] provides a recent collection of papers dealing with many aspects of the explosive working of metals. Pearson, in Chapter 1 of Reference [2], describes the explosive hardening of austenitic manganese steels subjected to severe impact and abrasion. These steels are used in railroad frogs, rock crusher jaws, grinding mills and similar devices. To explosively harden a steel, a thin layer of explosive is detonated in contact with the surface to be hardened, usually at grazing incidence. The propagation of the shock through the material increases the metal hardness (BHN) throughout the material. This also increases the yield and tensile strength of the metal, making it more resistant to impact wear and with less tendency to deform. Duvall [3] discusses shock wave propagation in metals.

Pearson, in Reference [2], discusses explosive compaction where explosive loads are applied either directly or through a loading system to compact powders. Two methods involve the use of gun powder cartridges and the use of explosives to drive pistons into the powder compaction chamber. Explosive compaction can produce parts from powders that cannot be produced by conventional pressing. Improved material properties with high press densities can be produced. Explosive compaction is extremely valuable in the powder metallurgy field.

Pearson, Chapter 1 and El-Sobky, Chapter 6 of Reference [2], discuss explosive welding. We have briefly touched on this area and we will conclude our discussion with some of the major points of Reference [2].

Explosive welding is a solid phase welding process in which high explosives are used to join the weld surfaces in a high velocity collision. This collision produces severe, localized plastic flow at the interface between the two surfaces. Explosive welding is used to weld metal combinations many of which cannot be welded by conventional means.

The weld is usually formed by oblique impact of the plate surfaces with the weld, progressing from the apex along the collision interface by a process similar to the collapse of a shaped-charge liner. The parameters involved in explosive welding include the physical and mechanical properties of the metals to be welded, the type and amount of explosive used, the mode of initiation, the initial geometry of the weld operation and the type and geometry of buffer sheets (if used) between the metal and the explosive. These parameters influence the collision angle, the impact velocity and the collision point velocity.

It is generally agreed that jet formation at the collision point is essential for welding, e.g., El-Sobky, Chapter 6 of Reference [2]. This is because, at least in part, jetting produces chemically clean surfaces which allow interatomic bonding under the high pressure conditions.

The jet-no-jet criterion, or the limiting condition for jet formation, discussed earlier, is based on the studies of Cowan and Holtzman [4], Walsh, et al [5], Chou, et al [6] and Harlow and Pracht [7]. These studies relate to shock formation and critical collapse angles and are also applied to shaped-charge jets. The mathematical description for the explosive welding of oblique plates involves relationships similar to those used in jet formation theory and in the Gurney type equations. In addition to Gurney, impact

velocity equations are given by Deribas, et al [8] and others as reviewed by El-Sobky, Chapter 6 of Reference [2]. El-Sobky reviews the jet formation criterion as well as minimum impact pressures and standoff distance requirements which must be met. El-Sobky notes that the collision velocity and plate impact velocity should be less than the bulk speed of sound of either welding component. However, Wylie, et al [9] suggests that the bulk speed of sound may be exceeded by as much as 25% with satisfactory welds. It is interesting that this coincides with the jet-no-jet criterion observed by Harrison, et al [10,11,12] for copper jets, i.e., Mach number 1.23. Also, the visco-plastic critical Reynolds number criterion, discussed earlier, was derived from explosive welding experiments [13,14].

A major area of study in explosive welding is the interfacial periodic deformation or the interfacial waves. Often a regular wavy interface pattern appears, but the nature of the interfacial waves vary depending on the materials and system geometry used.

When regular waves are produced, they are very similar to the surface deformations found on solid surfaces subjected to erosive action of high speed liquid films, jet drags, e.g., in pump and steam turbine blades, and at the air-sea interface, e.g., ocean waves. A review of the mechanisms for wave formation are given by El-Sobky in Chapter 6 of Reference [2].

A good general discussion of explosive welding is given in Reference [15]. Jetting phenomena, the weld interface, and the explosive load and standoff distance required for various weld combinations are discussed. Other excellent sources of information include the USSR sources, given in the discussion on the visco-plastic jet formation model and viscosity measurements [13,14]. Schroeder [16] recently edited a text on explosive welding and related areas. Deribas [17] authored a classic text on explosive welding and work-hardening. Duvall [3] presents an excellent supplementary discussion on shock propagation and transmission through solids. Sewell [18] also discusses explosive welding regarding jet-no-jet criterion.

This concludes the discussion of explosive working of metals. The information provided in this section is not complete, nor was it intended to be. The intent was merely to provide an overview of explosive welding and related fields. Our goal was to provide a brief introduction and a few fundamental references into this field and to note the similarity to shaped-charge jetting phenomenon.

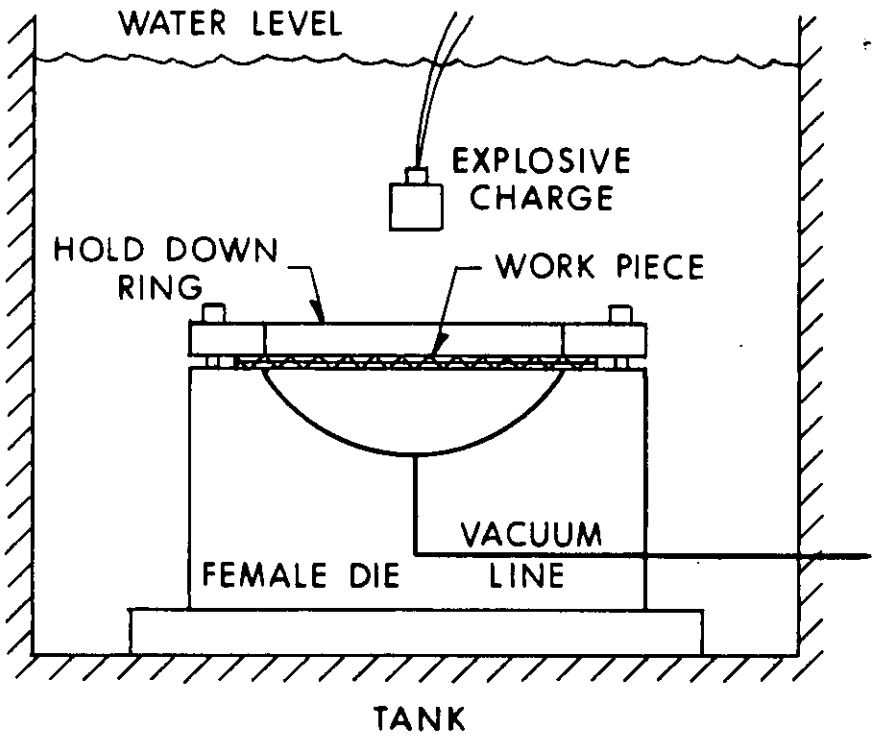

Figure 1. Explosive Forming.

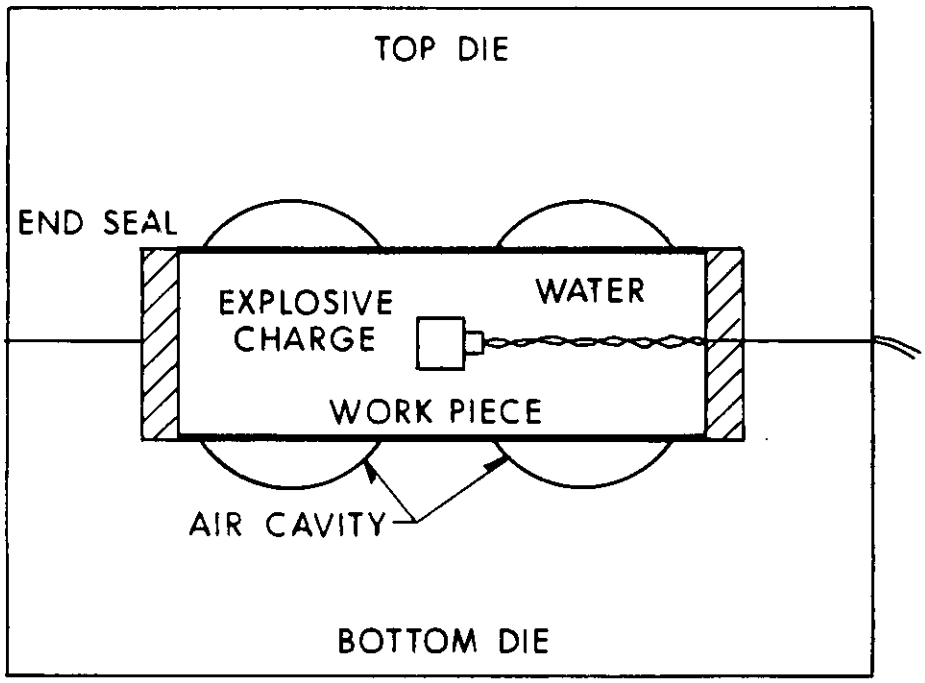

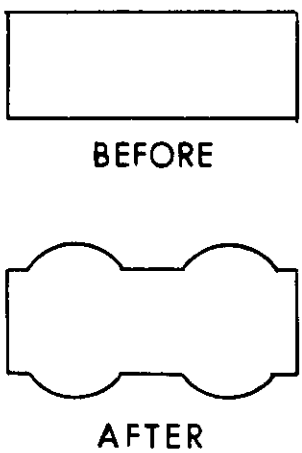

Figure 2. Bulging Cylinder Tube.

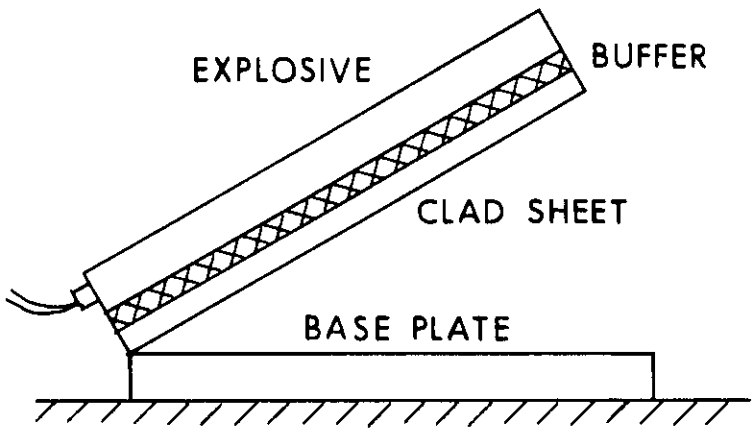

Figure 3. Surface Cladding.

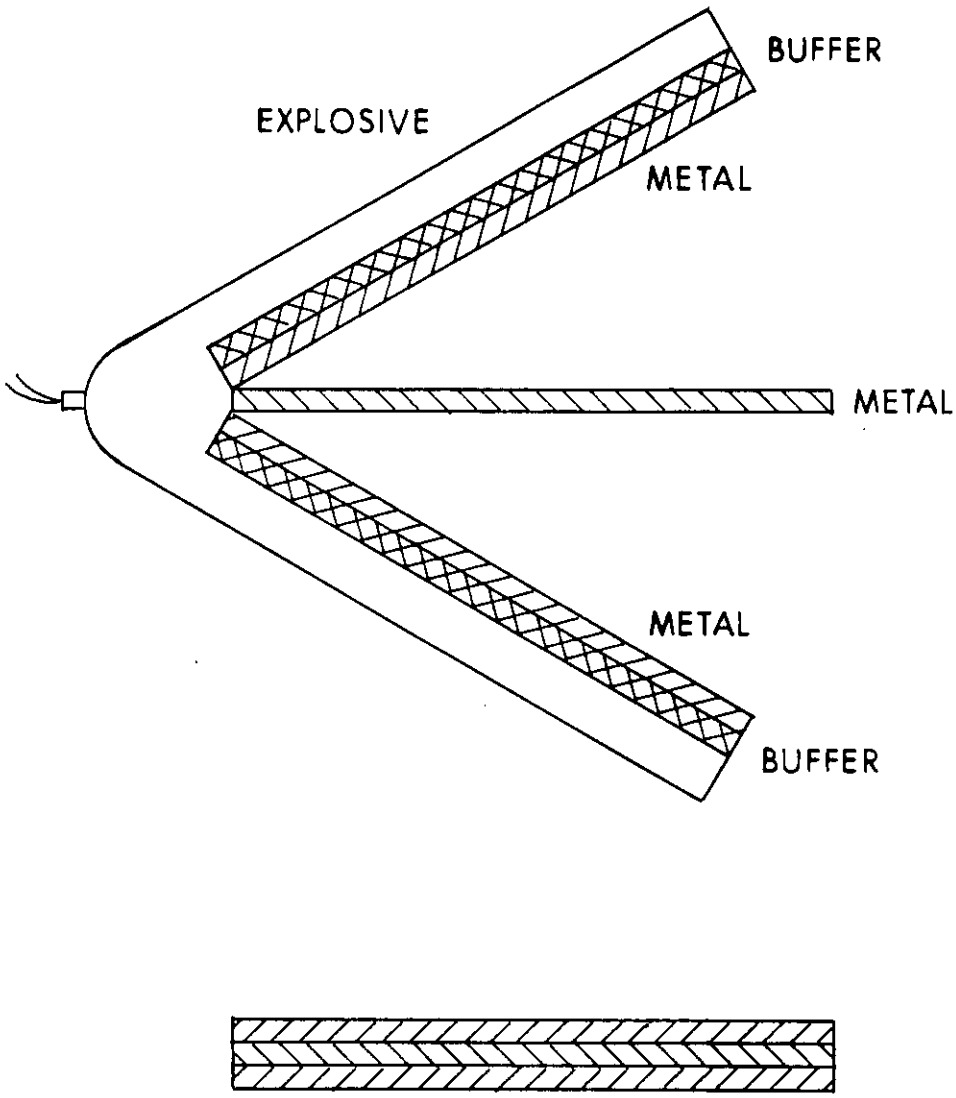

Figure 4. Explosive Welding, a Three Layer Weld (Sandwich).

REFERENCES
Section XI

1. John S. Rinehart and John Pearson, Explosive Working of Metals, Macmillan Comp., N.Y., 1963.

2. Explosive Welding, Forming and Compaction, edited by T. Z. Blazynski, Applied Science Publishers, N.Y., 1983.

3. George E. Duvall, "Shock Waves in Solids," International Science and Technology, April 1963.

4. G. R. Cowan and A. H. Holtzman, "Flow Configurations in Colliding Plates: Explosive Bonding," J. Appl. Phys., Vol. 34, No. 4, pp. 928 - 939, April 1963.

5. J. M. Walsh, R. G. Shreffler and F. J. Willig, "Limiting Conditions for Jet Formation in High Velocity Collisions," J. Appl., Phys., Vol. 24, No. 3, pp. 349 - 359, 1953.

6. P. C. Chou, J. Carleone and R. R. Karpp, "Criteria for Jet Formation from Impinging Shells and Plates," J. Appl. Phys., Vol. 47, pp. 2975 - 2981, July 1976.

7. F. H. Harlow and W. E. Pracht, The Physics of Fluids, 9, pp. 1951 - 1959, 1966.

8. A. A. Deribas, V. M. Kudinov, F. I. Matveenkov and V. A. Simonov, "Determination of the Impact Parameters of Flat Plates in Explosive Welding," Fizika Goreniya i Vzryva, Vol. 3, No. 2, pp. 291 - 298, 1967.

9. H. K. Wylie, P. E. G. Williams and B. Crossland, "Further Experimental Investigation of Explosive Welding Parameters," Proc. 3rd Int. Conf. of the Center for High Energy Rate Forming, University of Denver, Colorado, 1971.

10. J. T. Harrison, "Improved Analytical Shaped Charge Code: BASC," Ballistic Research Laboratory Technical Report No. ARBRL-TR-02300, March 1981.

11. J. T. Harrison, "BASC, an Analytical Code for Calculating Shaped Charge Properties," Proc. 6th Int. Symp. on Ballistics, Orlando, FL, 27 - 29 October 1981.

12. J. T. Harrison, R. DiPersio, R. Karpp and R. Jameson, "A Simplified Shaped Charge Computer Code: BASC," DEA-AF-F/G-7304 Technical Meeting: Physics of Explosives, Vol. II, April - May 1974, Paper 13 presented at the Naval Ordnance Laboratory, Silver Spring, MD.

13. W. P. Walters, "Influence of Material Viscosity on the Theory of Shaped-Charge Jet Formation," BRL Memorandum Report, ARBRL-MR-02941, August 1979.

14. W. P. Walters and J. T. Harrison, "Modeling of the Shaped-Charge Jet Formation," Proceedings of the Army Symposium on Solid Mechanics, 1980 - Designing for Extremes: Environment, Loading and Structural Behavior, AMMRC MS 80-4, September 1980.

15. "Explosive Welding," Mechanical Engineering, May 1978.

16. High Energy Rate Fabrication, edited by J. W. Schroeder, Foster Wheeler Development Corp., Livingston, N.J., 1984. (ASME Special Publication, Book No. H00381).

17. A. A. Deribas, Physics of Explosive Work-Hardening and Welding, Nauka, Novosibirsk, 1972.

18. R. G. S. Sewell, "Effects of Velocity and Material Properties on Design Limits for Linear Shaped Charges," NAVWEPS Report 8793, NOTS TP 3894, October 1965.

DISTRIBUTION LIST

Copies	Organization
2	Commander MICOM Research, Development and Engineering Center ATTN: Library Joel Williamson Redstone Arsenal, AL 35898
1	Assistant Secretary of the Army (R&D) ATTN: Assistant for Research Washington, DC 20310
2	Commander US Army Material Technology Laboratory ATTN: AMXMR-RD, J. Mescall Tech Lib Watertown, MA 02172
1	Commander US Army Research Office P.O. Box 12211 Research Triangle Park NC 27709-2211
1	Commander US Army Foreign Science and Technology Center ATTN: AIAST-IS 220 Seventh Street, NE Charlottesville, VA 22901-5396
1	Commander Det S, USAOG USAINSCOM ATTN: IAGPC-S Ft. Meade, MD 20755
2	Commander Naval Air Systems Command ATTN: Code AIR-310 Code AIR-350 Washington, DC 20360
1	Office of Naval Research Department of the Navy 800 N. Quincy Street Arlington, VA 22217
10	Commander Naval Surface Weapons Center ATTN: Code DG-50 DX-21, Lib Br N. Coleburn, R-13 T. Spivok W. Reed, R10A R. Phinney C. Smith E. Johnson W. Bullock C. Dickerson White Oak, MD 20910
1	Commander Naval Surface Weapons Center ATTN: Code 730, Lib Silver Spring, MD 20910
1	Commander Naval Surface Weapons Center ATTN: DX-21, Lib Br Dr. W. Soper Dahlgren, VA 22448
2	Commander Naval Weapons Center ATTN: Code 4057 Code 45, Tech Lib China Lake, CA 93555
2	David W. Taylor, Naval Ship R&D Center ATTN: D. R. Garrison/ Code 1740.3 H. Gray Bethesda, MD 20084
1	Commander Naval Research Laboratory Washington, DC 20375
1	USAF/AFRDDA Washington, DC 20330
1	AFSC/SDW Andrews AFB Washington, DC 20311
1	US Air Force Academy ATTN: Code FJS-41 (NC) Tech Lib Colorado Springs, CO 80840

DISTRIBUTION LIST

Copies	Organization
1	AFATL/DLJR (J. Foster) Eglin AFB, FL 32542
9	Director Lawrence Livermore Laboratory ATTN: Dr. J. Kury Dr. M. Wilkins Dr. E. Lee Dr. H. Horning Dr. M. Van Thiel Dr. C. Cline Dr. T. Ennis Dr. R. Wienguard Technical Library P.O. Box 808 Livermore, CA 94550
1	Battelle-Columbus Laboratories ATTN: Technical Library 505 King Avenue Columbus, OH 43201
2	Dyna East Corporation ATTN: P. C. Chou R. Ciccarelli 3432 Market Street Philadelphia, PA 19104-2588
1	Aerojet Ordnance Corporation ATTN: Warhead Tech. Dept. Dr. J. Carleone 2521 Michelle Drive Tustin, CA 92680
1	Physics International Company Tactical Systems Group Eastern Division ATTN: R. Berus P. O. Box 1004 Wadsworth, OH 44281-0904
4	Honeywell, Inc. Government and Aeronautical Products Division ATTN: C. R. Hargraves R. S. Kensinger G. Johnson J. Houlton 600 Second Street, NE Hopkins, NM 55343
5	Sandia Laboratories ATTN: Dr. W. Herrman Dr. J. Asay Dr. R. Longcope Dr. R. Sandoval Dr. M. Forrestal Albuquerque, NM 87115
1	Systems, Science & Software ATTN: Dr. R. Sedgwick P.O. Box 1620 La Jolla, CA 92037
2	General Dynamics Pomona Division ATTN: E. LaRocca, MZ4-40 R. Strike P.O. Box 2507 Pomona, CA 91769
5	University of California Los Alamos Scientific Lab ATTN: Dr. J. Walsh Dr. R. Karpp Dr. C. Mautz Mr. J. Repa Technical Library P.O. Box 1663 Los Alamos, NM 87545
1	University of Denver Colorado Seminary ATTN: Mr. R. F. Recht P. O. Box 10127 Denver, CO 80208
2	University of Illinois Dept of Aeronautical and Astronautical Engineering ATTN: Prof. A. R. Zak Prof. S. M. Yen Campus Police Building 101 N. Matthews Urbana, IL 61801
2	California Research and Technology ATTN: Dr. Ronald E. Brown Mr. Mark Majerus 11875 Dublin Blvd. Suite B-130 Dublin, CA 94568

DISTRIBUTION LIST

Copies	Organization
1	University of Dayton Research Institute ATTN: Dr. S. J. Bless Dayton, OH 45469
2	Southwest Research Institute ATTN: C. Anderson A. Wenzel 6220 Culebra Road P. O. Drawer 28510 San Antonio, TX 78284
2	Nuclear Metals Inc. ATTN: M. Walz W. Zimmer 2229 Main Street Concord, MA 01742
1	SRI International ATTN: Dr. L. Seaman 333 Ravenswood Avenue Menlo Park, CA 94025
1	Northrop Corporation Electro-Mechanical Division ATTN: Donald L. Hall 500 East Orangethorpe Avenue Anaheim, CA 92801
2	Boeing Aerospace Co. Shock Physics & Applied Math Engineering Technology ATTN: R. Helzer J. Shrader P. O. Box 3999 Seattle, WA 98124
1	McDonnell Douglas Astronautics Company ATTN: Bruce L. Cooper 5301 Bolsa Avenue Huntington Beach, CA 92647
1	Commander Air Force Wright Aeronautical Laboratory A. F. Systems Command ATTN: Dr. Lee Kennard, ASD/PMRRC USAF Wright Patterson AFB Ohio 45443
1	D. R. Kennedy and Associates Inc. ATTN: Donald Kennedy P. O. Box 4003 Mountain View, CA 94040
	Aberdeen Proving Ground
	Dir, USAMSAA ATTN: AMXSY-GI, B. Simmons

Copies	Organization
12	Administrator Defense Technical Info Center ATTN: DTIC-DDA Cameron Station Alexandria, VA 22304-6145
1	HQDA DAMA-ART-M Washington, D.C. 20310
1	Commander U.S. Army Materiel Command ATTN: AMCDRA-ST 5001 Eisenhower Avenue Alexandria, VA 22333-0001
1	Commander Armament R&D Center U.S. Army AMCCOM ATTN: SMCAR-TSS Dover, NJ 07801
1	Commander Armament R&D Center U.S. Army AMCCOM ATTN: SMCAR-TDC Dover, NJ 07801
1	Director Benet Weapons Laboratory Armament R&D Center U.S. Army AMCCOM ATTN: SMCAR-LCB-TL Watervliet, NY 12189
1	Commander U.S. Army Armament, Munitions and Chemical Command ATTN: SMCAR-ESP-L Rock Island, IL 61299
1	Commander U.S. Army Aviation Research and Development Command ATTN: AMSAV-E 4300 Goodfellow Blvd St. Louis, MO 63120
1	Director U.S. Army Air Mobility Research and Development Laboratory Ames Research Center Moffett Field, CA 94035

Copies	Organization
1	Commander U.S. Army Communications-Electronics Command ATTN: AMSEL-ED Fort Monmouth, NJ 07703
1	Commander ERADCOM Technical Library ATTN: DELSD-L (Reports Section) Fort Monmouth, NJ 07703-5301
1	Commander U.S. Army Missile Command Research, Development & Engineering Center ATTN: AMSMI-RD Redstone Arsenal, AL 35898
1	Director U.S. Army Missile & Space Intelligence Center ATTN: AIAMS-YDL Redstone Arsenal, AL 35898-5500
1	Commander U.S. Army Tank Automotive Cmd ATTN: AMSTA-TSL Warren, MI 48397-5000
1	Director U.S. Army TRADOC Systems Analysis Activity ATTN: ATAA-SL White Sands Missile Range, NM 88002
1	Commandant U.S. Army Infantry School ATTN: ATSH-CD-CSO-OR Fort Benning, GA 31905
1	Commander U.S. Army Development and Employment Agency ATTN: MODE-TED-SAB Fort Lewis, WA 98433
1	AFWL/SUL Kirtland AFB, NM 87117
1	Air Force Armament Laboratory ATTN: AFATL/DLODL Eglin AFB, FL 32542-5000

Copies	Organization
10	Central Intelligence Agency Office of Central Reference Dissemination Branch Room GE-47 HQS Washington, D.C. 20502

ABERDEEN PROVING GROUND

Dir, USAMSAA
ATTN: AMXSY-D
AMXSY-MP, H. Cohen

Cdr, USATECOM
ATTN: AMSTE-TO-F

Cdr, CRDC, AMCCOM
ATTN: SMCCR-RSP-A
SMCCR-MU
SMCCR-SPS-IL

USER EVALUATION SHEET/CHANGE OF ADDRESS

This Laboratory undertakes a continuing effort to improve the quality of the reports it publishes. Your comments/answers to the items/questions below will aid us in our efforts.

1. BRL Report Number_____ Date of Report_____

2. Date Report Received_____

3. Does this report satisfy a need? (Comment on purpose, related project, or other area of interest for which the report will be used.)_____

4. How specifically, is the report being used? (Information source, design data, procedure, source of ideas, etc.)_____

5. Has the information in this report led to any quantitative savings as far as man-hours or dollars saved, operating costs avoided or efficiencies achieved, etc? If so, please elaborate._____

6. General Comments. What do you think should be changed to improve future reports? (Indicate changes to organization, technical content, format, etc.)

CURRENT ADDRESS

Name

Organization

Address

City, State, Zip

7. If indicating a Change of Address or Address Correction, please provide the New or Correct Address in Block 6 above and the Old or Incorrect address below.

OLD ADDRESS

Name

Organization

Address

City, State, Zip

(Remove this sheet along the perforation, fold as indicated, staple or tape closed, and mail.)

FOLD HERE

Director
U.S. Army Ballistic Research Laboratory
ATTN: SLCBR-DD-T
Aberdeen Proving Ground, MD 21005-5066

NO POSTAGE
NECESSARY
IF MAILED
IN THE
UNITED STATES

OFFICIAL BUSINESS
PENALTY FOR PRIVATE USE, $300

BUSINESS REPLY MAIL
FIRST CLASS PERMIT NO 12062 WASHINGTON, DC
POSTAGE WILL BE PAID BY DEPARTMENT OF THE ARMY

Director
U.S. Army Ballistic Research Laboratory
ATTN: SLCBR-DD-T
Aberdeen Proving Ground, MD 21005-9989

FOLD HERE